2021

Geological Survey Paper 6:

Structural Geology of Frenchmans Cap, Central Tyennan Domain, Tasmania

Authors: D. R. Gray
M. J. Vicary

Date: 28/06/2021
Email: info@mrt.tas.gov.au
Website: www.mrt.tas.gov.au

REPORT No: GSP6

Aerial view of Frenchmans Cap at 1146m (centre background) and White Needle ridgeline (foreground). Barron Pass and Sharlands Peak are at centre-right. The heavily vegetated, glacial Livingstone Valley with Lakes Gertrude and Cecily is centre left. White, low-grade, quartzite of the Mary metamorphic sheet occupies the ridgelines with valleys in low-grade, dolomitic phyllite of the underlying Scotchfire metamorphic sheet.

Tasmanian Government

Mineral Resources Tasmania
mrt

Tasmanian Government

Mineral Resources Tasmania

Department of State Growth
www.mrt.tas.gov.au

Structural Geology of Frenchmans Cap, Central Tyennan Domain, Tasmania

David R. Gray[1] and Michael J. Vicary[2]
1. Consultant Structural Geologist to Mineral Resources Tasmania
2. Geological Survey Branch - Mineral Resources Tasmania

ARTICLE INFO

Published: 28 June 2021
Publisher: Mineral Resources Tasmania
Report No.: GSP6

KEYWORDS

Structural Geology
Frenchmans Cap
Central Tyennan Domain

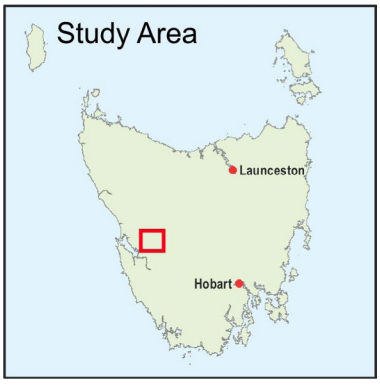

ABSTRACT

The Frenchmans Cap region belongs to the Central Tyennan domain, within the Proterozoic core of Tasmania. It is made up of three west-dipping, stacked metamorphic sheets with the high-grade schists of the Franklin-Joyce metamorphic sheet at the highest structural level on the western side. These overlie the quartzite of Frenchmans Cap (Fincham-Mary metamorphic sheet) and the low-grade dolomitic schist of the Scotchfire metamorphic sheet at the lowest structural level on the eastern side.

Structure includes two oppositely-closing, regional-scale recumbent isoclinal folds with lower limbs transitional into intensely foliated high-strain zones (The southwest-closing Frenchmans Cap-Lions Head Ridge recumbent fold and the east-closing Agamemnon recumbent fold). These are part of two quartzite outcrop belts that attenuate and merge to the northwest, a pattern related to the recumbent fold cores and refolding by more open Devonian folds (the Clytemnestra Anticline, the Philps Peak Anticline and the Lake Vera Syncline). The younger Devonian deformation also reactivated the high-strain zone contact between the quartzite (Fincham-Mary metamorphic sheet) and dolomitic schist (Scotchfire metamorphic sheet). This is shown by brittle reverse fault offsets in the contact and in particular the uplift of the Clytemnestra block relative to Frenchmans Cap. Later oblique-slip cross-faults (including the Lake Sophie Fault and the North Col Fault) further offset the contacts and fold-axial surface traces.

The significant relief of the east and northeast faces of Frenchmans Cap itself show structural variation and zonation in the low-grade quartzite sequence as well as high-strain contact with the underlying dolomitic schist. Three structural zones include:

1. An upper zone with recumbent macro-isoclinal folds in apparent “bedding”
2. A middle strongly foliated zone with mesoscopic, isoclinal folds within transposed layering and
3. A lower intensely foliated zone overprinted by brittle faulting above the faulted contact with the underlying dolomitic schist/phyllite.

Quartzites in the Frenchmans Cap region commonly show a quartz mineral elongation lineation (Lelong or Lm), a rodding lineation (Lrod) and crenulation lineations (Lcren). In the high-strain parts, particularly in the lower limb

transition to the basal zone of the recumbent Frenchmans Cap and Agamemnon macro-folds, the fabrics are typified by strong to intense foliation and transposition layering/foliation (Sm), rodding fabrics within the transposition layering, mesoscopic isoclinal folds, rootless isoclinal fold pairs and multiple crenulation cleavages (Scc).

Transport direction vectors calculated from shear bands and macro-shear band boudins indicate the quartzite sheet was emplaced from west-to-east towards 110°-120°. Shear bands in the high-strain upper part of the Scotchfire dolomitic phyllite also show west-over-east shear emplacement.

Oppositely closing Frenchmans Cap (southwest-closing) and Agamemnon (east-closing) recumbent folds at the same structural level, combined with the convergence of the quartzite outcrop belts containing the hinge-lines to the north, support a possible macro- sheath pod geometry within this part of the Mary-Fincham metamorphic sheet. The proposed structure is ~6 km wide with a strike length of ~10 km and a sheath-closure at around the Franklin River. Pod thickness is estimated at ~ 500 m in the position of Frenchmans Cap.

1.0 Introduction

Frenchmans Cap is perhaps the most iconic of Tasmanian peaks (see Kleinig, 2012; Wilkinson, 2011). Capped by quartzite, the Pleistocene glaciation has resulted in a unique and rugged landscape (see Peterson, 1966; Collins, 1990) (Figure 1). Frenchmans Cap and surrounds, including Clytemnestra and Agamemnon ridges, provide a window into the structure and nature of the lower part of Central Tyennan block litho-tectonic sequence (Figures 2 and 3).

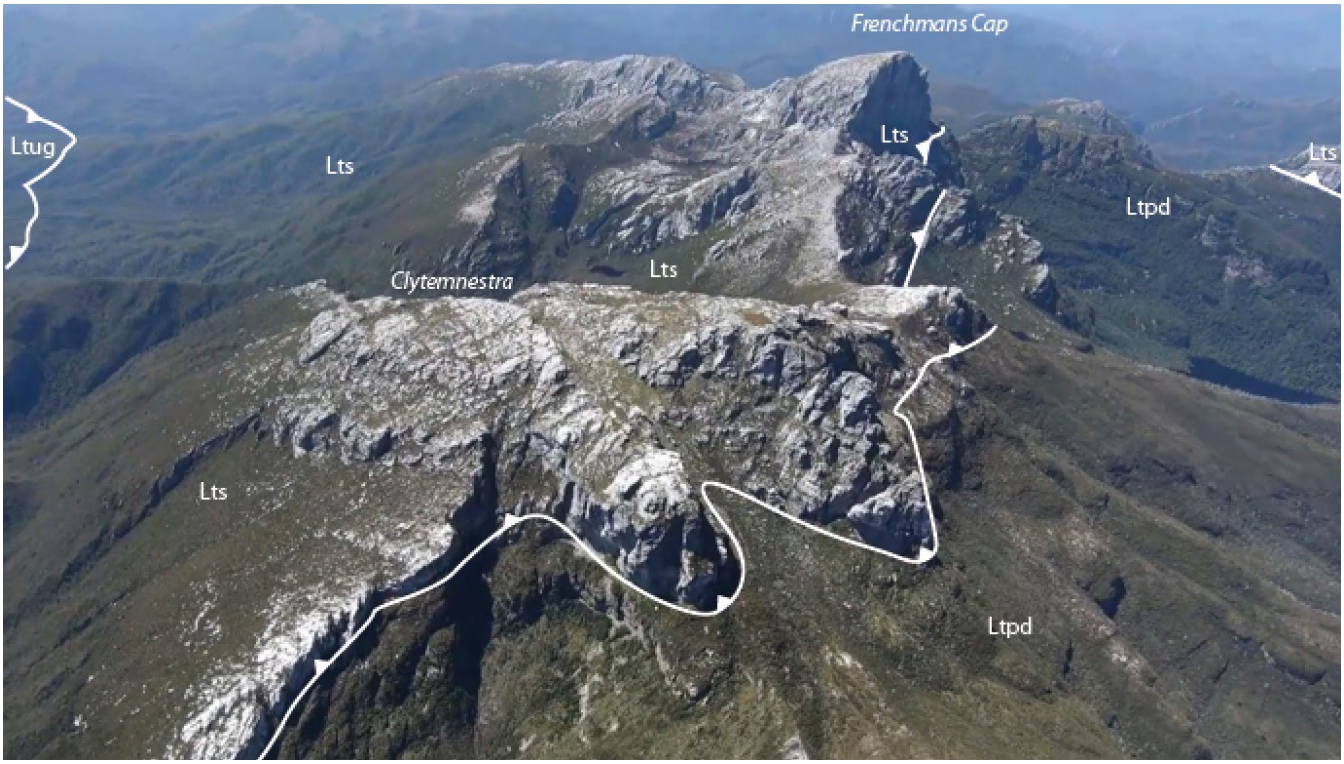

Figure 1. Aerial view from the south showing the imposing white quartzite ridges with Clytemnestra (foreground) and Frenchmans Cap (background) (photo by Wandering Foxbat). The quartzite is part of the low-grade Fincham-Mary metamorphic sheet (Lts). Contacts with the overlying high-grade Franklin-Joyce metamorphic sheet (Ltug) can be seen in the upper left, and the underlying low-grade Scotchfire metamorphic sheet (Ltpd) (photo centre) is highlighted by the barbed white lines. The Scotchfire sheet occupies the Livingstone valley (photo right).

The Tyennan block (after Carey, 1953; Turner 1989, fig. 2.10) represents the Proterozoic nucleus of Tasmania (Figure 2). It is the belt of Proterozoic quartzite and phyllite (quartz-chloritic pelite assemblage and garnetiferous schist-quartzite ± amphibolite assemblage) that extends from Cradle Mountain in the north, to Southwest Cape in the south (Figure 2b). The Tyennan block represents the major part of the Internal Zone of Berry (2014, fig. 4.2).

The Central Tyennan region (Figure 3) is made up of a stacked series of metamorphic sheets that have in part been folded into a series of regional-scale recumbent isoclinal folds. The metamorphic sheets include

1. High-grade Franklin-Joyce metamorphic sheet with garnet schists and schistose garnet quartzites (orange region, Figure 3) underlain by
2. Low-grade Fincham-Mary quartzites, schistose quartzites and phyllites (light blue region, Figure 3) underlain by
3. Low-grade Scotchfire dolomitic schist/phyllite (khaki region, Figure 3) as well as lenses of dolomite (olive green regions, Figure 3).

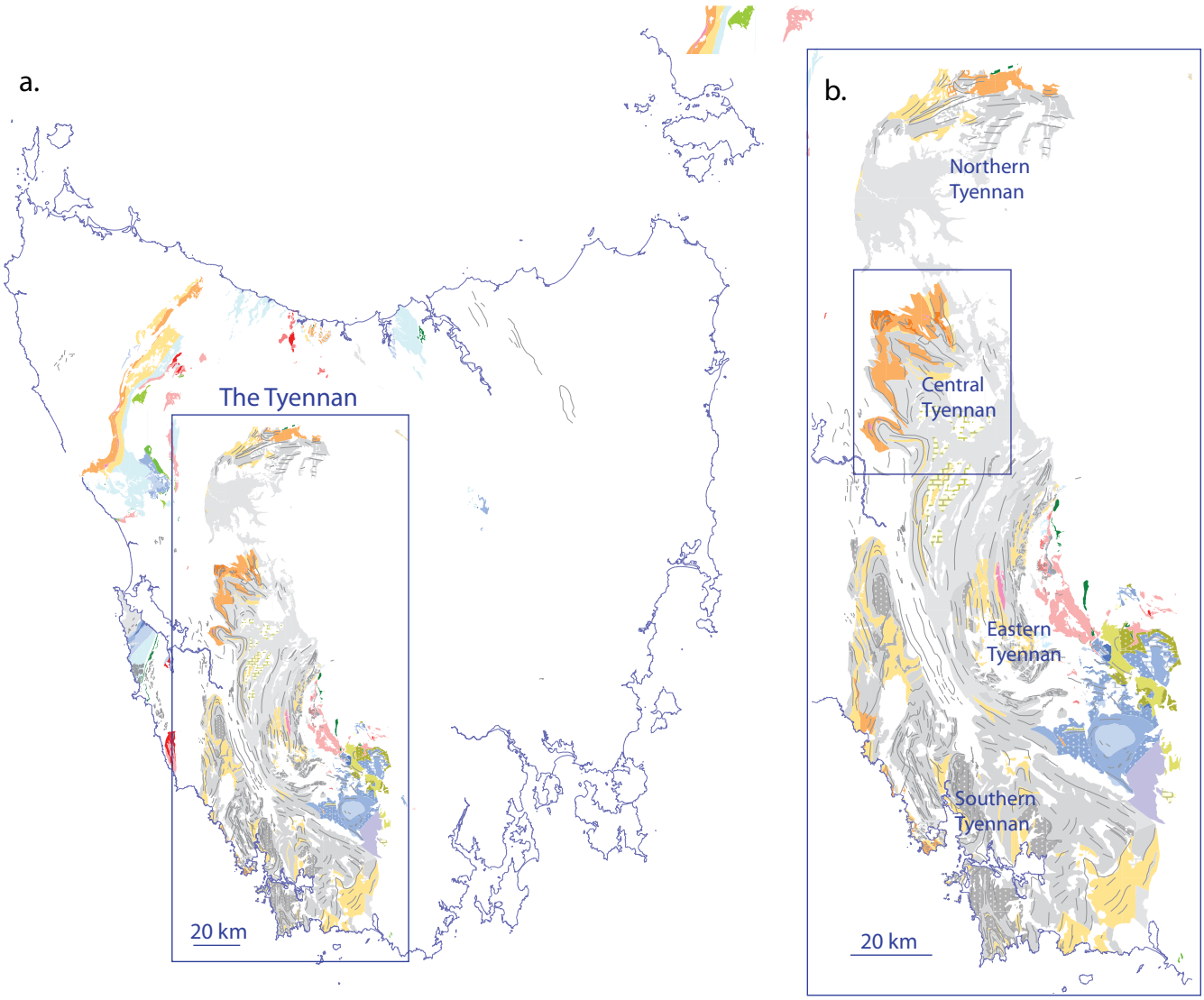

Figure 2. The Tyennan Proterozoic region of Tasmania. a) Tasmania map base (Mineral Resources Tasmania 1:25000 and 1:250000 Digital Geological Atlas). b) Location of the Central Tyennan region. Divisions within the Tyennan are after Berry (2014).

The Central Tyennan region (Figure 3) is made up of a stacked series of metamorphic sheets that have in part been folded into a series of regional-scale recumbent isoclinal folds. The metamorphic sheets include:

1. High-grade Franklin-Joyce metamorphic sheet with garnet schists and schistose garnet quartzites (orange region, Figure 3) underlain by:
2. Low-grade Fincham-Mary quartzites, schistose quartzites and phyllites (light blue region, Figure 3) underlain by:
3. Low-grade Scotchfire dolomitic schist/phyllite (khaki region, Figure 3) as well as lenses of dolomite (olive green regions, Figure 3).

Lenses of eclogite and amphibolite occur at the highest level in the high-grade Franklin-Joyce sheet (Spry, 1963; Raheim, 1976; Kamperman, 1984; Goscombe, 1990; Chmielowski, 2009; Palmeri et al. 2009; Chmielowski, & Berry, 2012; Brown et al., 2021). These lenses are enveloped by the high-grade schists (see Chmielowski, 2009, Palmeri et al. 2009, Brown et al., 2021) and are considered sills or flows in the shallow water Proterozoic sequences (Meffre et al., 2000).

Details and description of the Central Tyennan region are provided in Tyennan Structural Geology Series Publication 2 (Gray & Vicary, in prep.).

This Tasmanian Geological Survey Publication is the first in a series of papers on revisiting the structural geology of the Tyennan Proterozoic region. The aim of the Tyennan Structural Geology project has been to re-examine the structure of the Tyennan Proterozoic rocks in the context of ophiolite obduction and continental margin subduction-obduction (Berry & Crawford, 1988; see Berry 2014, fig. 4.10 in Corbett et al. eds. 2014). The main elements of this model are 1) the former passive continental margin (now preserved as the Rocky Cape autochthon), 2) the widespread mafic and ultramafic complexes in Tasmania (relicts of a middle Cambrian allochthonous sheet analogous to the Oman ophiolite), 3) high-P metamorphism of parts of the subducted margin, 4) the resultant stacked high-grade and low-grade metamorphic sheets that comprise the Tyennan (internal zone), and 5) the allochthonous, non-metamorphosed to very low-grade overlying sheets (external zone).

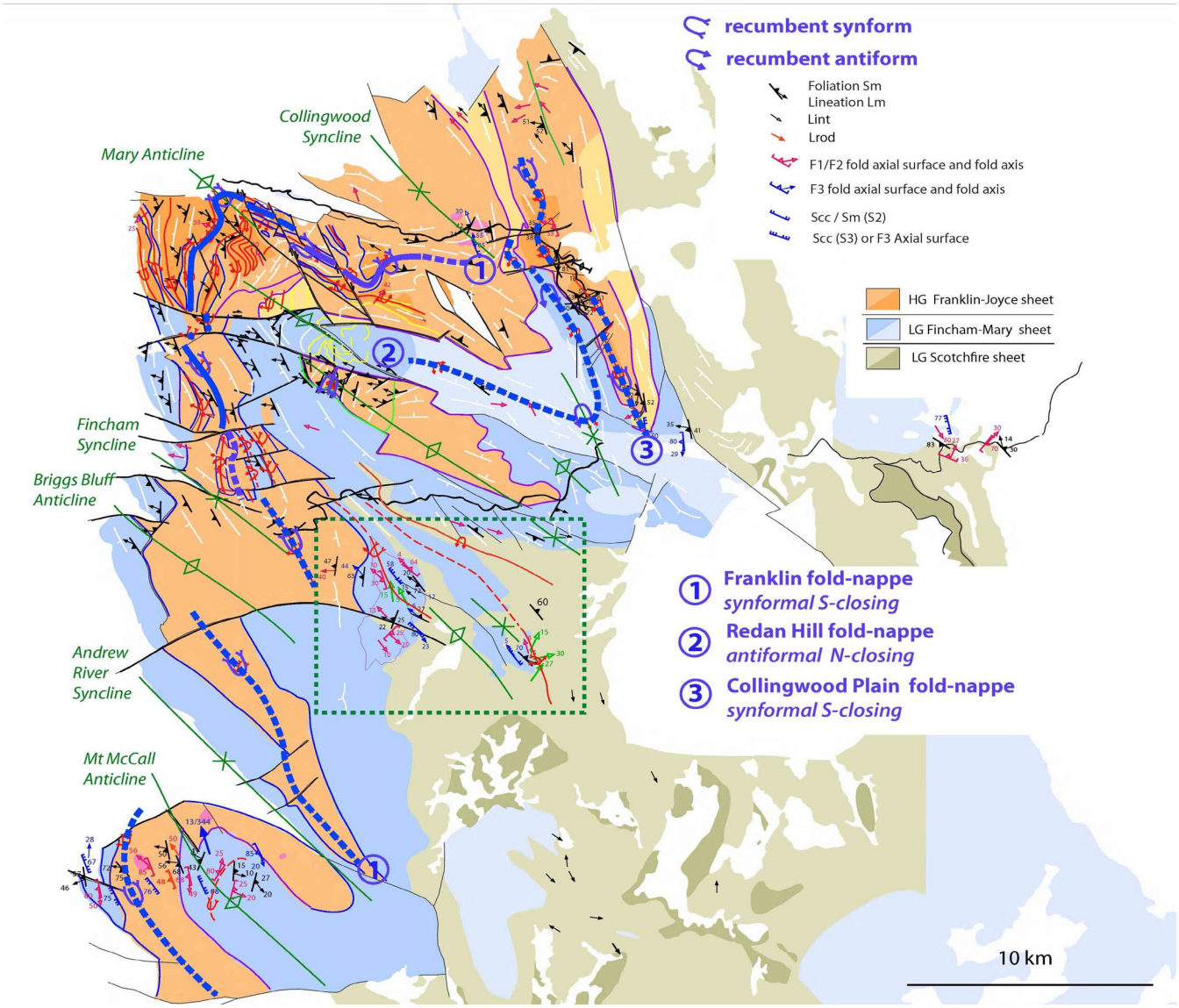

Figure 3. Central Tyennan litho-structural summary map showing the location of the Frenchmans Cap region (dashed box). Map base is from the Mineral Resources Tasmania 1:25000 and 1:250000 Digital Geological Atlas. The heavy blue and blue dashed lines show the axial surface traces of the three regional fold-nappes that dominate the structure of the Central Tyennan (see Gray & Vicary, in prep.). Orange: HG Franklin Metamorphic sheet; Dark orange: garnet quartzite; blue: LG quartzite-phyllite sequences of Fincham-Mary Metamorphic sheet; olive green: Scotchfire sheet.

Deformation of the Rocky Cape margin beneath the advancing ophiolite sheet has involved crustal-scale stacking of parts of the margin as sheets of different metamorphic grade, isoclinal folding and internal deformation of the sheets, and deformation or welding along their contacts as shear zones ±brittle faulting. Tasmania provides a 50-100 km extent-window into these underlying rocks, their internal deformation and the nature of their contacts due to the subsequent extensive removal of the ophiolite.

1.1 Background

The Frenchmans Cap area (dashed box, Figure 3) was mapped and described by Duncan (1974) with mapping undertaken in 1964 and 1965 as part of a PhD at the University of Tasmania (Duncan, 2021).

Structural mapping and reconnaissance was undertaken by the authors on a helicopter day-trip into Frenchmans Cap on March 28, 2020, involving a fly-around for photos, a traverse from Lions Head Ridge down to Lake Tahune and visits to Clytemnestra and Agamemnon.

B/W photographs taken by David Duncan (Duncan, 2021), along with structural data in Duncan (1974) and data collected by the authors, were used to update the Frenchmans Cap area structural map and structural interpretation. The Frenchmans Cap work has not been done in isolation but is part of a study of the structure and reinterpretation of the entire Tyennan region and the northwest coast. The results and understanding developed from this work will be included in other reports.

All structural attitude data mentioned in the text are with respect to True North unless otherwise indicated as magnetic.

All new structural data collected as part of this study are included as Tabulated data in Appendix 1.

1.2 Geology/Litho-tectonic units

The Frenchmans Cap region extending to the Franklin River consists of high-grade schist, quartzite, and low-grade dolomitic schist to phyllite (Duncan, 1974). Quartzite caps the ridges, dolomitic phylllite generally occupies the valleys and the high-grade schists crop out to the west of Frenchmans Cap (Figure 1).

The sequence consists of west-dipping, stacked sheets with the high-grade schists (Ltug) at the highest structural level to the west, overlying quartzite (Lts) and the underlying low-grade dolomitic schist to phyllite (Ltpd) at the lowest structural level to the east (Figures 3 and 4).

There is a conformity or sub-parallelism of foliations within and between the different units (Duncan, 1974), such that these units (sheets) are essentially "welded" together by deformation during emplacement along high-strain interfaces. The contact between the quartzites and the underlying dolomitic schist and phyllite has, however, been overprinted by brittle faulting (see fault trace in Figure 1).

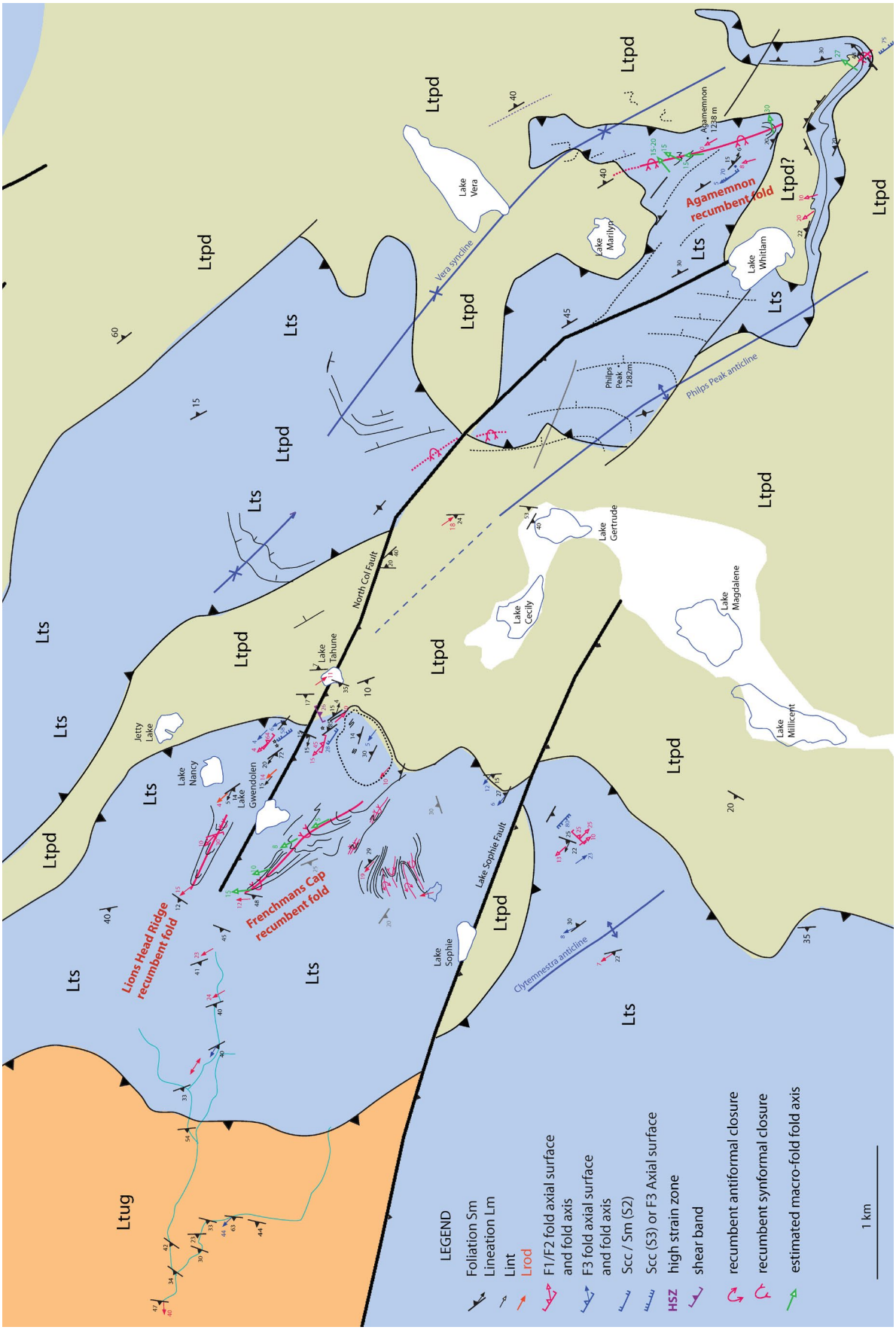

Figure 4. Structural summary map of the Frenchmans Cap area. The map base has been modified from the Mineral Resources Tasmania 1:250,000 Digital Atlas Series using structural data and observations from Duncan (1974, 2021) and those collected by the authors. Two main areas of quartzite (blue) include the Clytemnestra-Frenchmans Cap ridge domain on the west, and the Agamemnon-Philps Peak - Pine Knob domain on the east.

Ltug: high-grade schist (orange); Lts: quartzite (blue); Ltpd: low grade dolomitic schist/ phyllite (khaki).

Two outcrop belts of quartzite are separated by the glacial Livingstone Valley and referred to as the Clytemnestra-Frenchmans Cap domain in the west and the Agamemnon-Philps Peak-Pine Knob domain in the east (Figure 4).

The minimum apparent thickness of the quartzite sheet is ~300m.

Minimum thickness estimates at four geographic locations were calculated using the difference between maximum elevation at the location and the elevation of the contact (or inferred contact) with the underlying dolomitic schist.

1. Frenchmans Cap quartzite cap has an apparent structural thickness of 286m (1446m- 1160m: see Figure 11)
2. Clytemnestra quartzite cap apparent thickness is on the order of 220m-210m (north side 1271m - 1050m: 221m, whereas south side of ridgeline: 1271m-1060m: 211m)
3. Agamemnon quartzite cap apparent thickness estimates are from 240m to 280m (with north side 1238m-1000m: 240m and south side 1238m- ~950m: 280m)
4. Philps Peak quartzite cap ranges from 320m to 280m (west side 1282m-960m break in slope: 320m and north side: 1282m- 1000m: 282m).

1.3 Major Structural elements

Major structural elements in the area include:

1. Regional-scale, recumbent isoclinal fold structures:
   southwest-closing Frenchmans Cap (+Lions Head ridge) recumbent fold;
   east-closing Agamemnon recumbent fold;
2. Major open, upright fold structures:
   Vera Syncline;
   Philps Peak Anticline;
   Clytemnestra Anticline;
3. Thrust Fault contact between quartzite and dolomitic phyllite;
4. Steep Reverse/Strike slip Faults:
   North Col Fault;
   Lake Sophie Fault.

Analysis of photos taken on the ground and from the helicopter has enabled reconstruction of the macro-fold geometry (Figure 5). The reconstructed fold forms show the large-scale regional folds are aligned about the regional stretching direction (defined by the mineral elongation lineation in the quartzite). Within the axial surface envelopes the individual macro-folds show fold axis plunge and plunge direction changes along their fold lengths. Hinge-lines have curvilinear form and approach sheath form, particularly the Agamemnon recumbent fold.

The recumbent folds tend to taper towards their lateral-growth terminations with narrowing of hinges and approaching reclined geometry. Such changes in fold form and hinge curvature for the Frenchmans Cap recumbent fold require outcrop-truncation at South Col and with the Agamemnon recumbent fold truncation at Lake Vera.

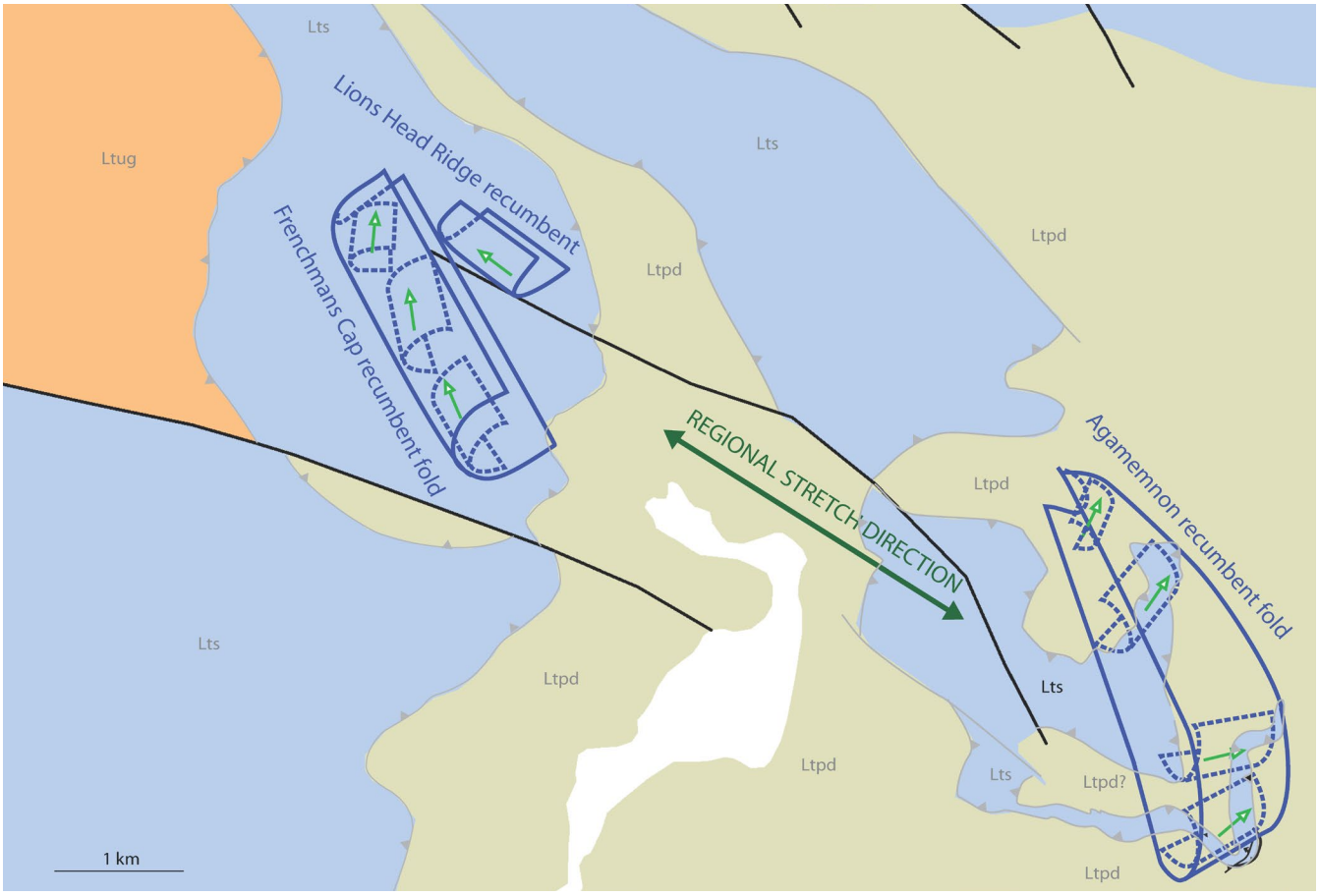

Figure 5. Geometry of the regional Frenchmans Cap, Lions Head Ridge and Agamemnon recumbent folds. These are large-scale recumbent isoclinal folds.

Given the apparent termination within quartzite outcrop belts, and the implied preserved geometry approaching half-sheath form (particularly for the Agamemnon recumbent fold) it is possible that the original recumbent fold length scales were in the order of 5-6 km. Current fold trace length scales are ~1.5 km and ~3 km for the Frenchmans Cap recumbent fold and Agamemnon recumbent fold respectively.

1.4 Nature of the Layering, Foliations and Lineations

Quartzites in the Frenchmans Cap region show high-strain fabrics typified by strong to intense foliation and transposition layering/foliation (Sm), rodding fabrics within the transposition layering, mesoscopic isoclinal folds, rootless isoclinal fold pairs, and multiple crenulation cleavages (Figure 6).

There are five types of layering and foliation (Figure 6):

1. So/Sm: compositional banding sub-parallel to a strong to intense foliation that has undergone recumbent isoclinal folding;
2. Intense foliation (dominant Sm) that is axial surface to the major recumbent isoclinal macro-folds. It is also the regional foliation that envelopes macro- to meso- fold "pods" at all scales up to the scale of the Frenchmans Cap recumbent isoclinal fold. This foliation is commonly associated with a marked rodding fabric.
3. Crenulation cleavages (Scc) associated with the development of transposition layering in the basal high-strain zones, or lower limb of recumbent folds.
4. Shear Band (S-C') foliation (Sb) as a form of extensional crenulation cleavage that reflects shear-induced, foliation-oblique late-stage flattening. These zones essentially secondary shear zones that record the overall shear sense and/or emplacement direction.
5. Spaced cleavage (Scl) a younger Devonian cleavage that overprints all three foliations listed above.

There are four types of lineations:

1. A mineral lineation (Lm) generally defined by mica and/or elongated quartz grains in the quartzite.
2. An elongation or stretching lineation (Lelong) most commonly shown by elongated quartz grains.
3. A rodding lineation (Lrod) that changes from an initial intersection lineation at high angle to the regional stretching direction, to a "herringbone" pattern where flattened mesoscopic fold hingelines become curvilinear and pulled apart, to eventually develop a strong, sub-parallel alignment with the regional stretching direction (Lstretch).
4. A crenulation lineation (Lcren) as tiny puckers or wrinkles within the foliation.

These fabrics, lineations and relationships are shown as insets in a structural profile through Lions Head-Frenchmans Cap-Clytemnestra (Figure 6).

There is a distinct structural zonation through the quartzite to the underlying high-strain contact with the dolomitic phyllite/schist. At outcrop-scale this is further subdivided into a zone of intense transposition layering/foliation immediately above the contact (Figure 6).

1.5 Orientation/Attitude Relationships of Structural Elements

The general relationships are shown in Figures 7 and 8 based on limited field measurement data collected during the helicopter sortie day trip. The stereonet plots show the dominant NW trend of most structural elements. These structural data are tabulated in Appendix 1.

Macro-Folds

- The Frenchmans Cap recumbent fold has a gentle (<15°) NNW plunge with a plunge direction varying by 30° from 320° to 350°. The great circle best fit to the fold axis range is 262°/12°N (Figure 8a).
- The Agamemnon recumbent fold has a moderate fold plunge (15°-25°) within a ~90° plunge direction range of 355° to 085°. The great circle best fit to the fold axis range is 332°/23°NE (Figure 8d).

Mesoscopic Folds

- Meso-folds associated with the Frenchmans Cap recumbent fold show gentle plunges (<13°) and a range of plunge directions of ~15° from 305° to 320° (Figure 8b).
- Meso-folds on the lower limb of the Agamemnon recumbent fold have moderately to steeply dipping north-south trending axial surfaces (Figure 8e).

Mineral Lineation

- Lm for the Frenchmans Cap domain shows a gentle plunge (<25°) and a plunge direction range of ~30° from ~300° to 330° (Figure 8c)
- Limited data for the Agamemnon domain gives an Lm plunging 12° towards 124° (Figure 8f)

Rodding Lineation

- Lrod for the Frenchmans Cap domain has a gentle plunge (<20°) and a ~315° to 320° range in plunge direction (Figure 8c).

1.6 Relationships between Fold Axes and The Regional Stretch Direction

Relationships between the mineral lineation (Lm), the rodding lineation (Lrod) and fold axes (FA) can be used to deduce the position of macro-fold hinges and help map out axial surface traces (see Alsop & Holdsworth, 1999). Lm is treated here as the regional stretching direction (Lstretch), as it is observed parallel to the quartz-grain elongation direction (Lelong) in some quartzites and to the X-direction when other strain markers are available. The rodding direction, as an intersection lineation (Lint), tracks the fold axis orientation but develops an irregular "herringbone" pattern when flattened, mesoscopic sheath-folds with markedly

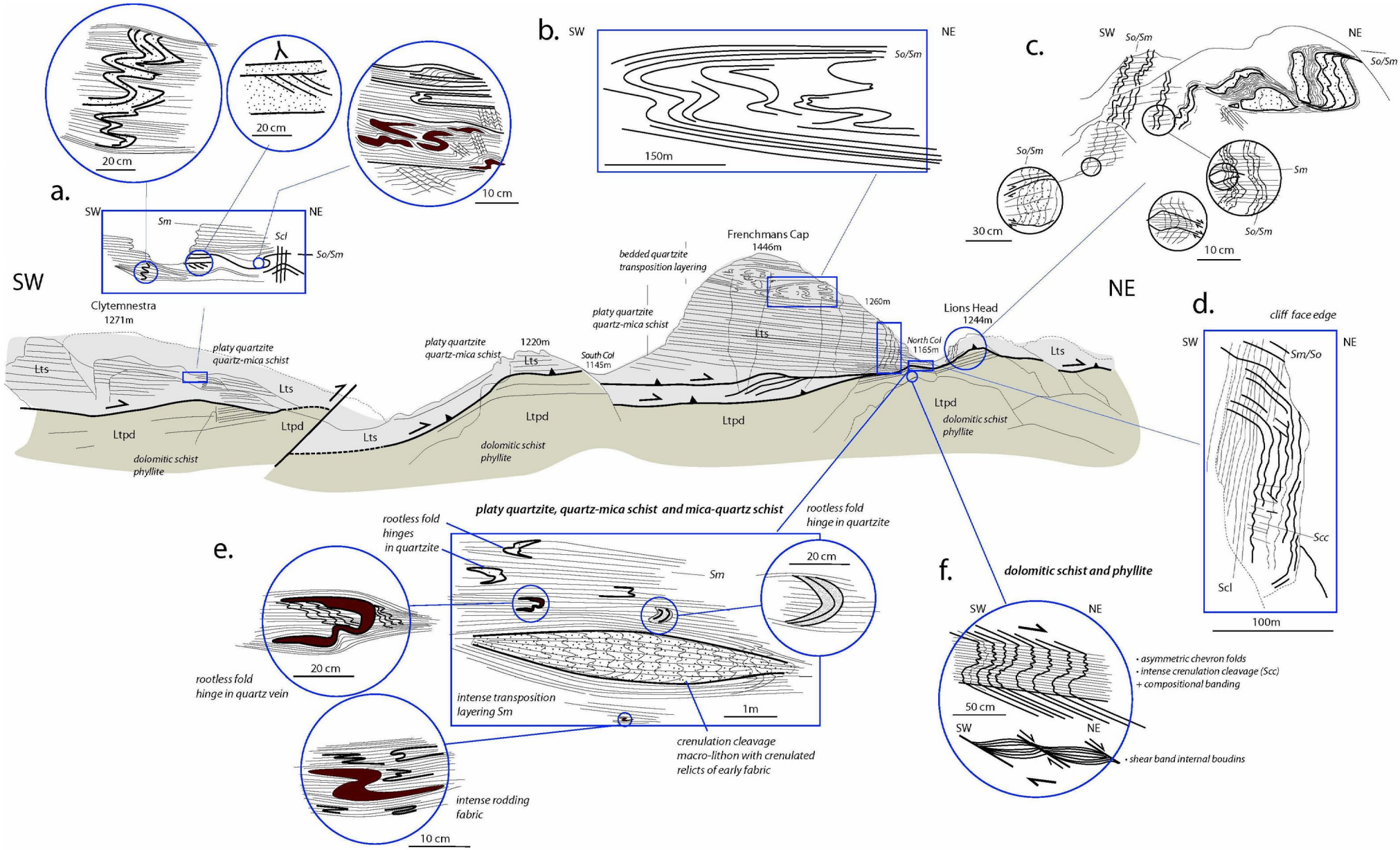

Figure 6. Clytemnestra - Frenchmans Cap structural profile showing the regional and local structural relationships and fabrics. a) Clytemnestra fabrics and structural relationships. b) Recumbent isocline geometry in the Upper Folded zone on east Wall of Frenchmans Cap. c) Fabrics and structural relationships at Lions Head (NW end exposure). d) Structural relationships on the NE wall, cliff edge track to Lake Tahune. e) Fabrics and meso-scale structure of the basal zone to the quartzite sheet (Intensely Foliated Transposition Zone). f) Fabrics and structural relationships in the upper part of the dolomitic schist -phyllite near the contact with the overlying quartzite sheet.

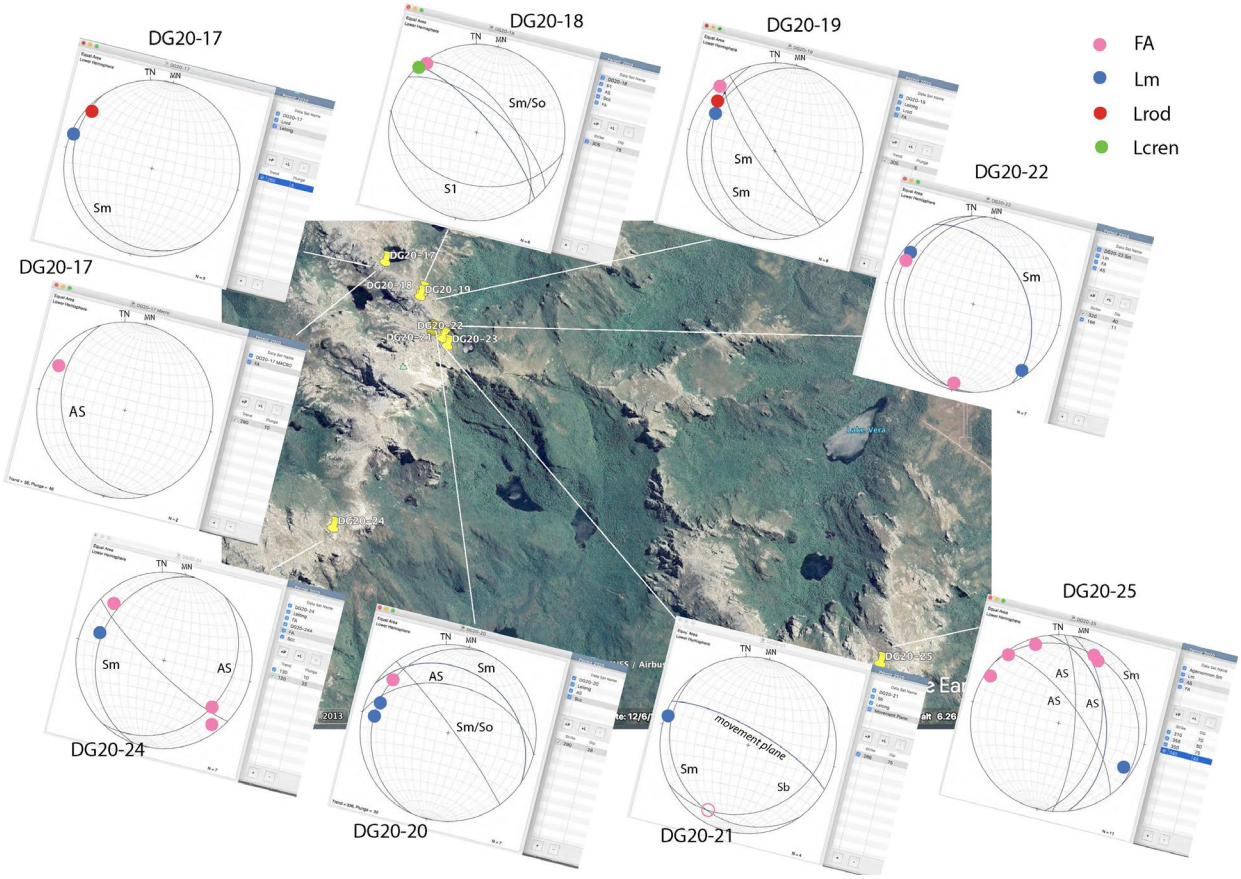

Figure 7. Structural data collected at Lions Head Ridge, Frenchmans Cap NE wall, Clytemnestra and Agamemnon plotted in stereonet form.

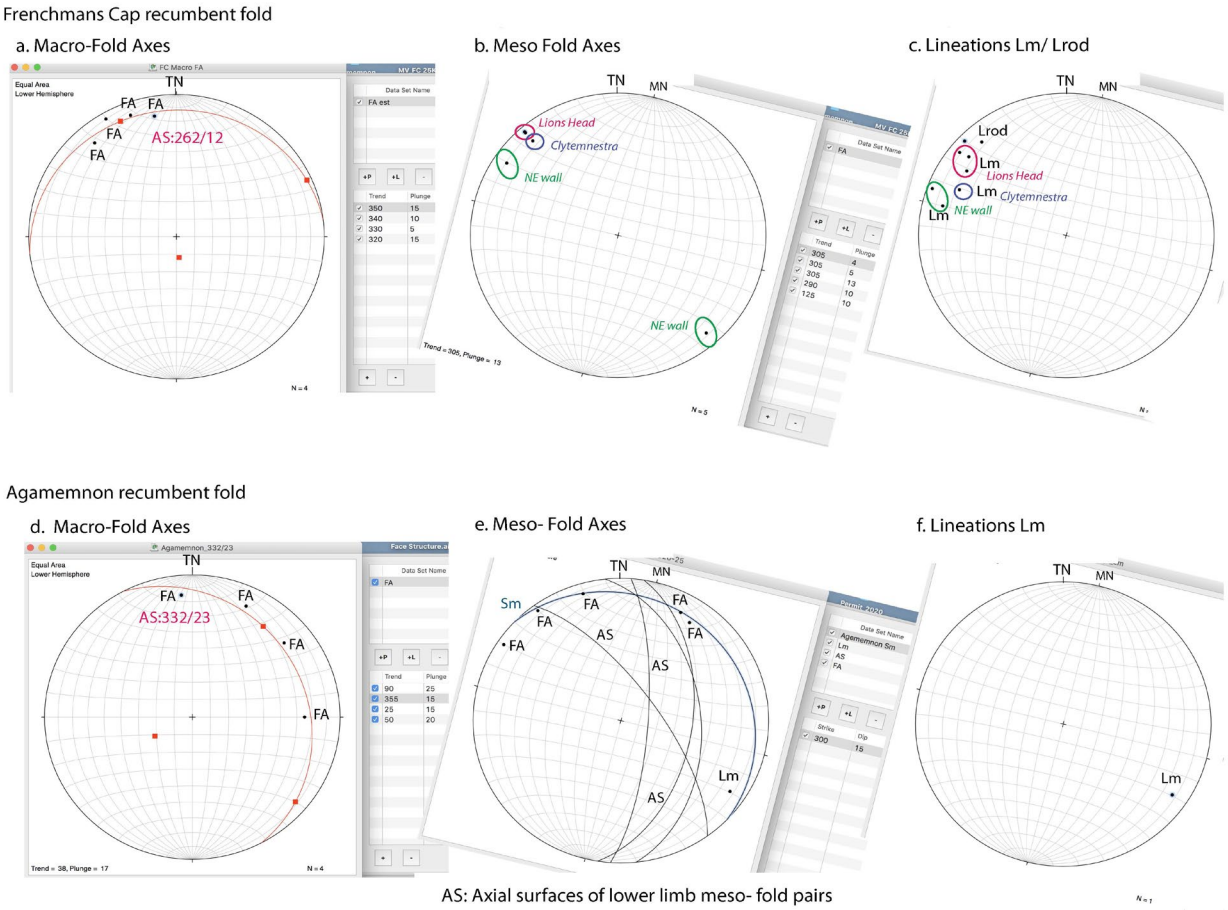

Figure 8. Stereonets showing estimated fold axis data for Frenchmans Cap (top row) and Agamemnon (bottom row) recumbent folds. Frenchmans Cap recumbent fold: a) Calculated macro-fold axes, b) Measured mesocopic-fold axes, and c) Mineral (Lm) and rodding (Lrod) lineation data. Agamemnon recumbent fold: d) Macro-fold axes, e) Measured mesoscopic fold axes, and f) Lineation Lm data for the fold lower limb.

curved hinge-lines develop. This occurs with increasing shear strain and shear-induced flattening in Sm. Alsop & Holdsworth (1999) noted that with curving hinge-lines typical of conical to sheath-like macro-folds the rotation direction changes across the axial surface trace in map view.

In the Frenchmans Cap region, mesocopic fold axes and the rodding lineation (Lrod) in quartzites from both the western Clytemnestra-Frenchmans Cap domain and in the eastern Agamemnon-Philps Peak-Pine Knob domain, show consistent clockwise rotation from Lm, or require counter-clockwise rotation of the FA towards Lm (Figure 9). This indicates the quartzite in both domains occurs on the same limb of a regional structure(s). With respect to each of the recumbent folds the hinges and lower limb are preserved, whereas the upper limbs have been eroded away. The implication is that the counter-clockwise relationship of fold axes to Lm reflects the lower-limb relationship for these recumbent folds. Upper limbs, if preserved would show a clockwise rotation sense.

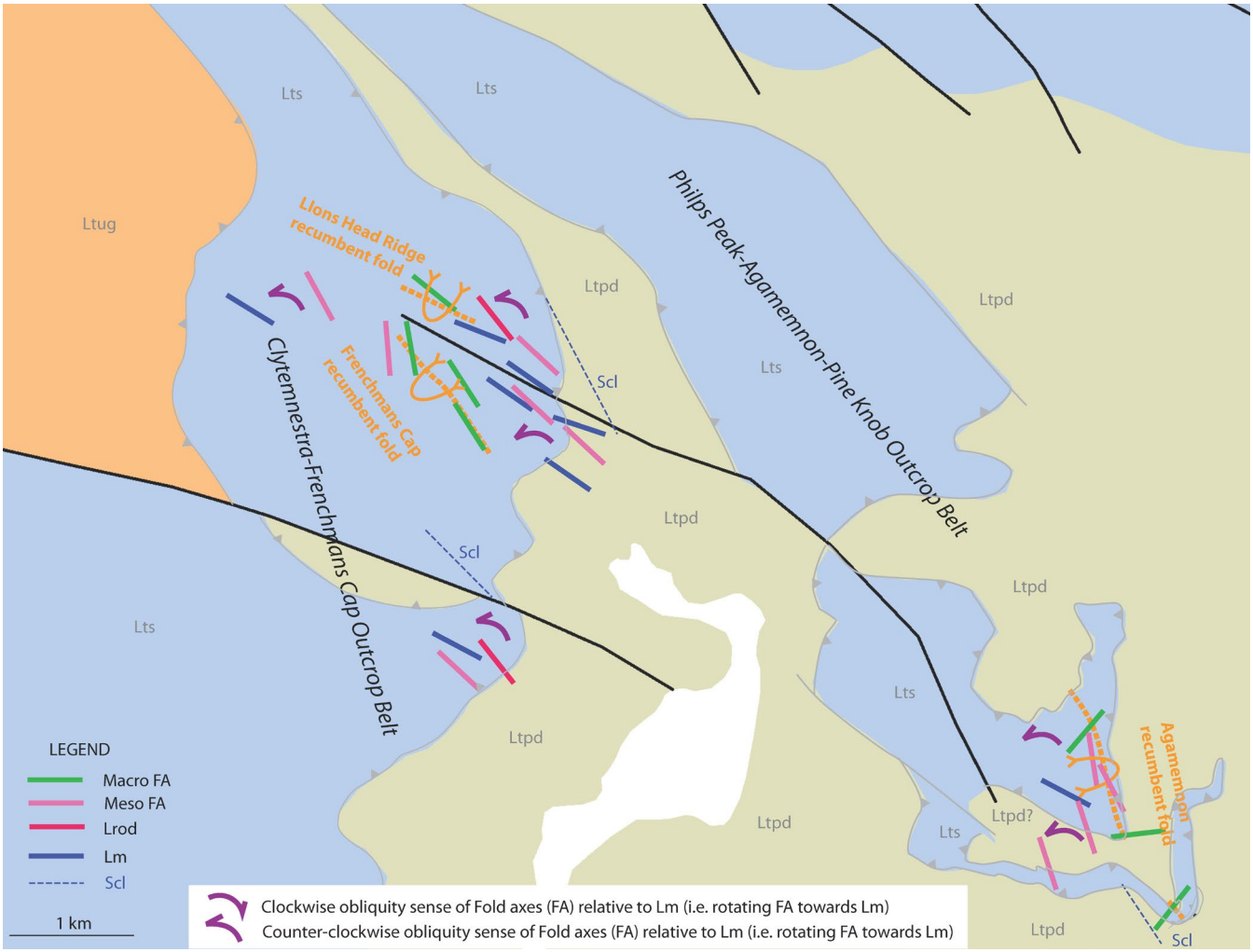

Figure 9. Frenchmans Cap region summary relationships between mineral lineation (Lm: dark blue lines), mescoscopic fold axes (FA: pink lines), axes of macro- or large-scale folds (FA: green lines), rodding direction (Lrod: red lines). The rotation direction (purple semi-circle with direction arrow) is defined by rotating the fold axis (FA) and/or Lrod towards the lineation Lm by closing the acute angle between them.

2. Using Frenchmans Cap faces to elucidate macro-structural geometry.

Interpretation of the structural geometry was made by examining all the faces of the peak of Frenchmans Cap as well as the walls of glacial cirques and cirque valleys extending from the main peak (Figure 10) using digital photographs taken from a helicopter.

A structural interpretation was made for each face of Frenchmans Cap peak (see Figures 11, 12, 13 and 15). Interpretation of the different faces posed different problems but all faces are variably fractured and jointed. There is also an overprinting younger Devonian sub-vertical cleavage (Scl). The southeast and east faces are mostly in shade, appear stained and/or with biological growths such as lichen, but provide a profile view of the fold structures in the upper folded zone or cap (Figure 14). Structural interpretation was hindered by photograph image resolution in some instances.

2.1 Quartzite Sheet Structural Zonation

The imposing northeast face visible from Lake Tahune (Figure 11), and the east and southeast faces visible from Barron Pass expose the maximum vertical section

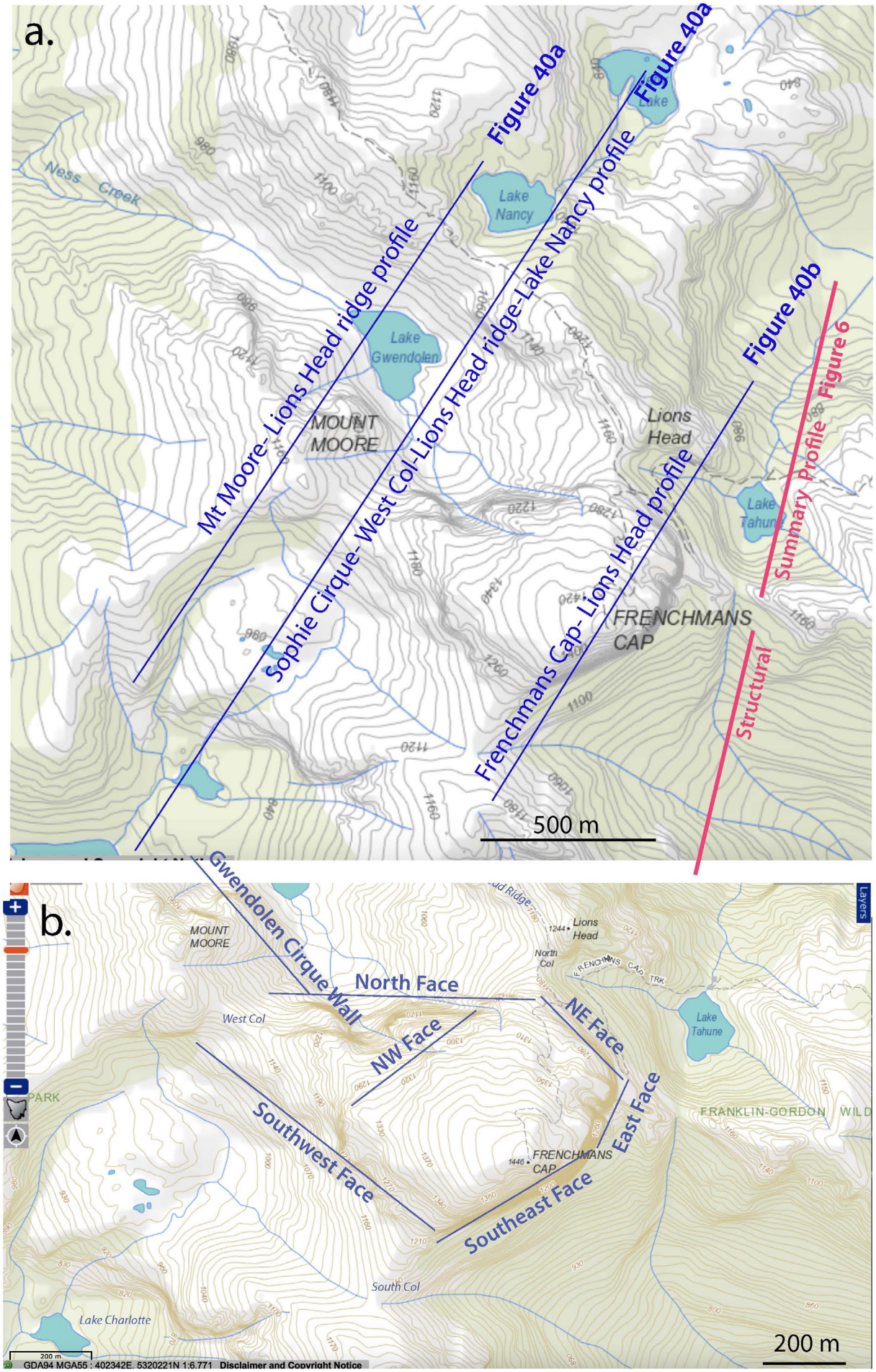

Figure 10. Frenchmans Cap topographic map with geographic elements. The base map is a Tasmanian ListMap topographic map. a) Positions of structural profiles including the schematic profile shown in Figure 6 (red line) and the structural profiles in Figure 40 (blue lines). b) Map Enlargement showing the Frenchmans Cap face delineation. These faces and other geographic features are referred to in the text.

through the quartzite and show three structural zones:

1. An upper zone with recumbent macro-isoclinal folds in apparent “bedding”;
2. A middle strongly foliated zone with mesoscopic isoclinal folds within transposed layering; and
3. A lower, intensely foliated, zone overprinted by brittle faulting above the faulted contact with the underlying dolomitic schist/phyllite (Ltpd).

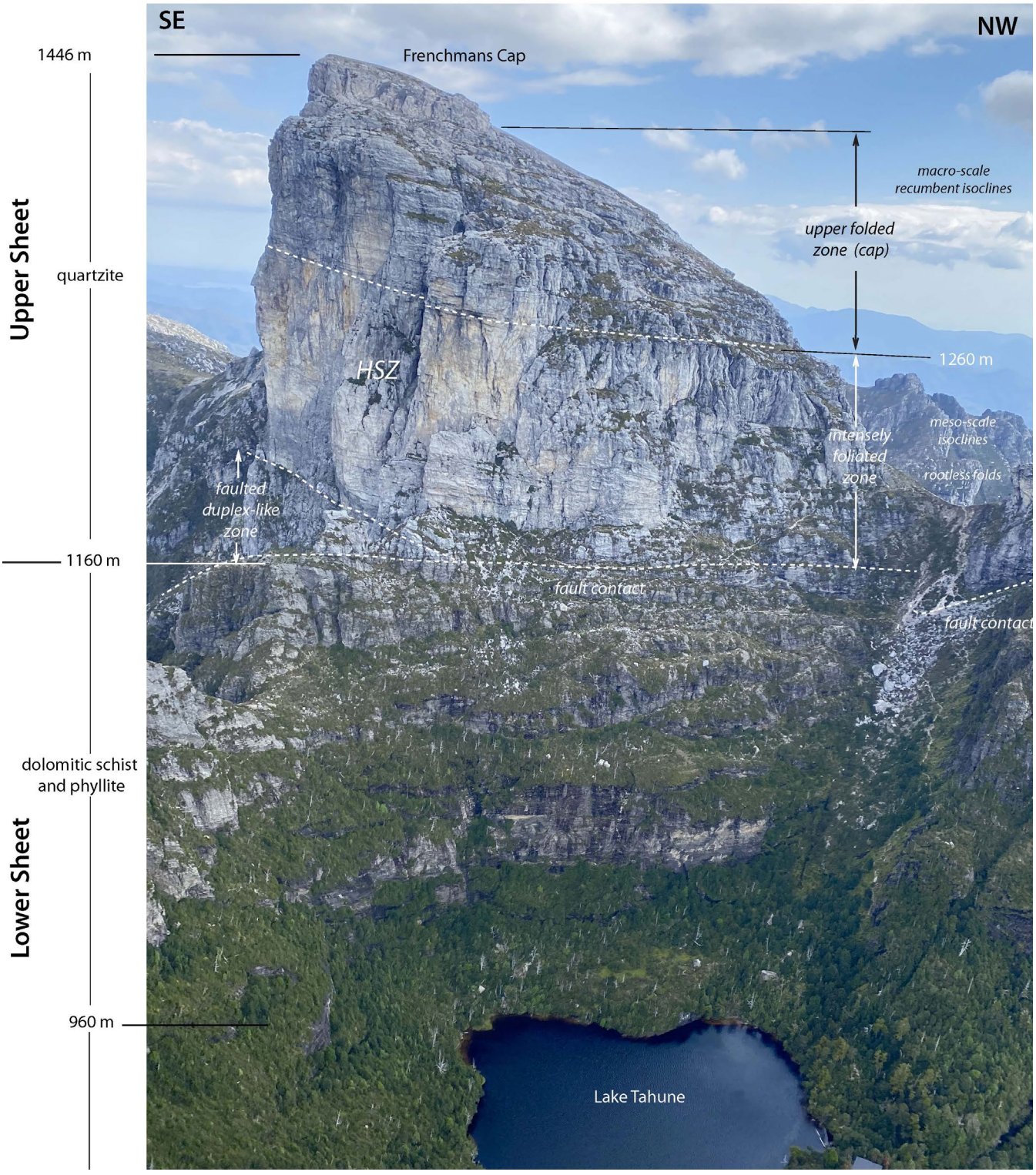

Figure 11. Structural zonation and changing structural character through the quartzite to the underlying dolomitic schist/phyllite from the top of Frenchmans Cap (1446m) to Lake Tahune (960m) over 500m of structural relief.

2.1.1 Upper Folded Zone

Folds in the upper folded zone are best observed in the east-south east face (Figure 12a) and the high northwest face (Figure 12b). These faces show the positions and geometry of the larger-scale recumbent, isoclinal hinges in the upper folded domain. In the east face the dominant recumbent isocline is south-closing (Figure 12c), whereas in the northwest face the largest recumbent fold is north-closing (Figure 12d). The north face provides linkage between the fold structures in the opposing southeast and northwest faces. The face shows apparent fold length-scales are on the order of tens of metres and not continuous over the exposed length of the Cap (Figure 13).

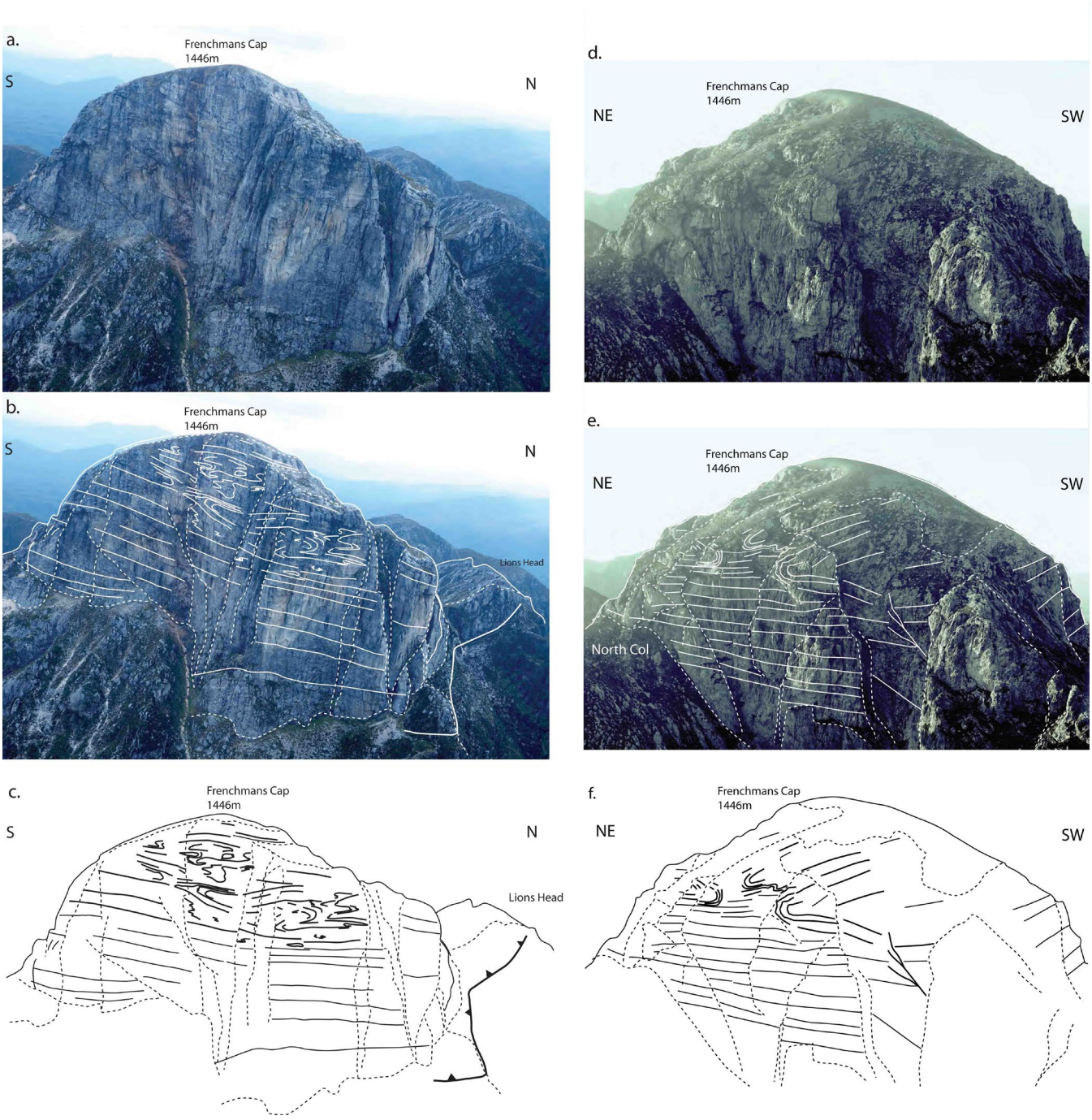

Figure 12. Aerial views of Frenchmans Cap with structural interpretations. a), b) and c) showing the east and southeast faces. d), e) and f) the northwest face from Lake Gwendolen valley. Middle row b) and e) show form-line interpretation on the face photographs shown in the upper row. Bottom c) and f) are line drawings of the faces with the form-line interpretation of So/Sm and Sm.

These structures and structural zonation are also visible on the northern face (Figure 13). The apparent convergence of the upper folded zone with the basal intensely foliated zone (HSZ) towards North col is due to a "cut-off" effect caused by the transgressive nature of a late brittle fault (see Section 4) to the high-strain zonation.

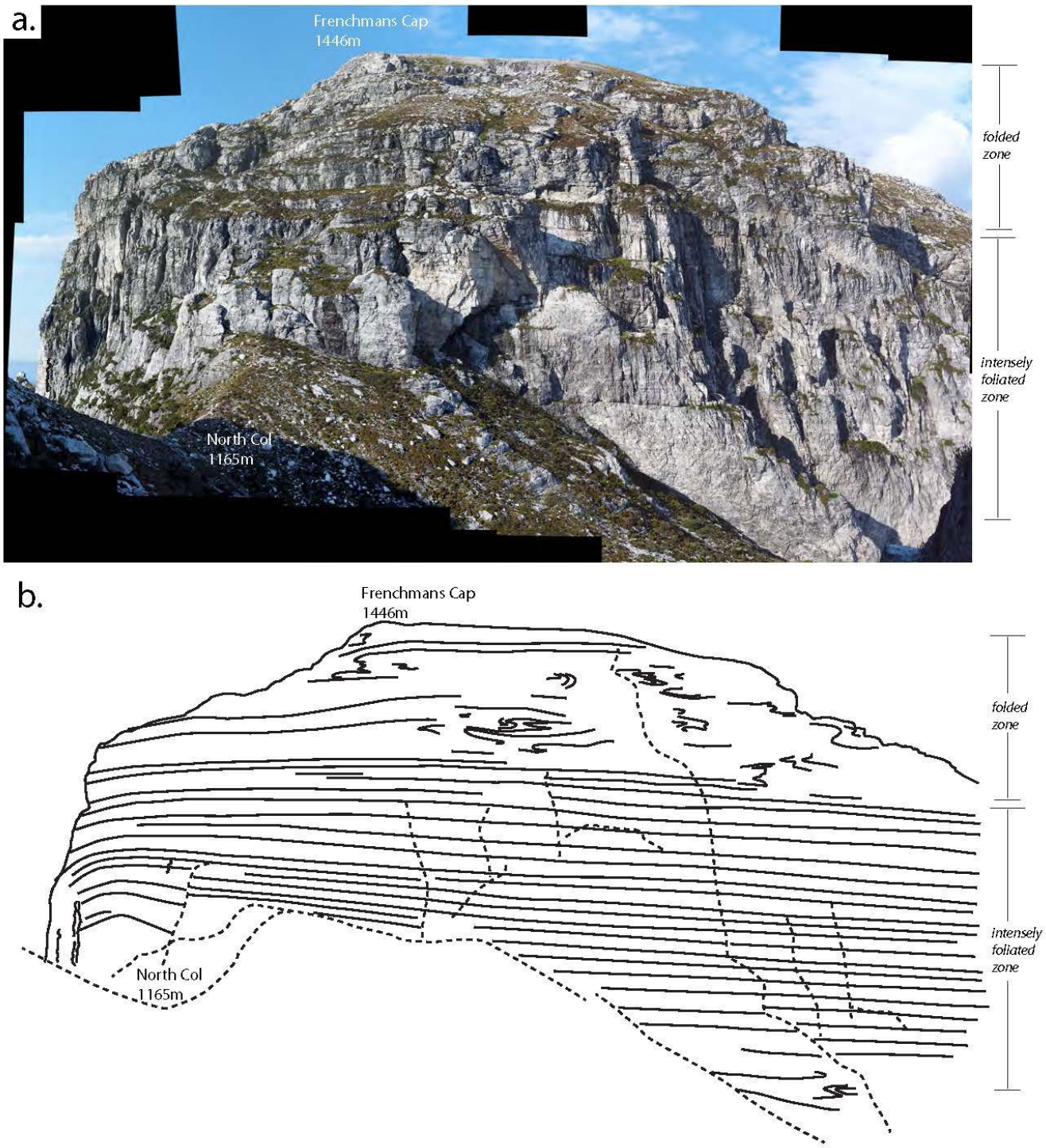

Figure 13. View of the north face of Frenchmans Cap from Lions Head Ridge. Note the domains of isolated isoclinal fold hinges in the upper folded zone.

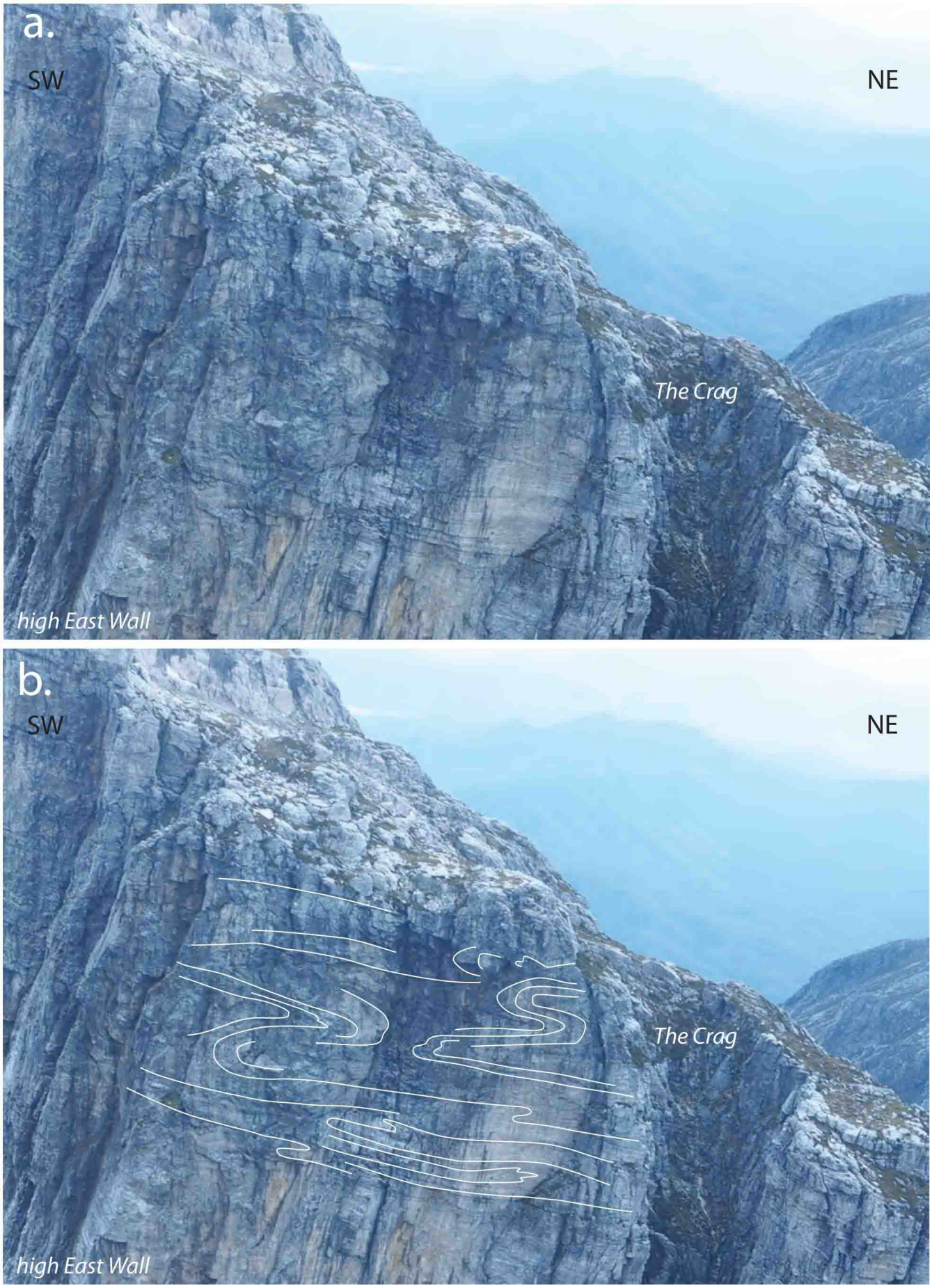

Figure 14. Fold closures on the high east wall within the Upper Folded zone. a) Non-annotated photo shows the difficulty in fold definition and structural interpretation due to a strong jointing and younger cleavage overprint, as well as surface colouration changes due to weathering and black lichen growth. b) form-line interpretation of So/Sm showing recumbent isoclinal fold closures.

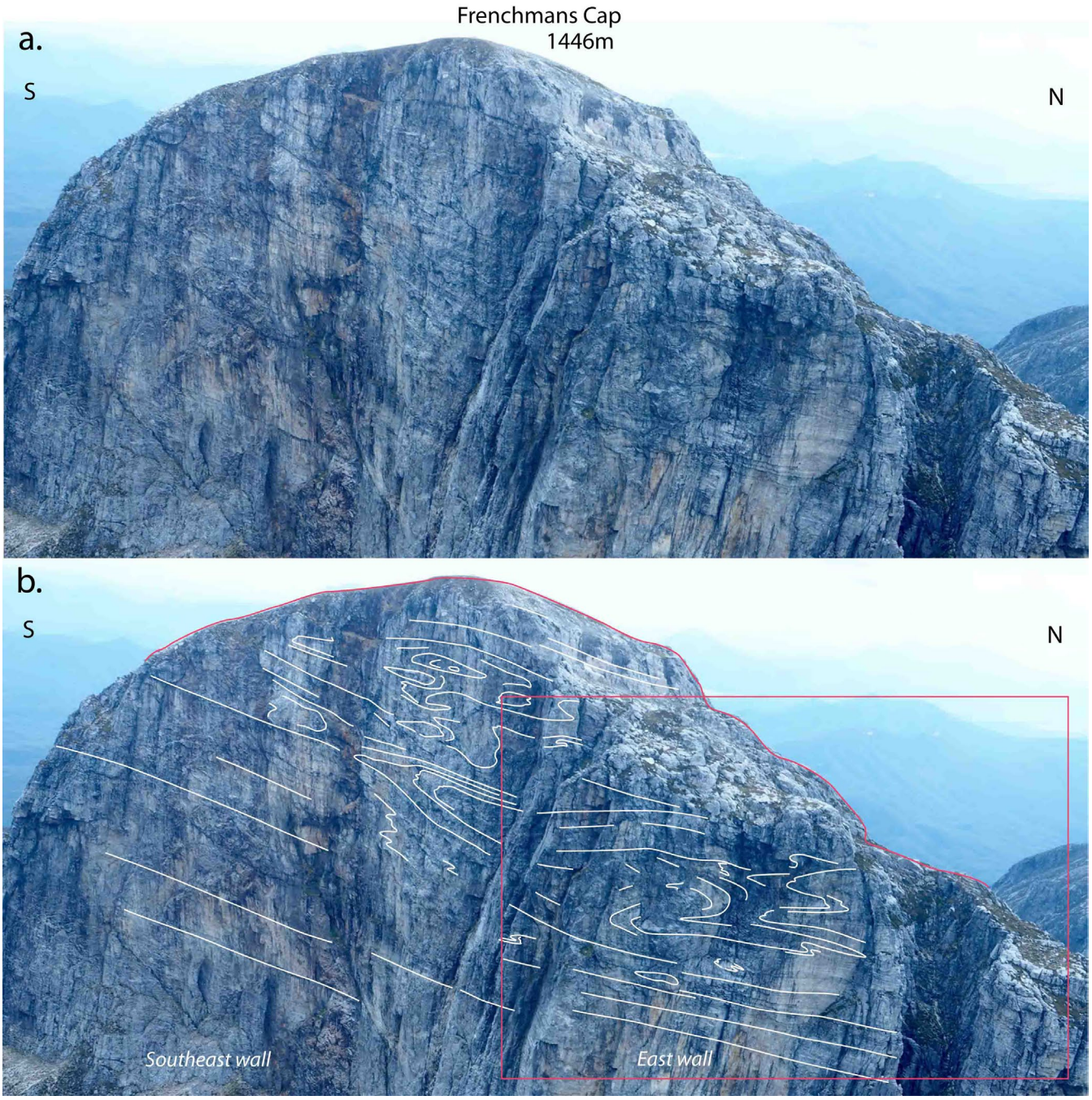

Figure 15. The Upper Folded zone of Frenchmans Cap. a) Phoptograph of southeast and east faces. b) Interpretation of the faces shown in a) with form-lines outlining the bedding/transposed layering So/Sm. The red box is that area shown in Figure 14.

2.1.2 Middle Strongly-Foliated Zone

The Middle Strongly-Foliated zone occupies most of the wall extent of Frenchmans Cap in the northeast and north faces (Figures 11 and 13). From a distance it appears as a "uniformly" foliated zone with little or no apparent structure. At the outcrop-scale, bedding So/Sm is present with a strong younger Devonian cleavage overprint (Scl: Figure 16). In this zone no large-scale recumbent isoclinal folds have been observed and the So/Sm foliation is overall sub-horizontal across most the faces of Frenchmans Cap (Figures 11, 13 and 14). Small-scale, mesocopic recumbent isoclines occur within Sm.

There is a rollover in So/Sm in the northeast wall suggesting presence of a large-scale north-closing recumbent closure (see northeast end of Frenchmans Cap-Lions Head profile in Figure 6). Such a closure is also supported by the So/Sm relationship in the adjacent Lions Head ridgeline exposures (Figure 17a, b, 18, and 19). Axial surfaces of the mesoscopic folds in the So/Sm are gently northeast-dipping and appear consistent from the wall exposure in the northeast face (Figure 16) through North Col to the Lions Head ridgeline (Figure 17 and 18) and Lions Head (Figure 19).

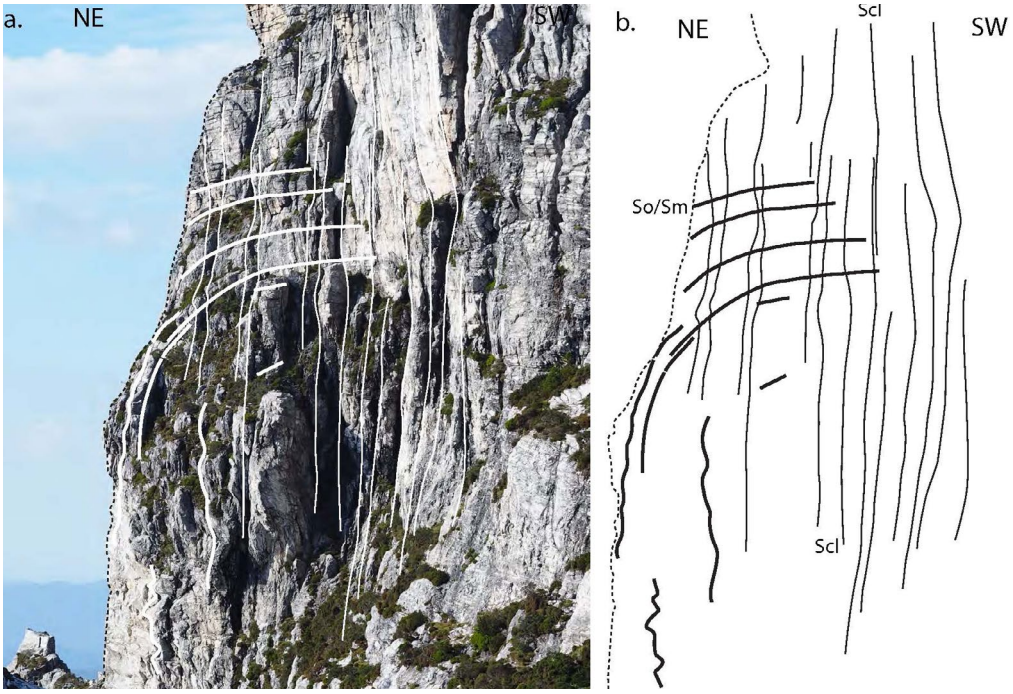

Figure 16. Middle Strongly-Foliated Zone exposed in the northeast wall of Frenchmans Cap (observed from the track below North Col looking to the southeast). Bedding So/Sm is highlighted by the thicker black lines in the interpretation. (b). Note the rollover in So/Sm and the steeply dipping limb in So/Sm apparent along much of the northeast wall. The significance of this geometry is discussed in Section 5.1.1. Scl: younger Devonian cleavage overprint.

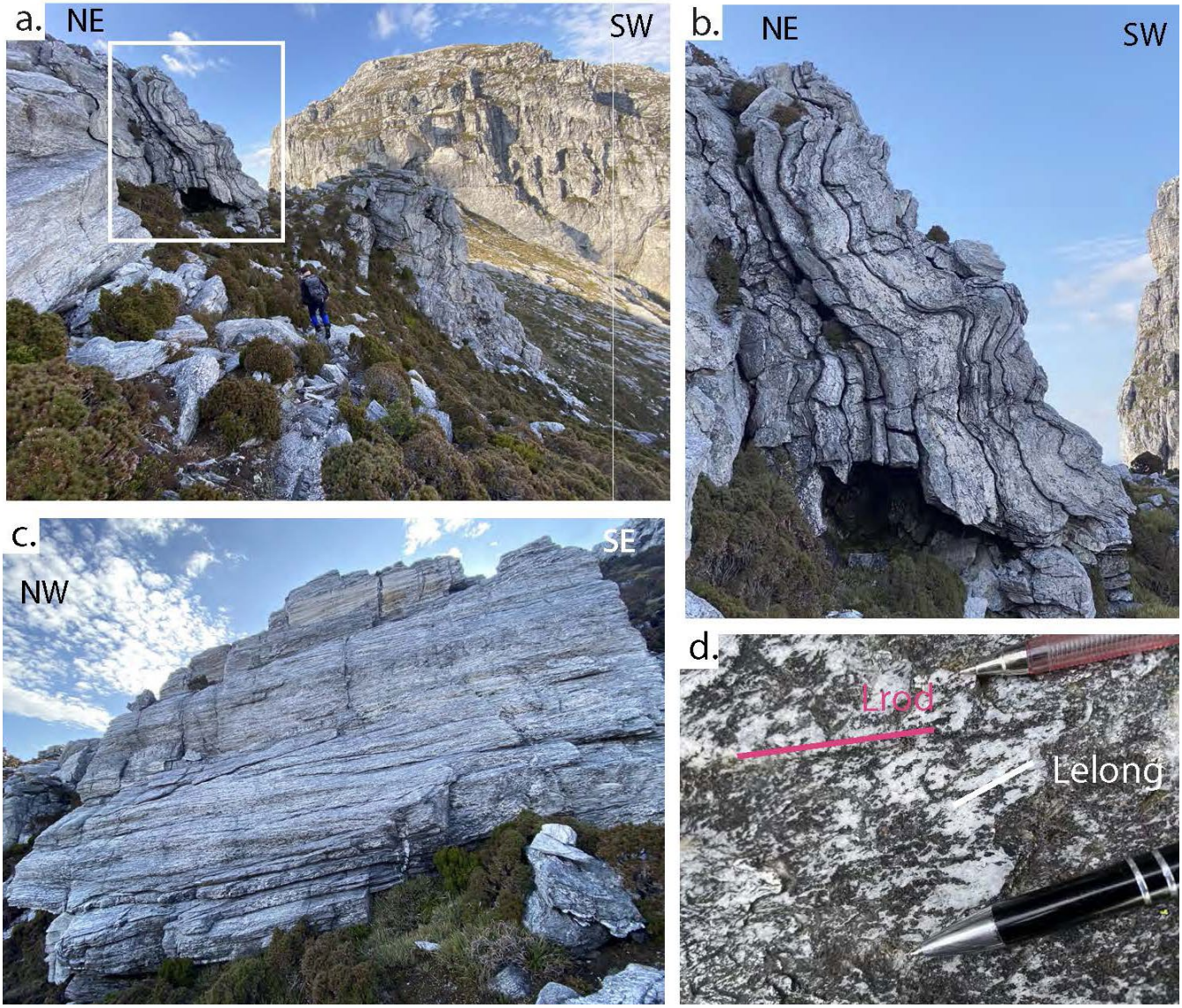

Figure 17. Bedding/Compositional Banding (So/Sm) character in outcrops, southwest side of Lions Head Ridge. a). Dipping compositional banding/transposition layering (So/Sm) with a strong banding- parallel foliation. b) Enlarged part of a) showing the So/Sm banding folded by open folds with sub-horizontal axial surfaces. c) View of dipping layering surface showing a pronounced rodding lineation. d) View onto foliation surface from c) showing the mineral elongation lineation and the rodding lineation.

The rollover occurs within quartzite "layering" typical of the Middle Zone. It is a transposition layering (So/Sm) with a strong foliation sub-parallel to the bedding-like, compositional banding (Figure 17). This banding So/Sm contains a mineral elongation lineation (Lm) and strong to intense rodding (Lrod) within the layering/banding (Figure 17c, d). The lineations are sub-parallel and gently northwest-plunging (Figure 17d and Figure 18) and are sub-parallel to meso-fold hinges (FA : pink dots) and a crenulation lineation (Lcren) (Figure 18).

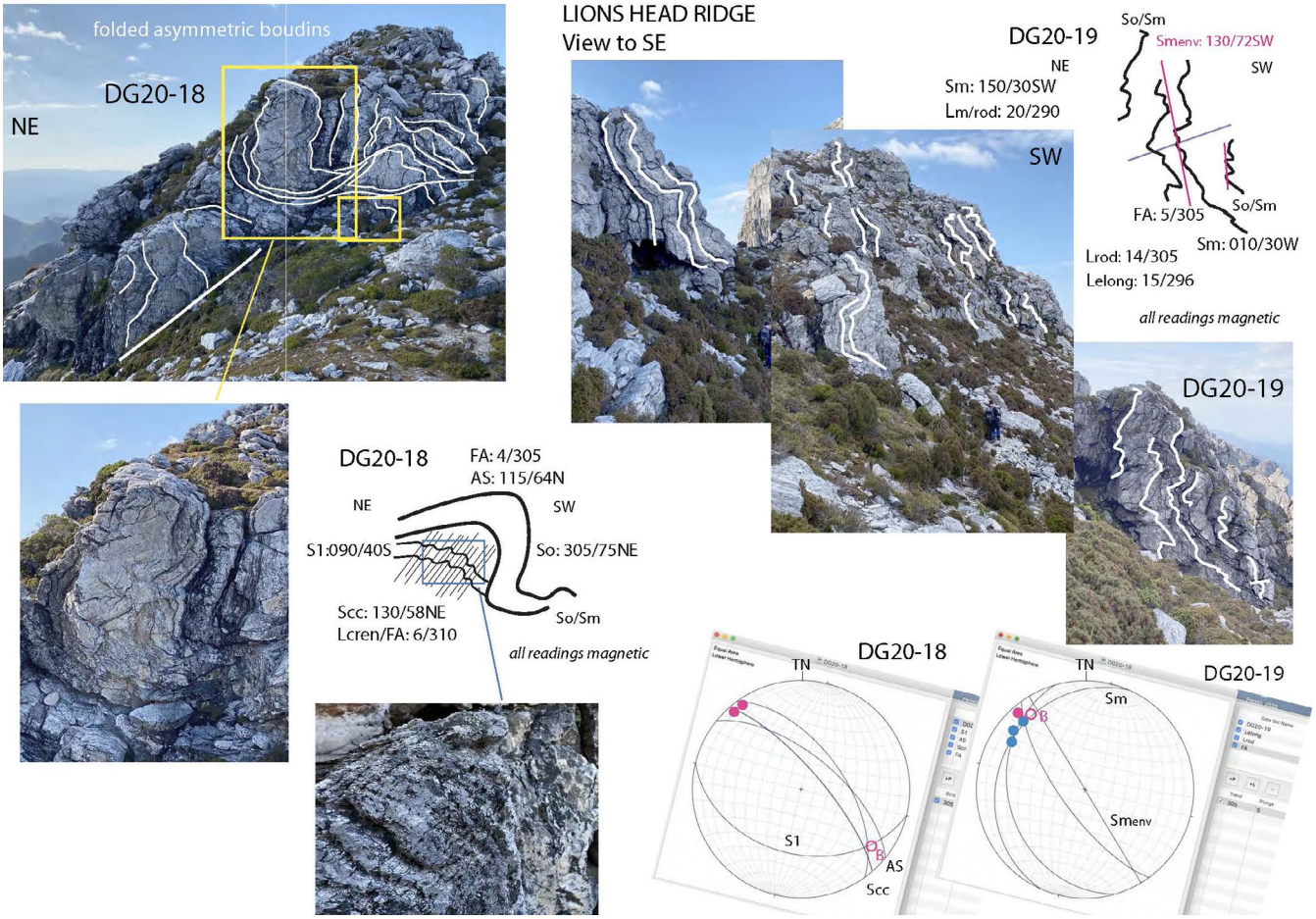

Figure 18. Composite photo profile on the Lions Head ridgeline showing the continued rollover of So/Sm from the northeast face of Frenchmans Cap (Figures 16 and 17a) across North col into Lions Head. The So/Sm shows metre-size, asymetric shear-band boudins (bottom left). Two sets of gently northwest-plunging coaxial folds refold the So/Sm. The fold axial surfaces of the first set are gently northeast-dipping (inset sketch for DG20-19) and are refolded by a set with moderate to steeply northeast-dipping axial surfaces and axial surface crenulation cleavage (Scc) (see inset sketch DG20-18). Stereonets show great circle traces for foliations S1, Sm and Scc. Fold axes (FA: pink dots) and lineations (Lm: blue dots).

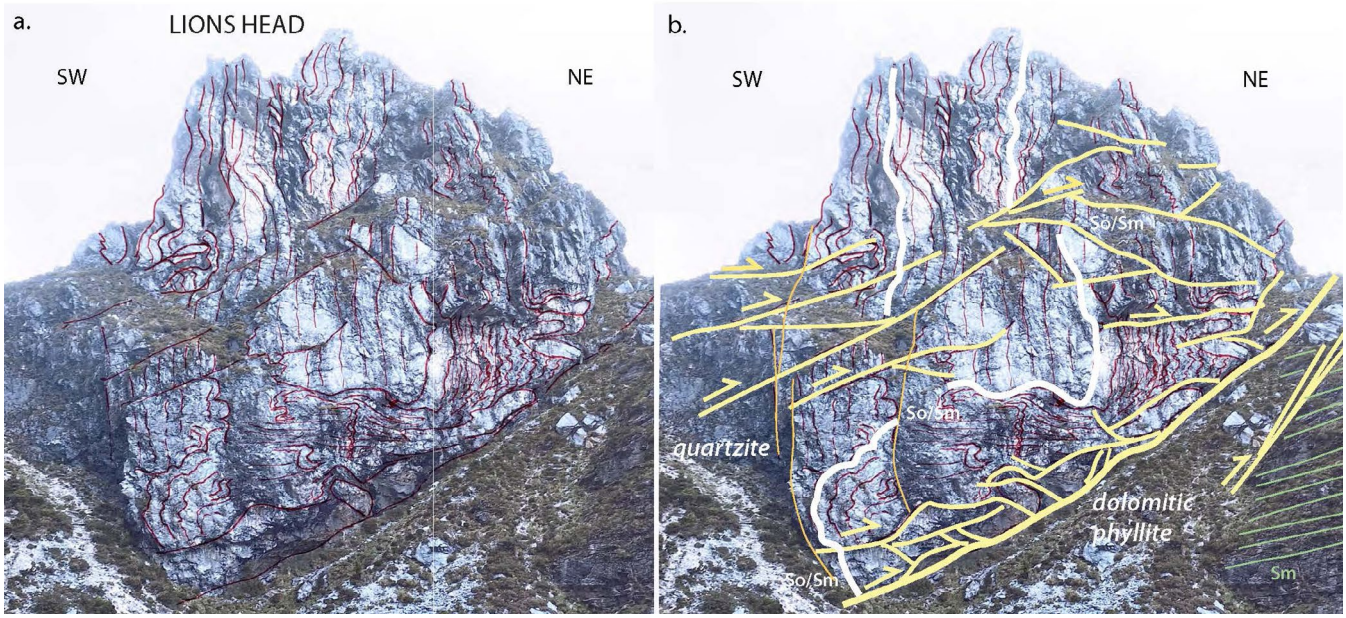

Figure 19. Structure of Lions Head. a) Lions Head viewed from the northeast face track to Lake Tahune. b) Formline interpretation of a). The dominant So/Sm layering is folded by folds with gently northeast-dipping axial surfaces (compare with composite photo profile in Figure 18, a view of the ridgeline behind Lions Head). White lines are So/Sm. Yellow lines are brittle fault traces that juxtapose the quartzite (hanging wall) in a southwest-over northeast sense over the dolomitic phyllite in the footwall (below the fault). Pale green lines (lower right) are foliation traces in the dolomitic phyllite. Thin orange lines are late, steep, sub-vertical faults with little or no apparent offset.

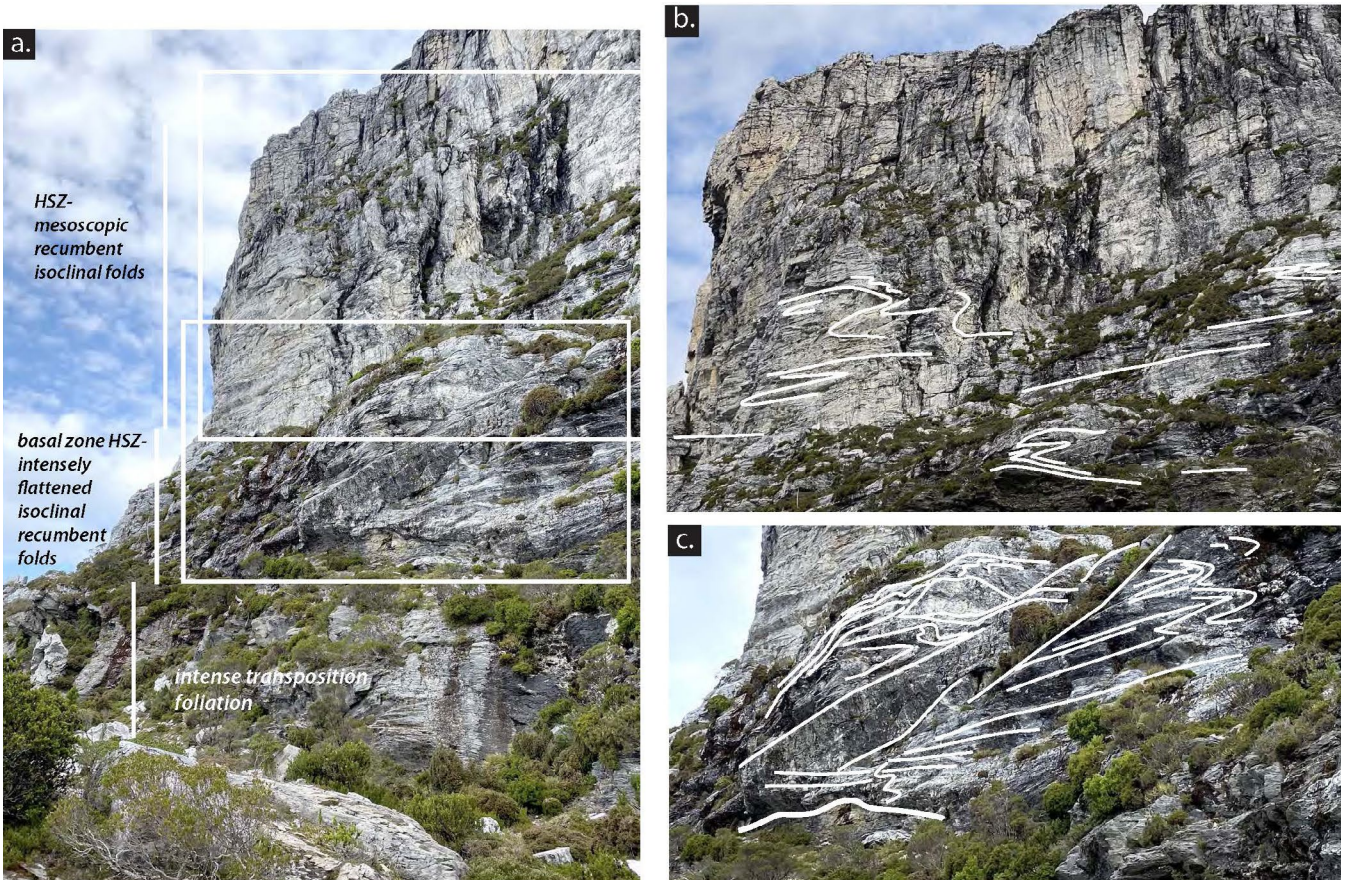

Figure 20. Mesoscopic recumbent isoclines visible in the northeast face of Frenchmans Cap. a) Northeast face photo showing the structural zonation with the upper part a high-strain zone (HSZ) with mesoscopic recumbent isoclinal folds, a middle zone with intensely flattened isoclinal recumbent folds transitional into a zone of intense transposition layering at the contact with the underlying Scotchfire dolomitic phyllite. The white boxes show the positions of enlargements b) and c). b) Enlargement of the upper part of the cliff. c) Enlargement of the lower part of the cliff showing an oblique view of isoclinal, recumbent folds cut bv brittle thrust/reverse faults. These folds become more attenuated towards the interface with the Zone of Intense Transposition Layering/foliation (see lower part of photo in a)).

The mesoscopic folds define a strain gradient into the basal high-strain zone of the quartzite sheet (Figure 20). These folds become more attenuated with flattened form (Figure 20c) towards the Lower Intensely-Foliated Transposition zone (see Figure 11).

2.1.3 Lower Intensely Foliated Transposition Zone

Strong to intense transposition layering/foliation dominates the lowest part of the quartzite sheet (Figures 21 and 22).

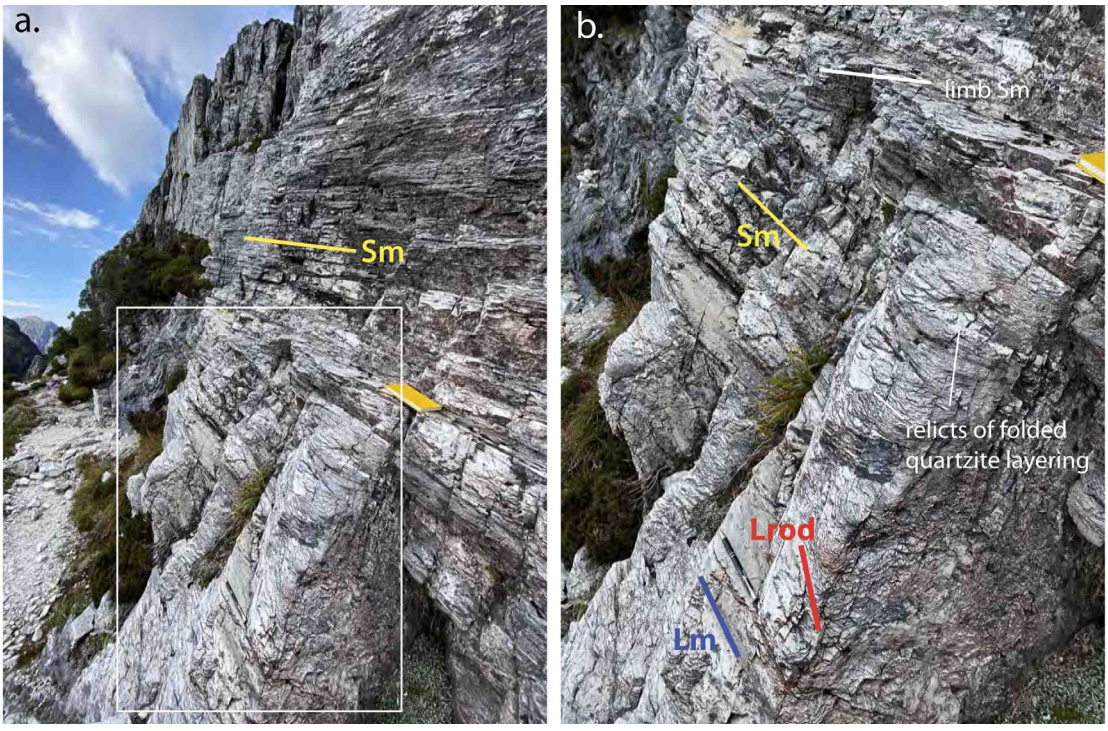

Figure 21: Intense transposition layering on Irenabyss Track near junction with Summit Track. View is to the southeast. a) View along northeast wall with Lake Tahune track shown on left side of photo. Relict folded quartzite layering is preserved as fragments within the dominant Sm. The foliation Sm surfaces show discordant mineral lineation (Lm) and rodding lineation (Lrod). b) Enlargement of the white outlined area in a).

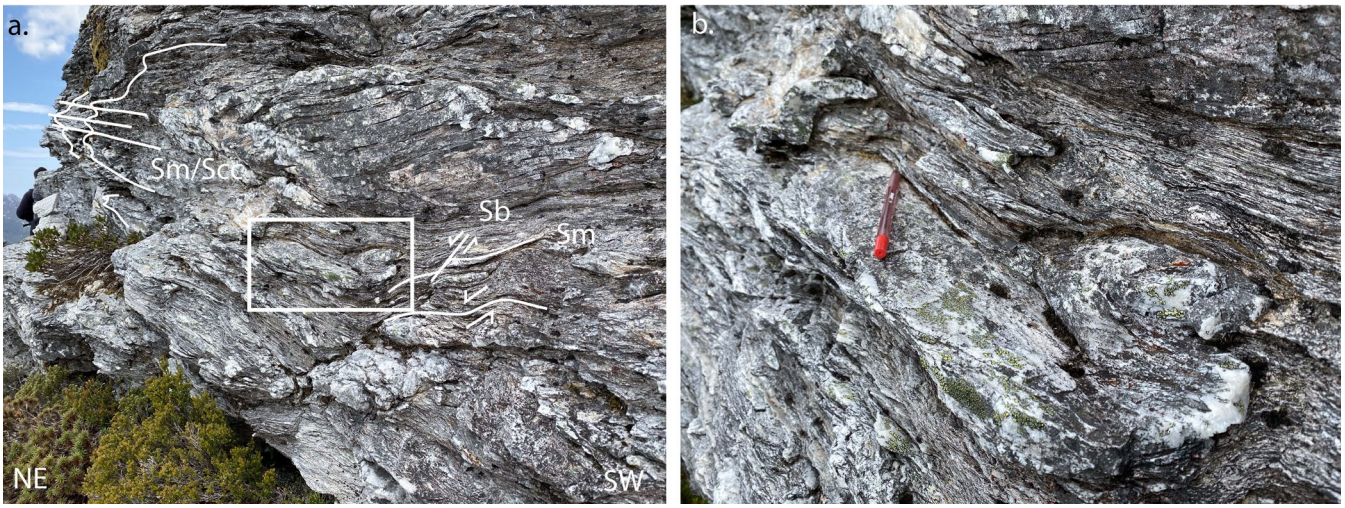

Figure 22. Upper part of the Lower Intensely-Foliated Transposition Zone. Views are to the southeast. a) Isoclinally folded quartzite showing recumbent isoclines in Sm and So/Sm (transposed quartzite layering), and shear band (Sb) giving southwest-over-northeast emplacement. b) Close-up of asymmetric fold pair in thin quartzite band shown in (a) by white outlined area. The mesoscopic fold pair displays varying direction of plunge, with the upper hingeline straight out of page (almost normal to the plane of the photo) and the lower hingeline almost parallel to plane of the photo. The red pen is parallel to the mineral lineation (Lm).

It is made up of zones of sub-horizontal crenulation cleavages mostly preserved as pods that are enveloped by the dominant foliation Sm within this zone (Figure 22a). Small-scale, rootless, asymmetric, isoclinal fold pairs occur as relicts of the Sm/So layering in the dominant Sm (Figures 22b and 23a). Hinges of these folds are sub-parallel to Lm and define Lrod (Figure 21b).

Towards the contact with the underlying dolomite there is pronounced development of sub-horizontal crenulation cleavage (Scc/Sm) (Figure 23). The Scc is sub-parallel to Sm outside the crenulated zones. With increasing strain this becomes the dominant transposition layering Sm (Figure 23).

In parts of the basal Intensely Foliated Transposition Zone (Figure 24a) the crenulation cleavage domains show earlier-formed differentiated layering Sm folded as classic chevron folds in the development of the surrounding or enveloping dominant Sm (Figure 24b and c).

3. Emplacement Shear Sense

3.1 Shear Bands

Shear bands in the basal, high-strain transposition zone for the quartzite sheet show northwest-over-southeast movement sense with transport towards ~120° (Figure 25).

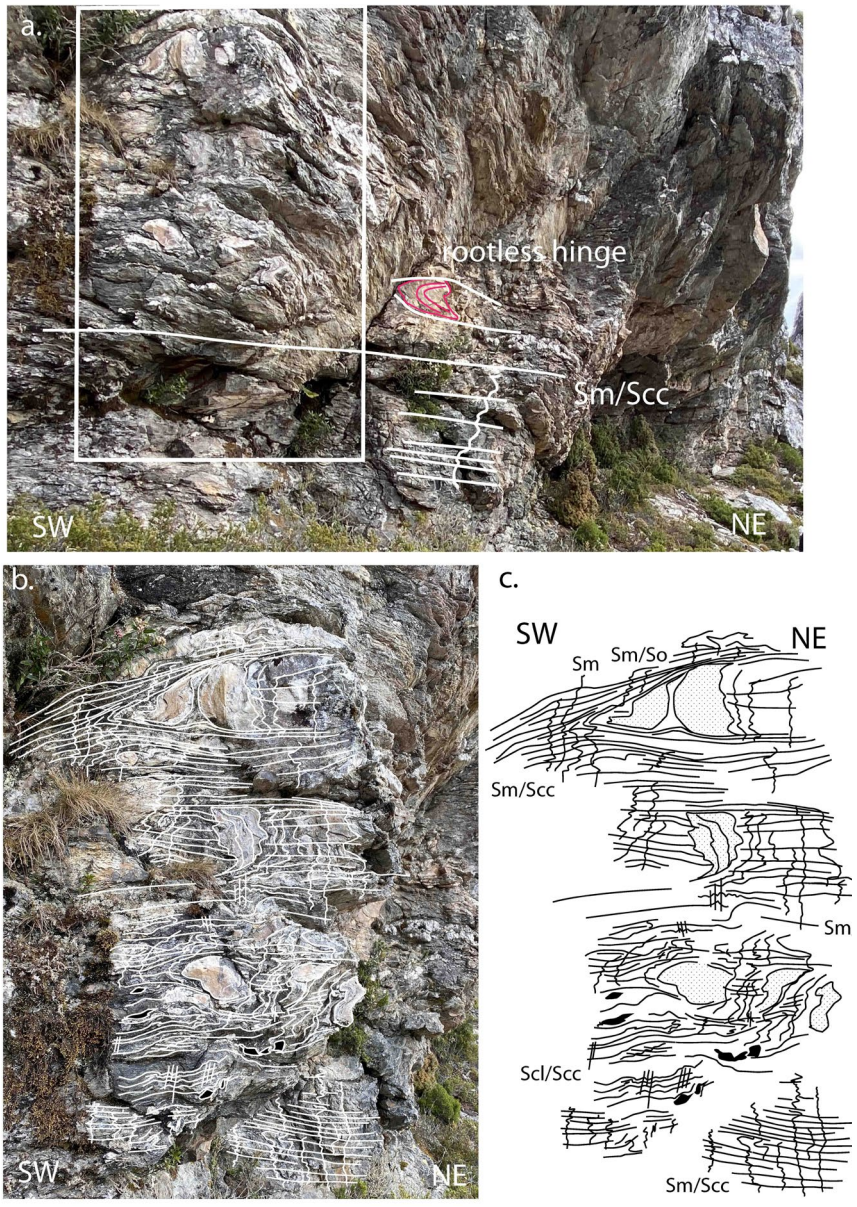

Figure 23. Basal high-strain zone of the quartzite sheet showing marked transposition layering developing from sub-horizontal crenulation cleavage (Sm/Scc). Rootless quartzite isocline hinges occur in Sm/So (stippled regions), folded by a steeply dipping Sm that gets crenulated by Sm/Scc. A younger cleavage (Scl) overprints all these fabrics and is axial surface to upright, northwest-trending minor folds. Irregular shaped black segments are boudinaged quartz veins.

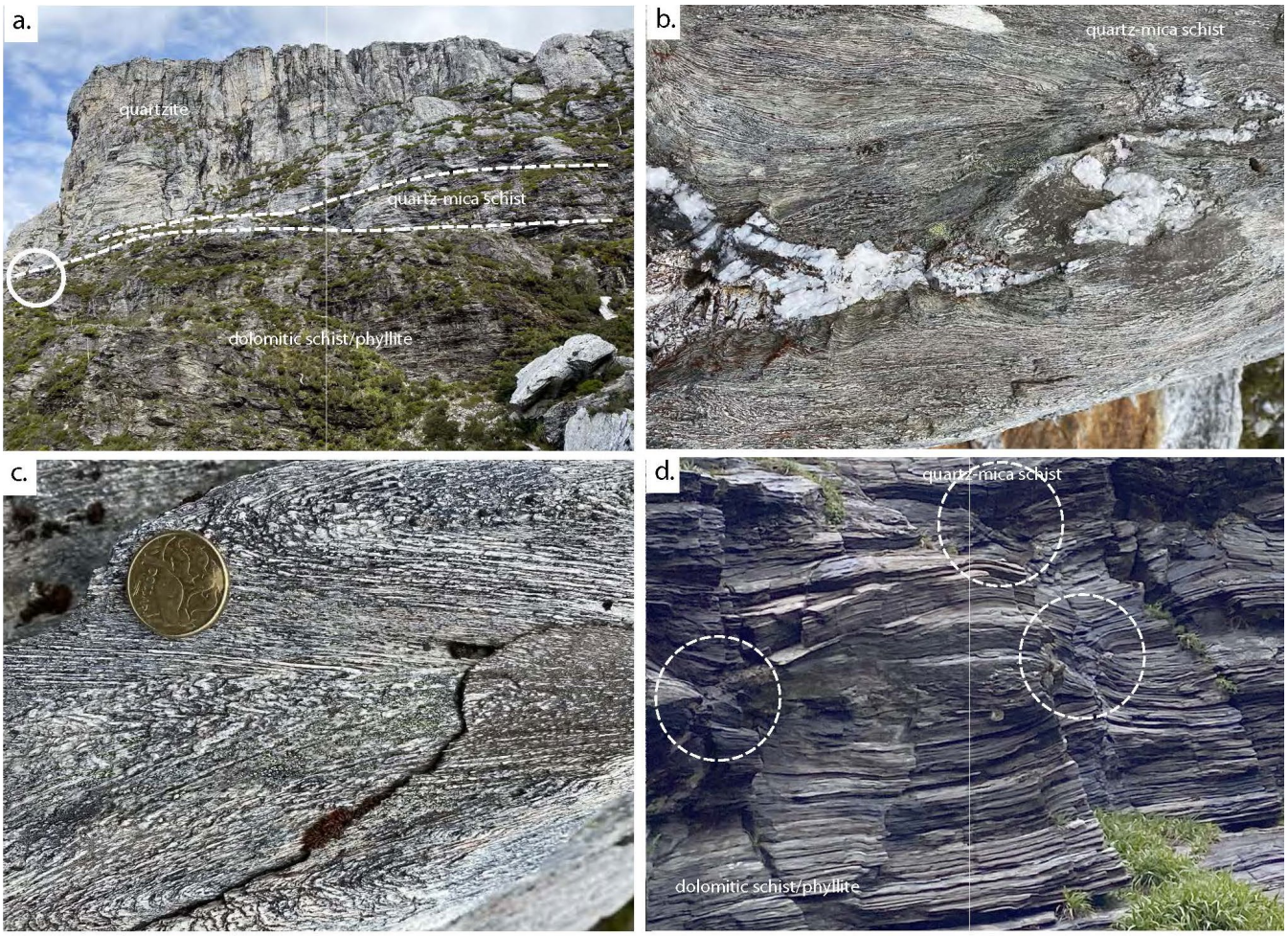

Figure 24. Deformation zones and fabrics within the contact high-strain between the quartzite sheet and underlying dolomitic phyllite. a) View of contact taken from Lake Tahune track showing domains of quartzite with isoclines, the basal quartz -mica schist and the dolomitic phyllite. b) Quartz-mica schist transposition fabrics with internal boudin, isoclinally folded quartz veins and limb-hinge domains/banding from chevron folding with ongoing transposition. c) Close up of transposition layering development due to chevron style folding within the basal high-strain zone. d) Asymmetric internal-boudin development within the dolomitic phyllite. Track photo above the Lake Tahune hut.

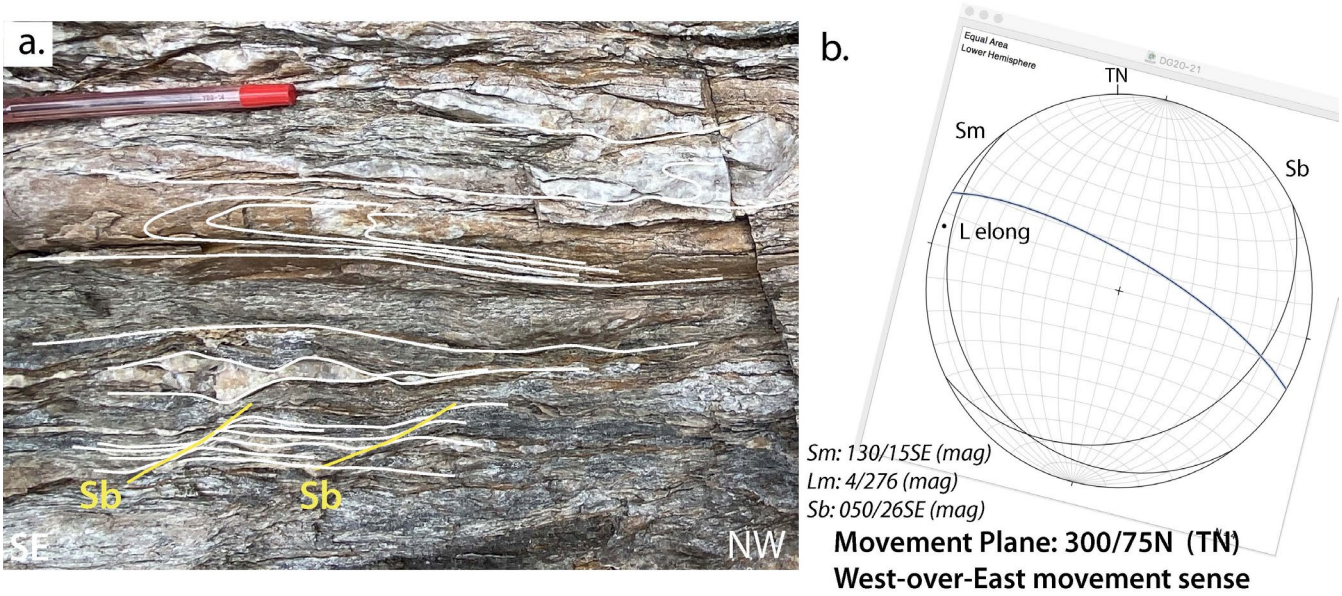

Figure 25. Isoclinal fold hinges (axes parallel to plane of the photograph) and shear bands developed within Sm of the basal zone. b) Stereonet plot with derivation of the movement plane and transport direction toward 120° (northwest-over-southeast sense).

3.2 Folded asymmetric shear-band boudin of quartzite

So/Sm layering at the northwest end of Lions Head further indicates west-over-east transport towards ~102° (Figure 26).

Asymmetric, internal, shear-band boudins in the upper part of the Scotchfire dolomitic phyllite below Lions Head also show west-over-east movement sense (Figure 24d).

Shear bands and shear-band boudins indicate that the quartzite sheet was emplaced from west-to-east towards 102°-120° (Figure 27).

4. Brittle Faulting

Brittle faulting is a late-stage, probably-Devonian reactivation between the overlying quartzite of the Fincham-Mary sheet and the underlying dolomitic phyllite of the Scotchfire sheet. This is superimposed on the marked strain gradient and apparently conformable foliation relationships across the contact (i.e the contact is a "welded" strain contact where the units were internally deformed during emplacement).

The Lake Tahune track follows the strike of the foliation and brittle fault(ing) at the contact zone, such that the contact appears horizontal (i.e. strike normal view as shown in Figure 11 with white fault-traces appearing sub-horizontal and sub-parallel to the Sm foliation traces). The actual relationship between the faulting and the high-strain zone contact can be observed at Lions Head and South Col (Figures 28 and 29). Here the views are strike-parallel and show the obliquity and discordance of the fault plane relative to the high-strain zone base of the quartzite and to the foliation in the footwall dolomitic phyllite. Estimates of the fault strike and dip are similar and are 174/45W (Lions Head) and 169/35W (South Col) (see Figure 30).

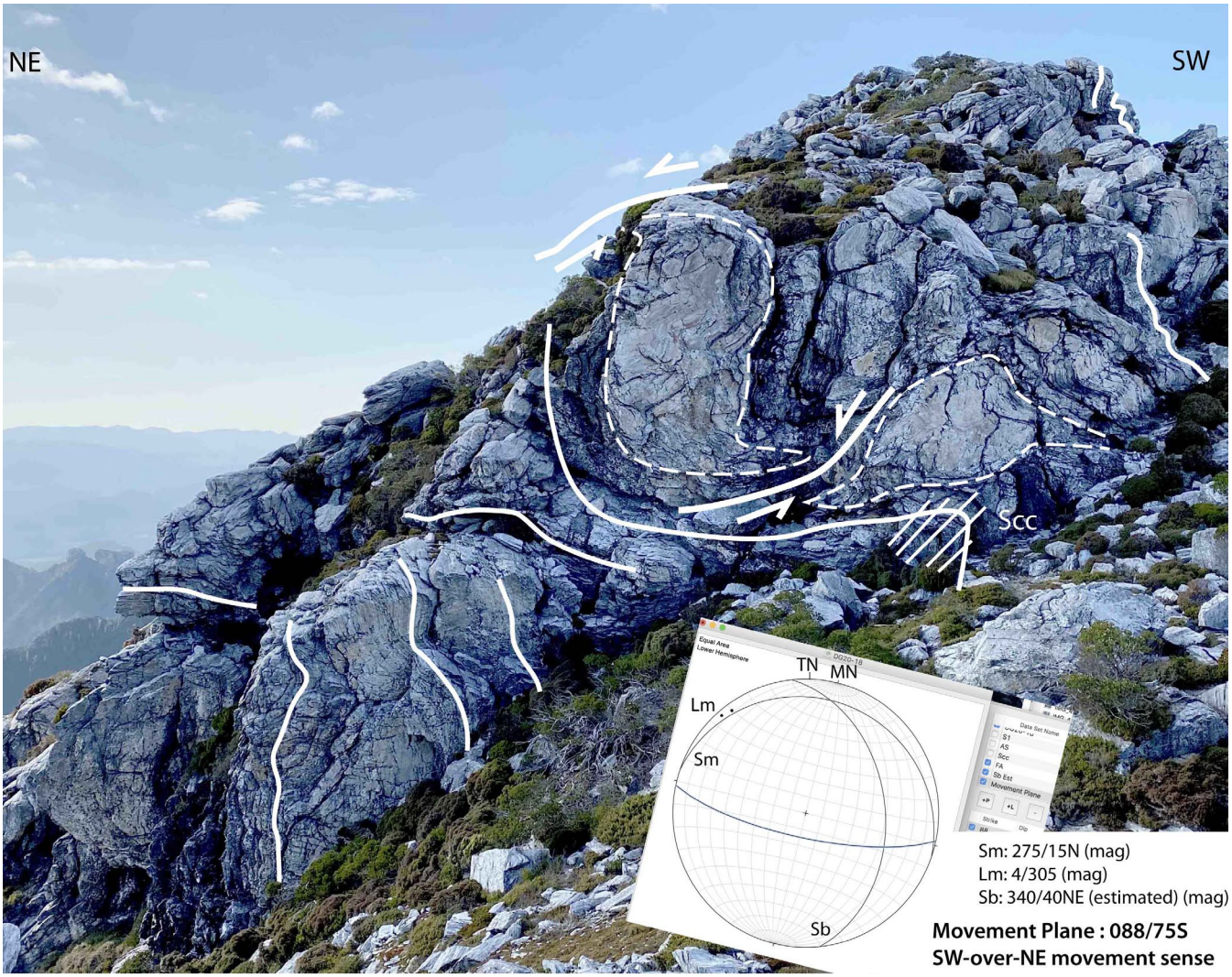

Figure 26. Large-scale, asymmetric shear-band boudin in thick quartzite layer formed during early transposition layering development. This is re-folded by asymmetric folds with northeast-dipping axial surface crenulation cleavage. The location is the northwest end of the Lions Head ridge (see also Figure 18). The inset Stereonet plot shows derivation of the movement plane and transport direction. Transport direction is towards ~102°. See Figure 27 for position.

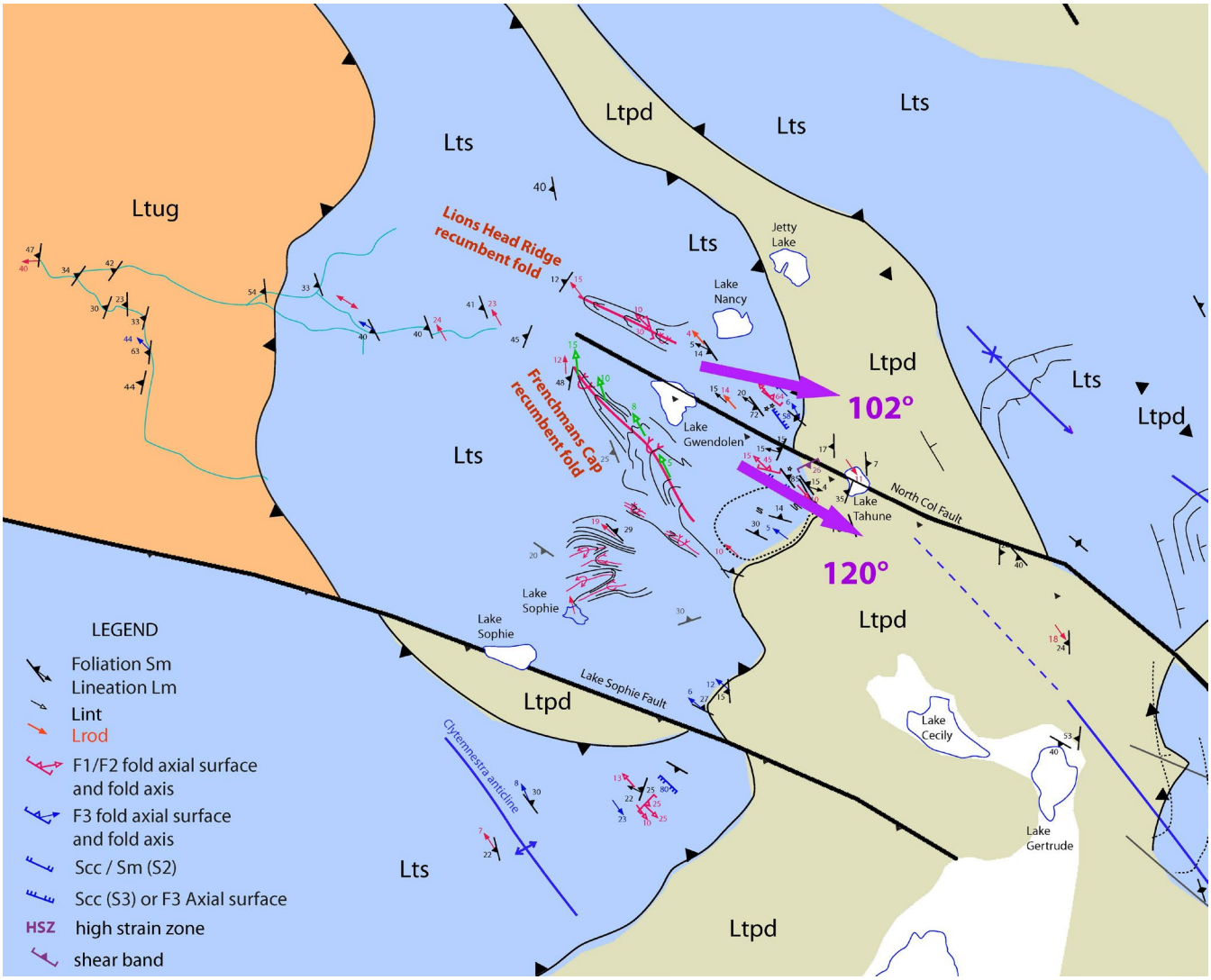

Figure 27. Transport direction vectors (purple arrows) calculated from shear bands and macro-shear band boudins (see Figures 25 and 26). Orange Ltug: high-grade schist; blue Lts: low-grade Frenchmans Cap quartzite sequence; khaki Ltpd: Scotchfire dolomitic phyllite.

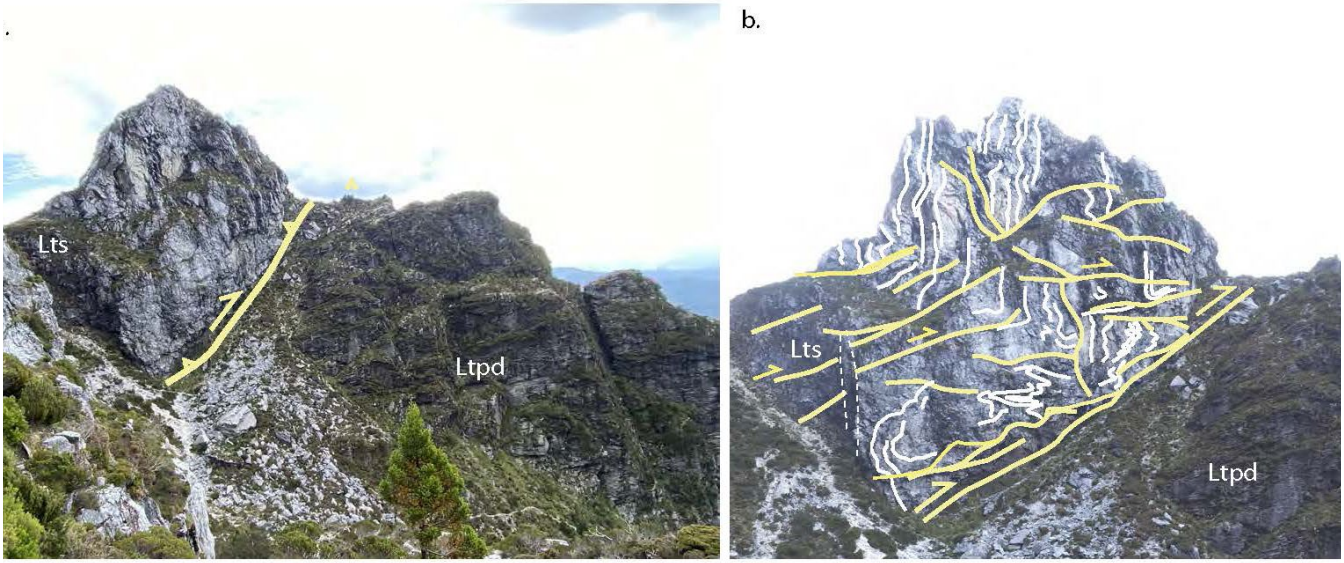

Figure 28. Thrust-reactivated contact between quartzite (Lts) and the underlying dolomitic phyllite (Ltpd) at Lions Head (yellow fault trace) with suggestion that Sm in both the hanging wall and footwall is sub-parallel. b) Enlargement of Lions Head showing that this is not the case. A brittle faulting zone exists some 10-20m above the basal thrust fault and is made up of a series of flat-thrust faults that cut strongly folded So/Sm.

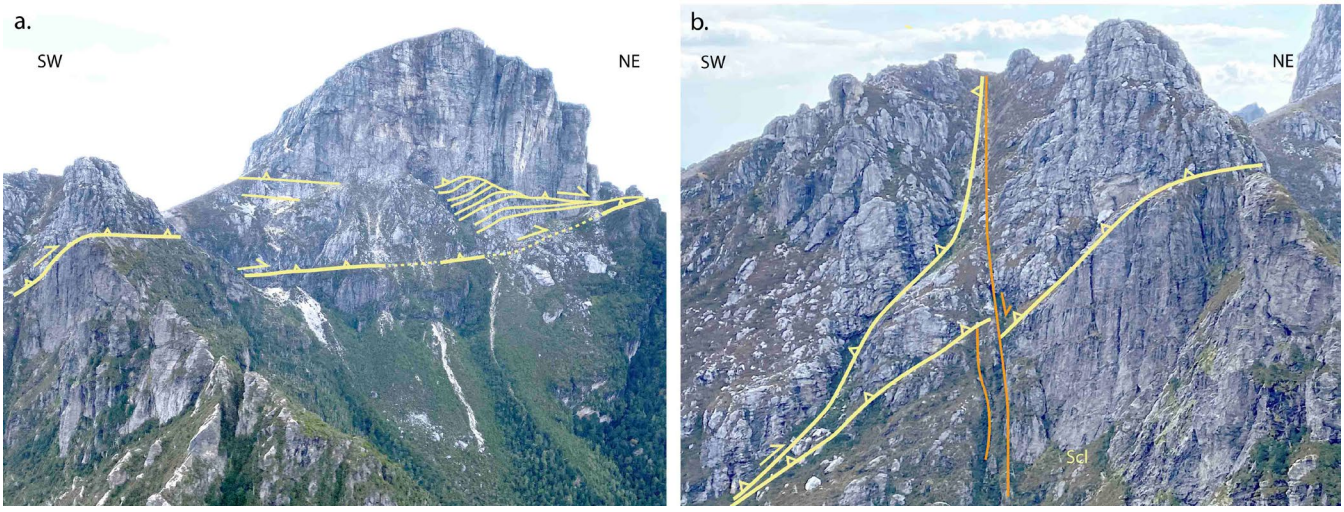

Figure 29 (Above). Thrust-reactivated contact (yellow traces) between quartzite (Lts) and the underlying dolomitic phyllite (Ltpd) near South Col. b) Splay off basal thrust contact with reactivation and offset by a younger steep fault (orange). Note the discordance of both Sm in the footwall and hanging wall.

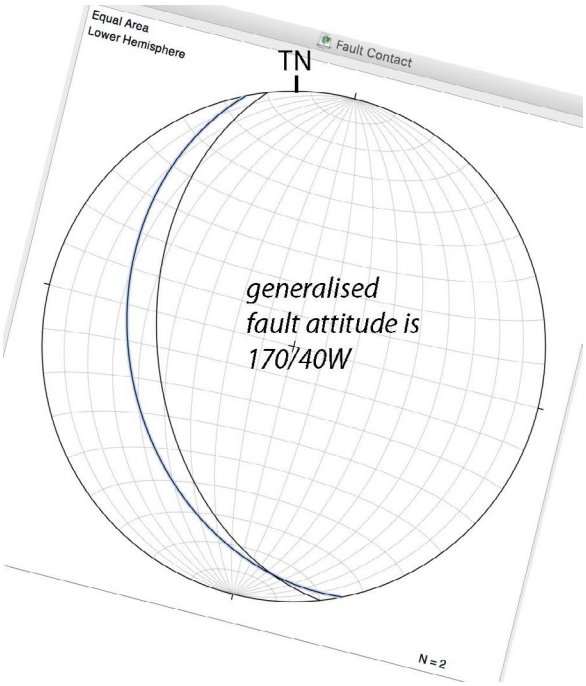

Figure 30 (Left).Attitudes of faults from Lions Head and South Col plotted as stereonet great circle traces. The faults define the contact between the quartzite and the underlying dolomitic phyllite. A generalised fault attitude is ~170°/40°W.

Figure 31 (Below). Aerial view of Clytemnestra, from the vicinity of Mt Moore, showing quartzite capping the ridge and the contact (white fault) with the underlying brown dolomitic phyllite. Another fault (yellow) along the Lake Sophie glacial valley offsets this contact and elevates the Clytemnestra quartzite relative to the quartzite of South Col. Late north-striking and west-dipping normal faults in the west (photo right side) clearly offset the quartzite contact with the Scotchfire dolomitic phyllites.

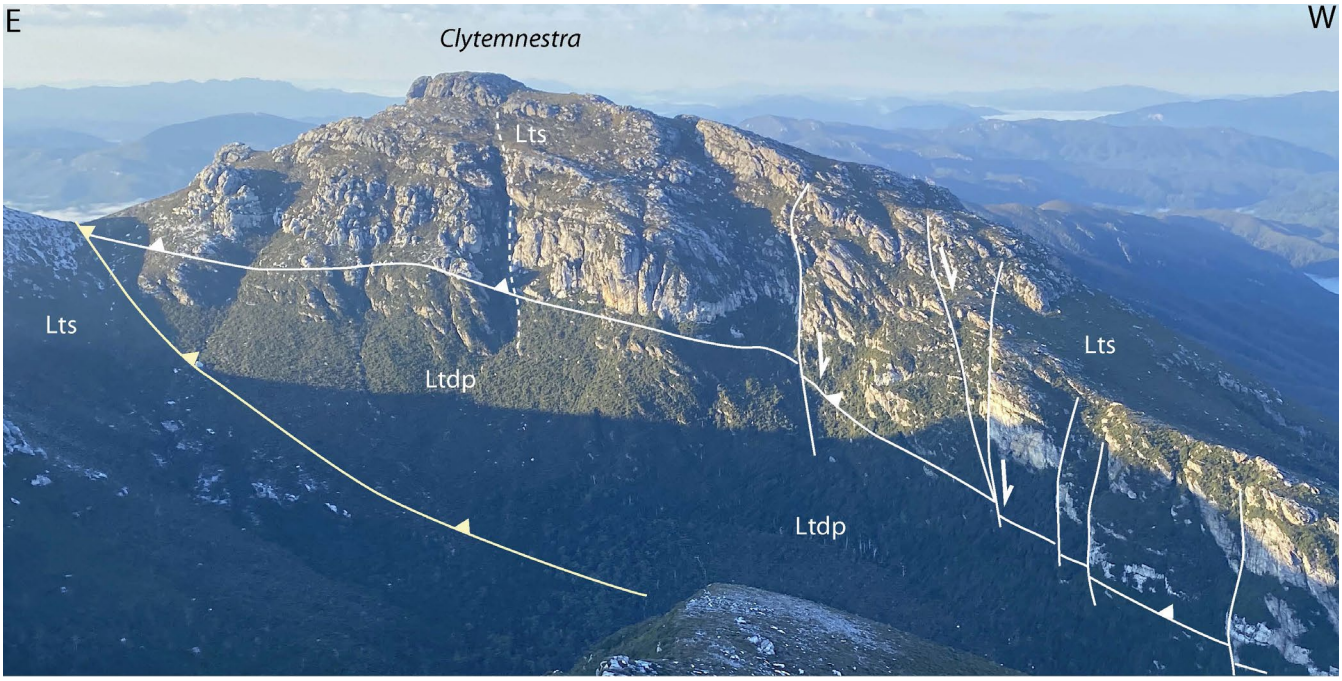

The fault contact between the Fincham-Mary sheet and the structurally lower Scotchfire sheet can also be seen along the base of Clytemnestra (Figure 31). Here this fault is cut by a younger fault passing along the Lake Sophie glacial valley (i.e. Lake Sophie Fault of Figure 4) producing a small wedge or inlier of dolomitic schist/phyllite (see also Ltpd slice below and north of Clytemnestra in Figure 4). Late north-trending and west-dipping normal faults also offset the quartzite contact with the Scotchfire dolomitic phyllites (Figure 31).

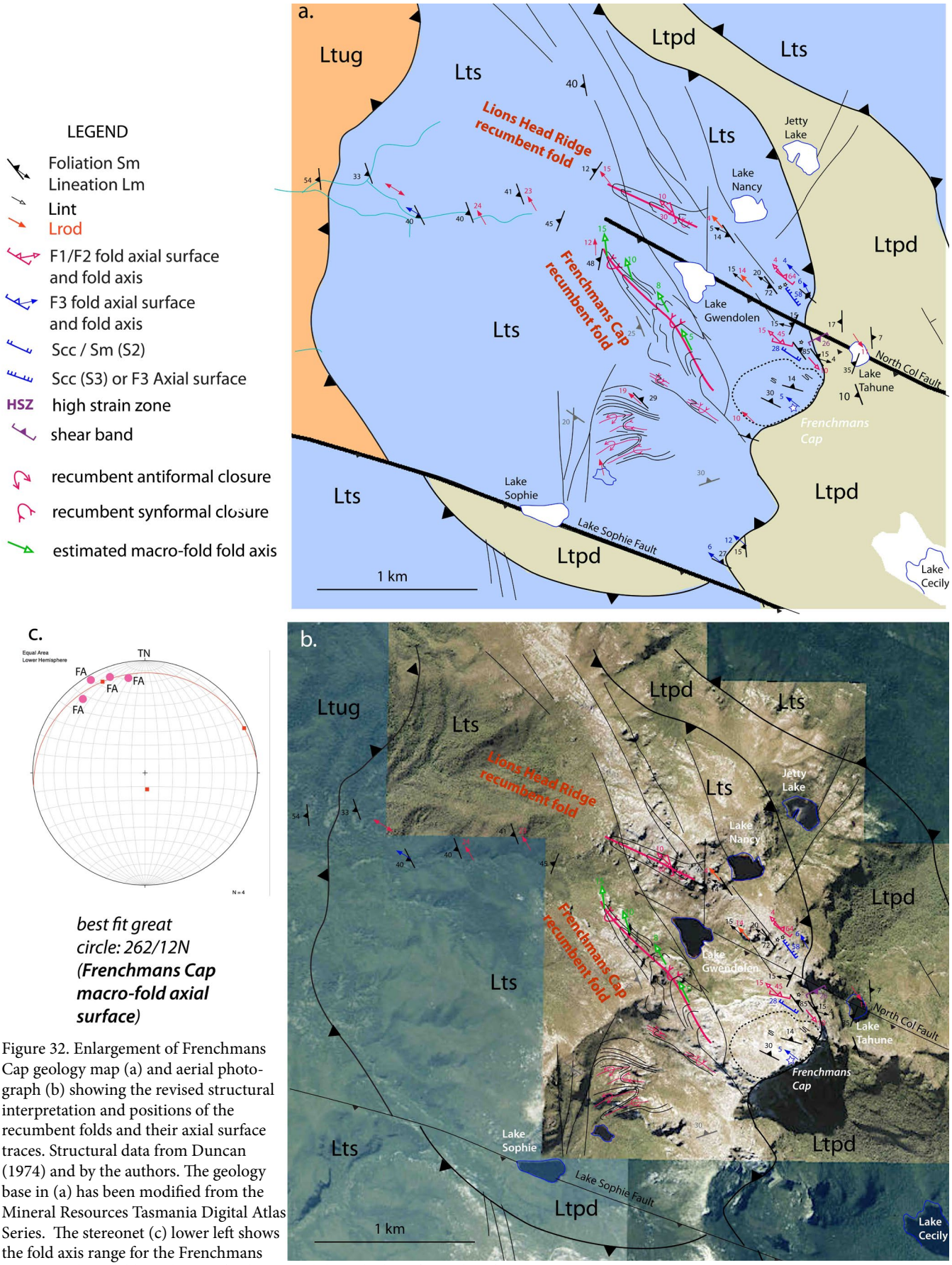

Figure 32. Enlargement of Frenchmans Cap geology map (a) and aerial photograph (b) showing the revised structural interpretation and positions of the recumbent folds and their axial surface traces. Structural data from Duncan (1974) and by the authors. The geology base in (a) has been modified from the Mineral Resources Tasmania Digital Atlas Series. The stereonet (c) lower left shows the fold axis range for the Frenchmans Cap recumbent fold southwest of Lake Gwendolen. The best-fit axial surface is 263/12N.
Orange Ltug: high-grade schist; blue Lts: low-grade Frenchmans Cap quartzite sequence; khaki Ltpd: Scotchfire dolomitic phyllite.

5. Regional Folds

5.1 Frenchmans Cap Recumbent Fold

The main fold structure in the Frenchmans Cap quartzite is a southwest-closing synformal recumbent fold structure southwest of Lake Gwendolen (Figures 5 and 30). An oblique section through the fold is shown along the west wall of the Gwendolen cirque valley (Figures 33, 34, 35, 36 and 37). It has pod-like form elongated in the direction of the regional stretching direction, shown by the mineral lineation (Lm) and/or rodding lineation (L rod), and is enveloped by the regional schistosity/foliation (Sm).

An oblique view of the Frenchmans Cap recumbent fold looking up Gwendolen cirque (Figure 38) shows the changes in geometry and apparent down-plunge taper with decreasing elevation to the level of Lake Gwendolen. The aerial view above South Col (Figure 39) provides a part profile view of the lower limb to hinge transition of the Frenchmans Cap recumbent fold.

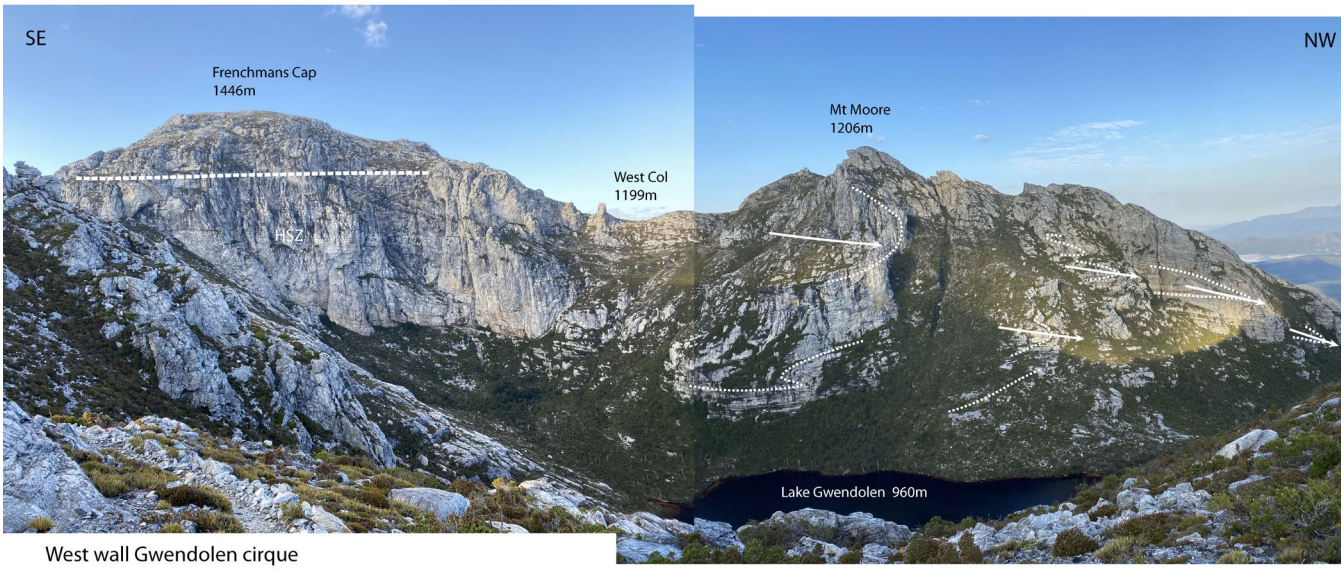

Figure 33. Composite photograph of Gwendolen cirque western wall providing a longitudinal profile of the Frenchmans Cap macro-fold. The photographic section is parallel to the deformation movement plane that contains the mineral lineation and stretch direction. White dashed line is interface of the Upper Folded Zone with the Middle Strongly-foliated Zone. White dotted lines are formlines of bedding traces in the cirque valley wall. White arrows denote the changes in macro-fold plunge from West Col to the end of the wall in the northwest. Due to slight obliquity of these hingelines with respect to the cirque wall they represent axial-surface intersection traces that contain the Frenchmans Cap macro-fold hingelines.

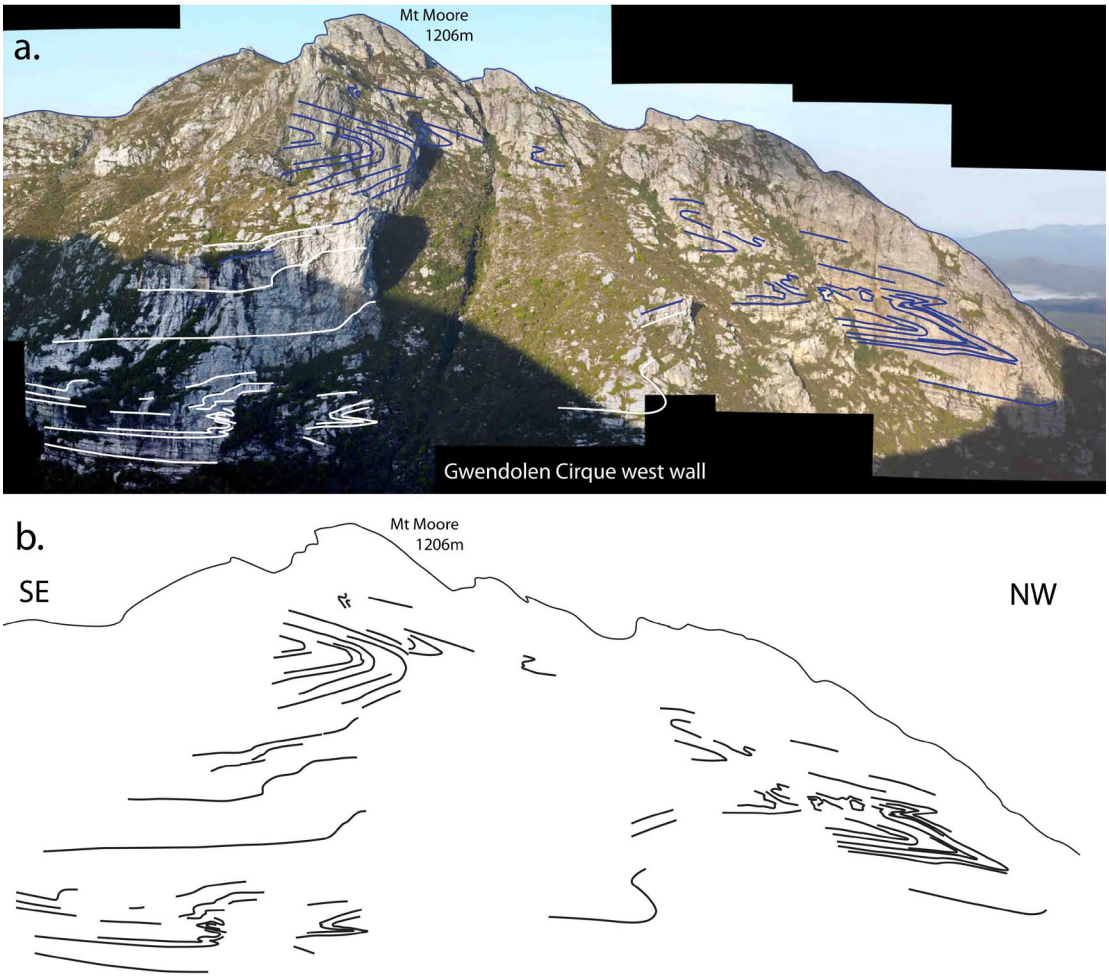

Figure 34. View to the southwest of the west wall of Gwendolen cirque from the Lions Head ridgeline giving an extremely oblique intersection of the Frenchmans Cap recumbent fold, with b) structural interpretation by using So/Sm intersection traces in the cirque wall. The fold is closing into the cirque valley wall towards the southwest in the direction of the photo.

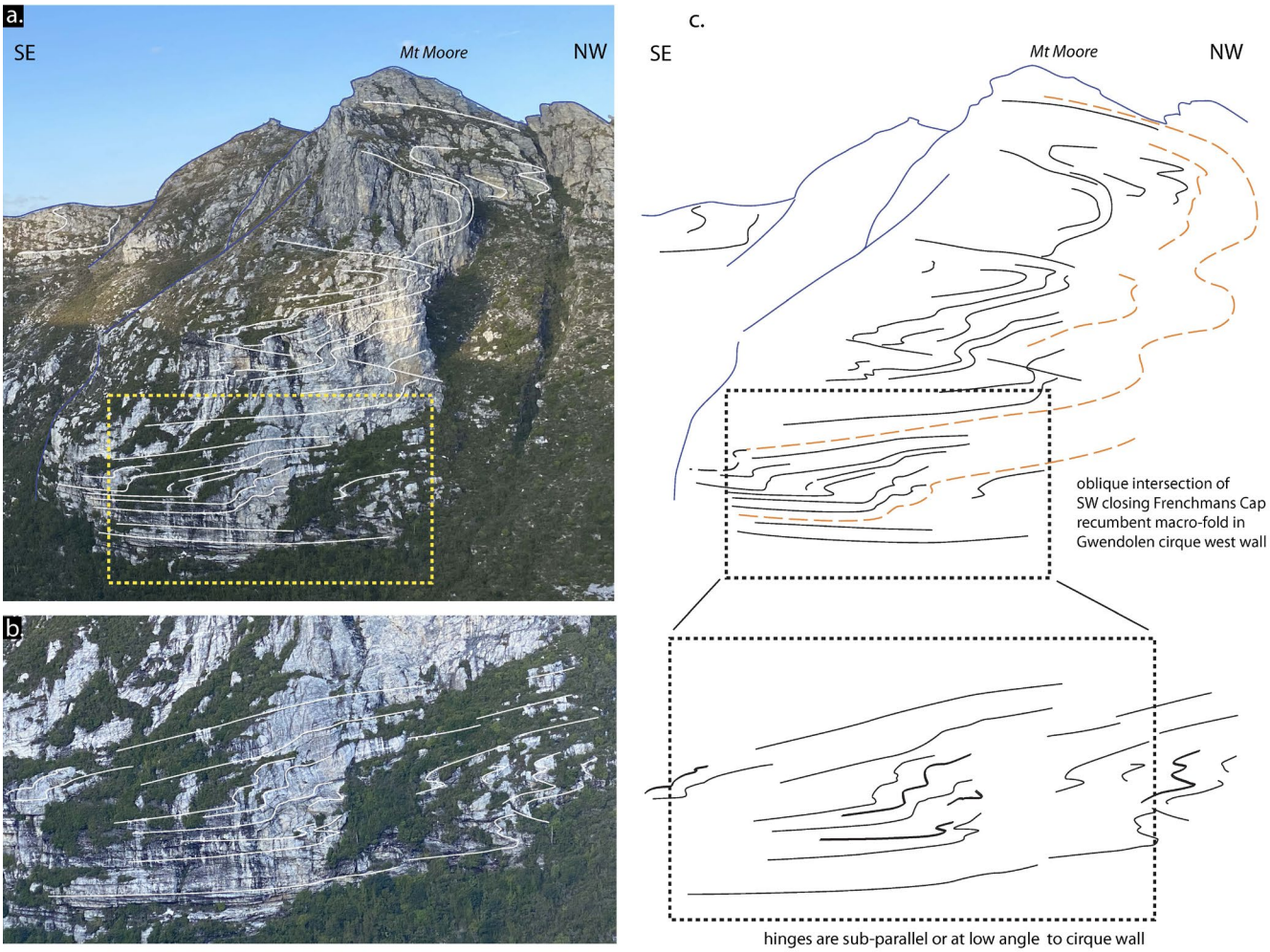

Figure 35. The closure geometry of the major southwest-closing Frenchmans Cap recumbent fold in an oblique view towards Mt Moore from the Lions Head ridgeline. View is towards the southwest. Broad, more rounded closure with partial upper limb exposed on Mt Moore and the attenuated lower limb in the lower part of the Gwendolen cirque wall. b) Flattened asymmetric fold pairs on the lower limb of the recumbent fold with similar form to the Dent des Morcles folds at the base of the Morcles Nappe in the Swiss Alps (see Ramsay et al., 1983; Dietrich & Casey, 1989).

Figure 36. Apparent flattened, attenuated nose to the Frenchmans Cap recumbent fold exposed in the northern end of the west wall of the Gwendolen cirque valley. The cirque wall is north-northwest to south-southeast trending. This is an oblique intersection of the fold where the wall is sub-parallel to the fold axis trend. An approximate profile view of the closure is shown in Figure 37.

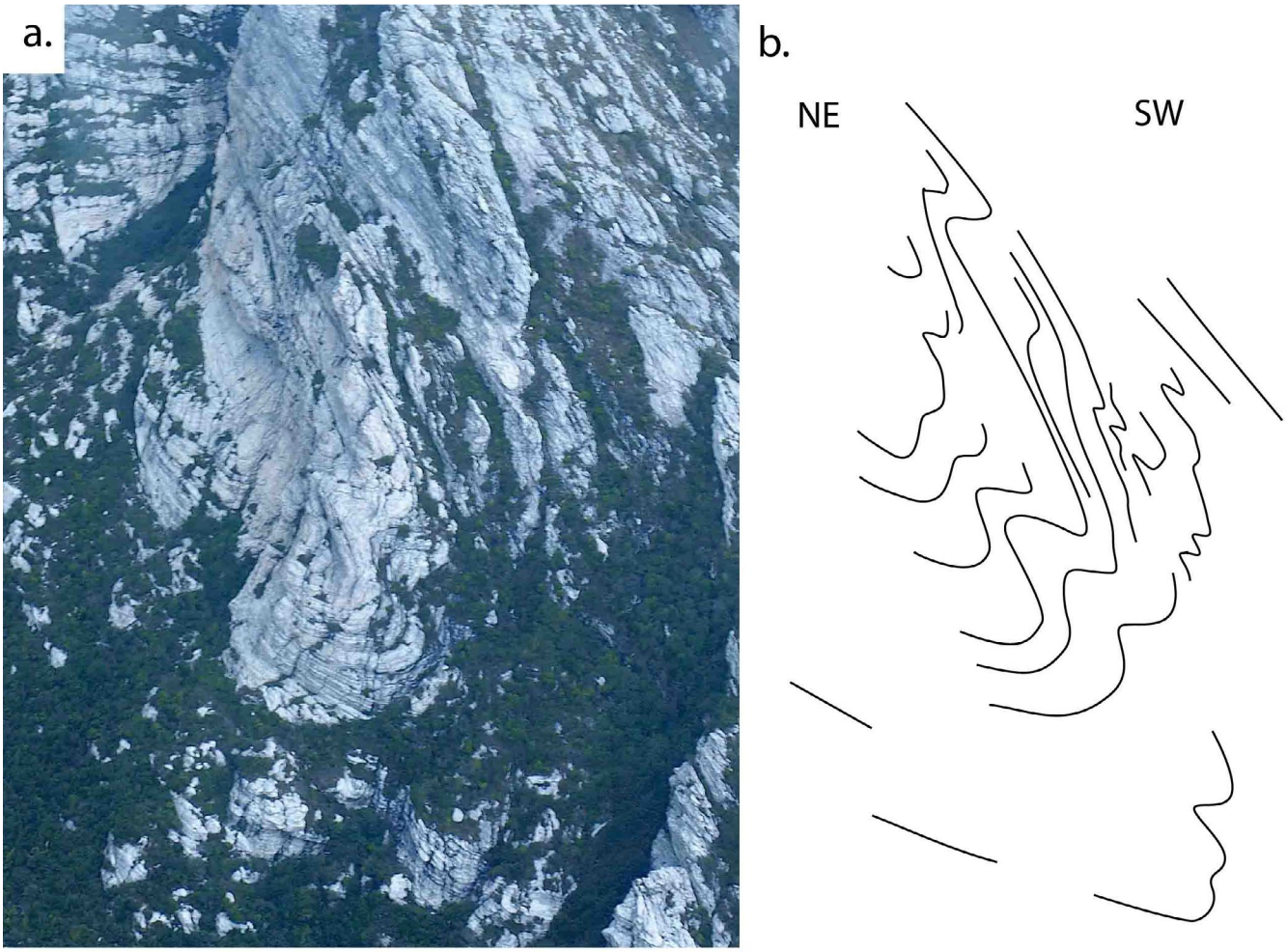

Figure 37. Approximate profile view of Frenchmans Cap recumbent fold-hinge (photo from helicopter towards the south-southeast). The profile is at the level of Lake Gwendolen in the west wall of Gwendolen cirque. This is the same hinge shown in Figure 36 above.

An oblique view of the Frenchmans Cap recumbent fold looking up Gwendolen cirque (Figure 38) shows the changes in geometry and apparent down-plunge taper with decreasing elevation to the level of Lake Gwendolen. The aerial view above South Col (Figure 39) provides a part profile view of the lower limb to hinge transition of the Frenchmans Cap recumbent fold.

5.1.1 Three Dimensional (3D) Recumbent fold Geometry

The profile geometry of the Frenchmans Cap recumbent fold is a large-scale, southwest-closing, recumbent isoclinal fold underlain by a high-strain zone that constitutes the fold lower limb (Figure 40a). The macro-fold geometry appears to taper or becomes less broad to the northwest in the direction of plunge (see Figures 34 and 38). Macro-fold axis variation along the west wall of Gwendolen cirque suggests a weakly curved hinge to this recumbent fold (see Figures 5, 32 and 33).

Superimposing the Frenchmans Cap profile section onto the other profiles (Figure 40b), with readjustment for fold plunge, indicates that the Upper Fold Zone is at a higher structural level and therefore forms a cap to the major recumbent fold exposed in Gwendolen cirque valley (Figure 40b).

The presence of moderate to steeply southwest-dipping So/Sm on Lions Head ridgeline (Figures 6c, 17, 18 and 19) and a sub-vertical So/Sm at the northeast face of Frenchmans Cap (see Figures 6d and 16) give an apparent closure northeast closure (Figure 42b). This would produce a closed loop or "eye fold" form typical of a large-scale sheath fold inside the Middle Strongly Foliated Zone. Compare the differences in geometry between the sections in Figure 40a and 40b.

This poses the question: a macro-sheath fold, a SW closing recumbent fold or a combination of the two? (see Figure 41).

Possible 3D geometries include 1) a major northwest-plunging, southwest-closing recumbent synform (recumbent fold) open to the northeast i.e "canoe on its side " geometry (Figure 41c), or 2) a major, northwest-plunging, closed sheath-fold pod enveloped by the dominant schistosity i.e. "tapered sleeping bag" geometry (Figure 41a).

Interpretation 2 is critically dependent on the So/Sm relationships along Frenchmans Cap northeast face and at Lions Head (see Figures 16, 17, 18 and 19). Continua-

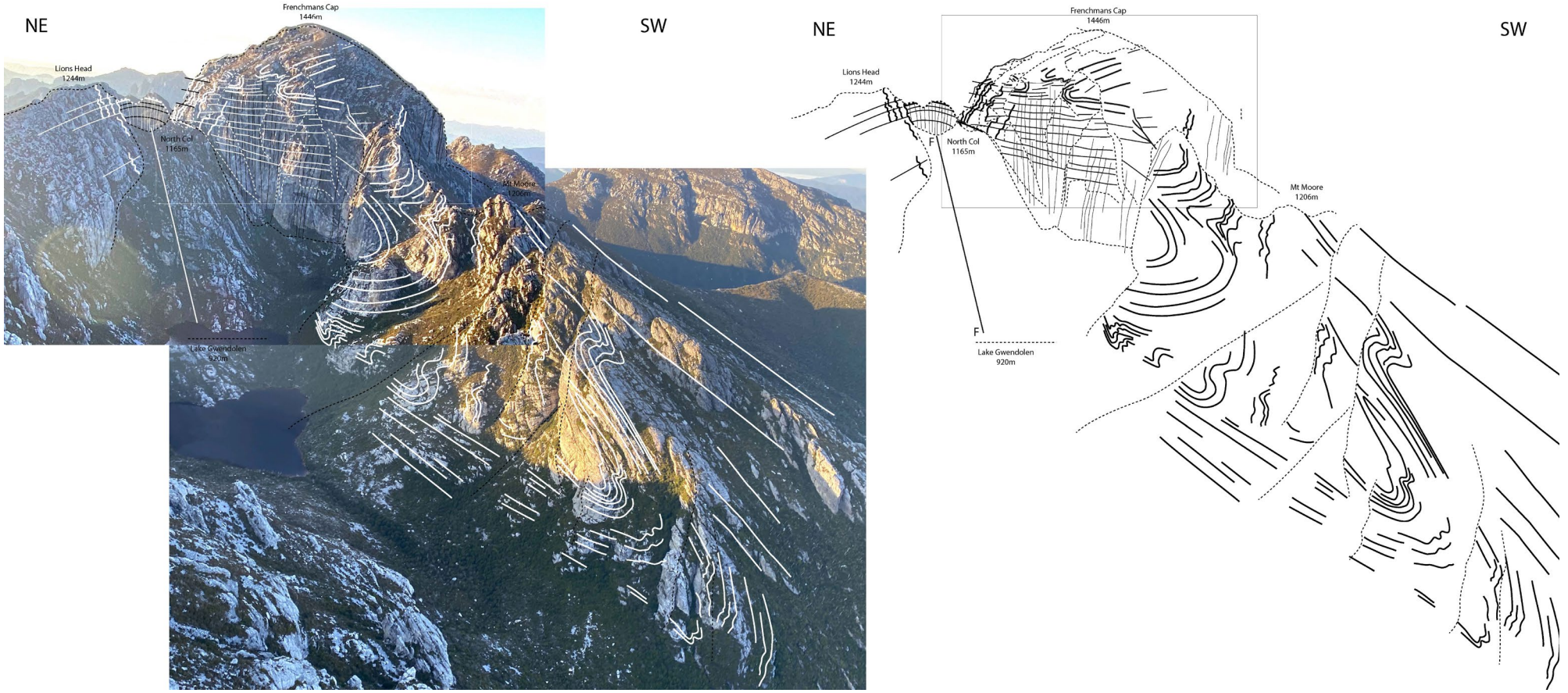

Figure 38. Composite, oblique view of Frenchmans Cap recumbent fold along the Gwendolen cirque west wall and northwest face of Frenchmans Cap. The geometry is based on formline traces of layering So/Sm from the photographs. The recumbent fold profile has an apparent taper in the plunge direction to the northwest.

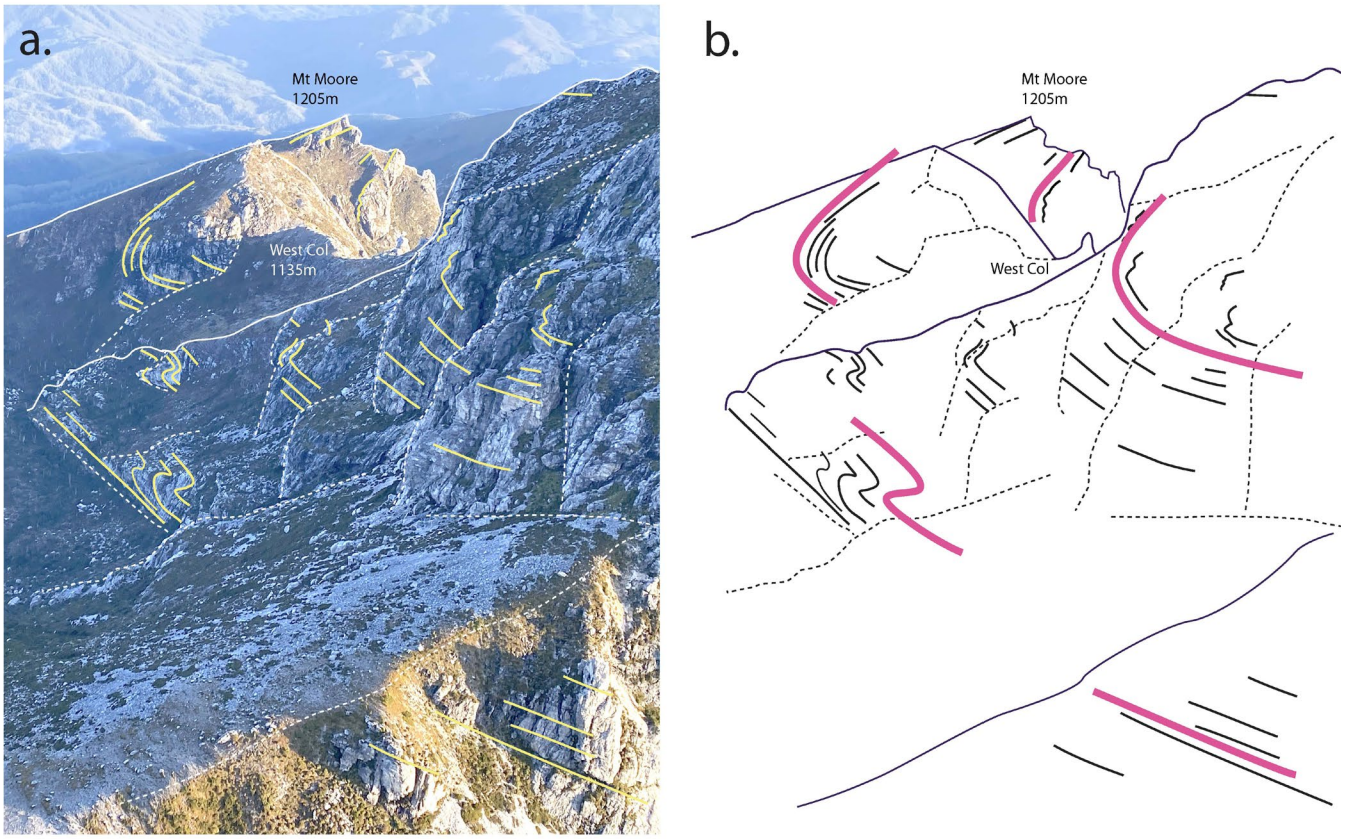

Figure 39. Down-plunge view of the Frenchmans Cap recumbent fold as seen in an oblique view of southwest face of Frenchmans Cap. The view is towards Mount Moore and the West Col (towards the north-northwest). a) Annotated photo taken from helicopter above South Col. b) Approximate profile view of the Frenchmans Cap recumbent fold through West Col based on the photo interpretation in a).

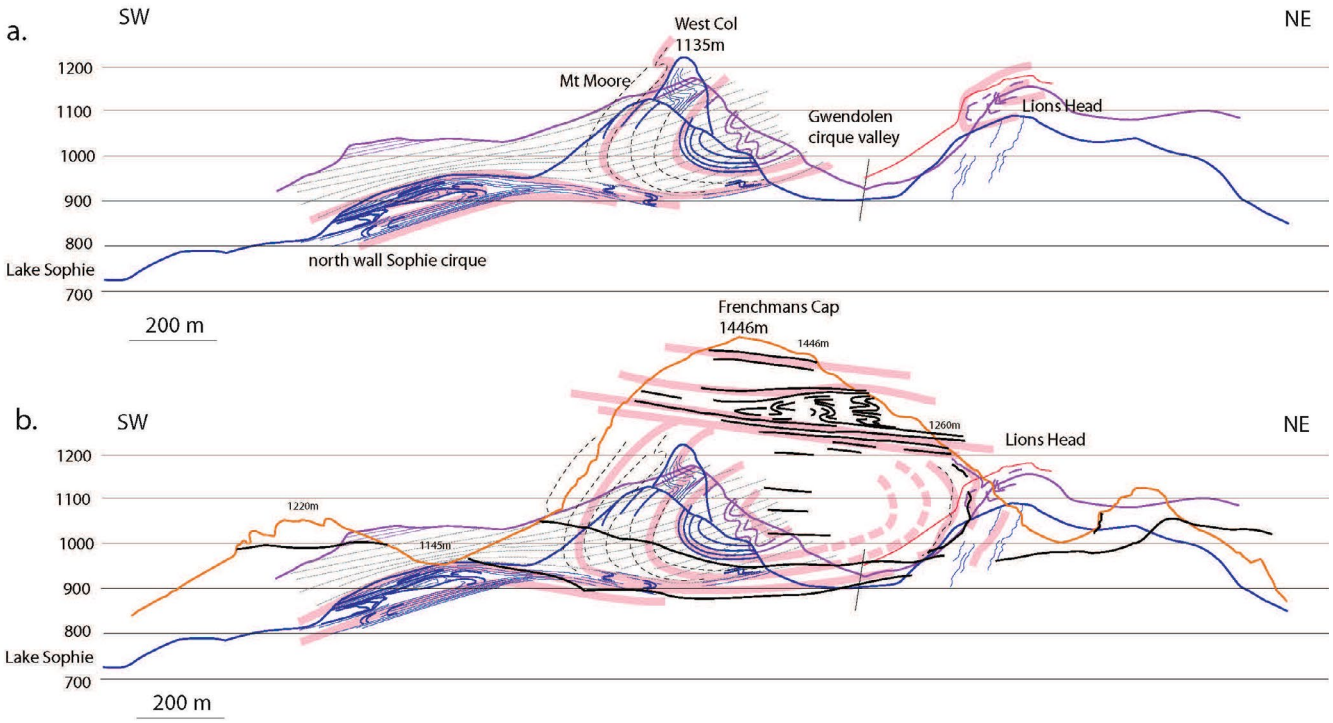

Figure 40. Stacked topographic profiles with structural interpretations. Vertical: horizontal scale. a) Two profiles including Sophie cirque-West Col profile (blue line) and Mt Moore - Lions Head ridge profile (purple line), and b) Three stacked profiles including the above plus Frenchmans Cap profile (orange profile). Thicker pink lines are generalised formlines in So/Sm depicting the Frenchmans Cap fold geometry. The positions of the profiles are shown in Figure 10a.

tion of the southwest facing closure onto the Lions Head ridgeline (see Section 5.2) would suggest that the major, synformal recumbent fold remains open to the northeast at this level. This is an apparent contradiction: at the position and level of North Col there appears to be closure to the northeast (refer Figures 16, 17 and 18) to give an "eye-fold" geometry, whereas at the position and level of Lake Gwendolen the major structure appears open to the northeast. This would suggest that the macro-fold geometry is changing along the length of the structure and could be a combination of the two geometries as discussed above (see Figure 41b).

Better high-resolution photographs are needed for the northwest face of Frenchmans Cap to resolve the relationships in the high-strain domain (see Figures 10 and 11).

5.1.2 Clytemnestra Basal High-Strain zone

Clytemnestra provides examples of structural relationships along the basal high-strain zone that constitutes the lower limb of the Frenchmans Cap recumbent fold. Clytemnestra consists of intense high-strain fabrics and foliations with a classic "swirly" nature related to rodding, relict isocline "pods" and overprinting zones of crenulation cleavage (Figures 42 and 43).

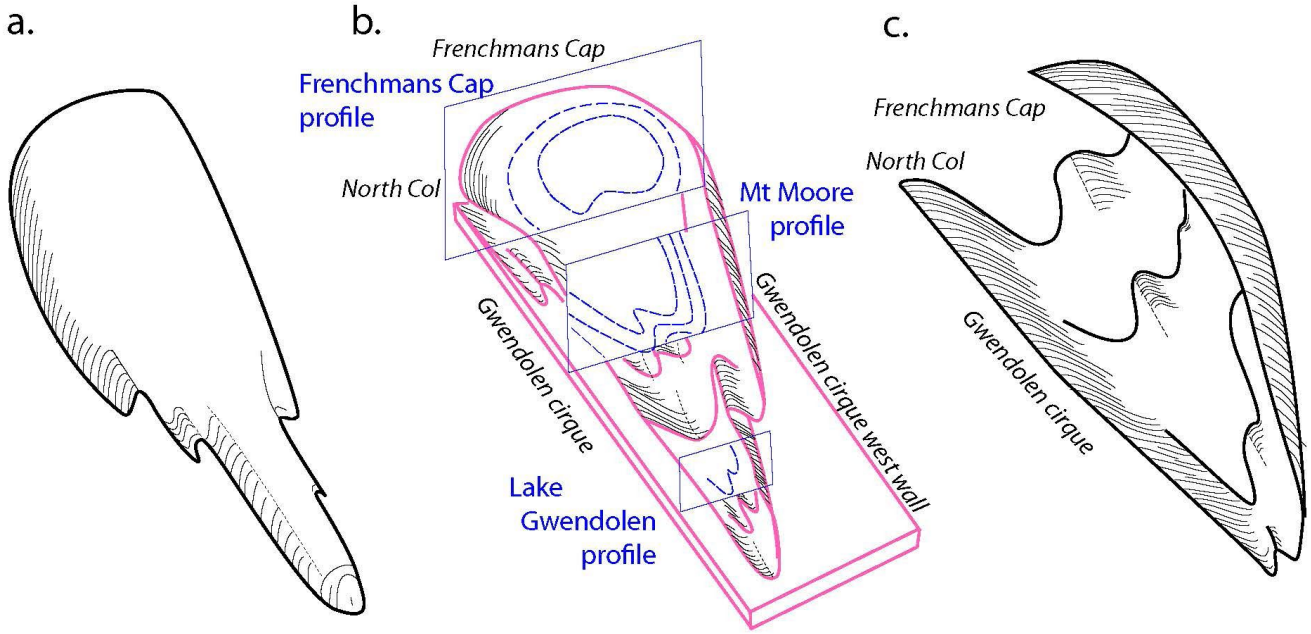

Figure 41. Two possible geometrical reconstructions for the Frenchmans Cap recumbent fold. a) and b) represent an elongated sheath-fold geometry, with analogy to a "sleeping bag". a) Sheath geometry with closed form of the outer layer. b) Same sheath geometry as in (a) but showing three slices or structural profiles through the sheath pod. The Frenchmans Cap profile shows closed loops in So/Sm to explain the geometry in the northeast face and at Lions Head ridgeline. c) Southwest-closing synformal closure open to the northeast with geometry analogous to a "tilted canoe".

Isolated or rare mesocopic isoclines occur as small pods or augens at metre-scales within the Intensely Foliated Transposition Layering zone (Figures 42a and 43a, b).

The strong rodding fabric (Figure 43c) shows transition into an intensely foliated platy quartzite with rootless fold hinges and relict sub-horizontal crenulation cleavage(s) at low angles to the dominant Sm (Figure 43d).

5.1.3 Sophie Cirque Fold Pod

The Sophie cirque north wall contains isolated, metre to ten-metre scale, recumbent isoclinal folds (Figures 44 and 45) within and enveloped by a lower-limb high-strain zone beneath the southwest-closing Frenchmans Cap recumbent fold. The folds occur in an augen- or pod-like zone (the Sophie Cirque Fold Pod) enveloped by intense high-strain foliation above the contact with the underlying dolomitic phyllite (compare with small-scale examples: Frenchmans Cap northeast face high-strain zone in Figure 23 and on Clytemnestra in Figures 42a and 43a).

5.2 Lions Head Ridge Recumbent Fold

A major, large-scale southwest-closing recumbent isoclinal hinge occurs along the northwestern continuation of Lions Head ridge (Figure 46).

It is likely that this closure is part of the major Frenchmans Cap recumbent fold, with axial surface projection across the Gwendolen cirque valley onto Lions Head ridgeline, with minor offset along the North Col Fault (Figure 47).

The recumbent fold lower limb is transitional into high-strain transposition layering fabrics exposed on the col above Lake Nancy (Figure 48). This layering is associated with marked rodding of fold hinges and the development of a pronounced rodding lineation (Figure 48a and b). Multiple crenulation cleavages reflect transposition cycling during Sm layering development (Figure 48c and d).

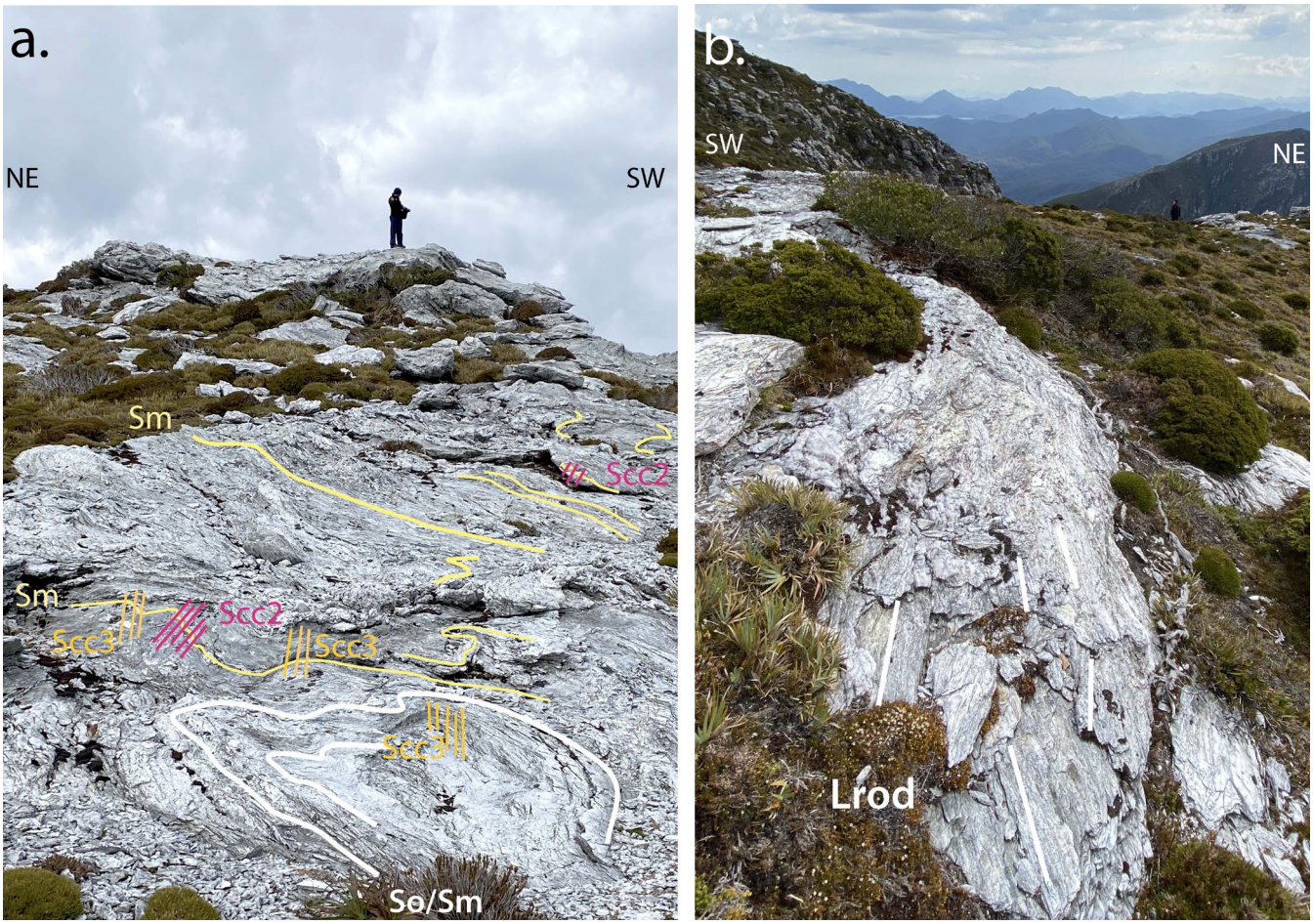

Figure 42. Clytemnestra fabrics and foliations. a) Classic "swirly" and pod-like nature of high-strain fabrics, north end of Clytemnestra. Sheath-like "eye" closure (white outline) within the dominant Sm (yellow) overprinted by an asymmetric fold set with northeast-dipping axial surface crenulation cleavage (pink Scc). Younger, upright crenulation cleavage set (orange Scc) is probably related to the Devonian deformation. b) Pronounced rodding lineation within gently NE-dipping Sm.

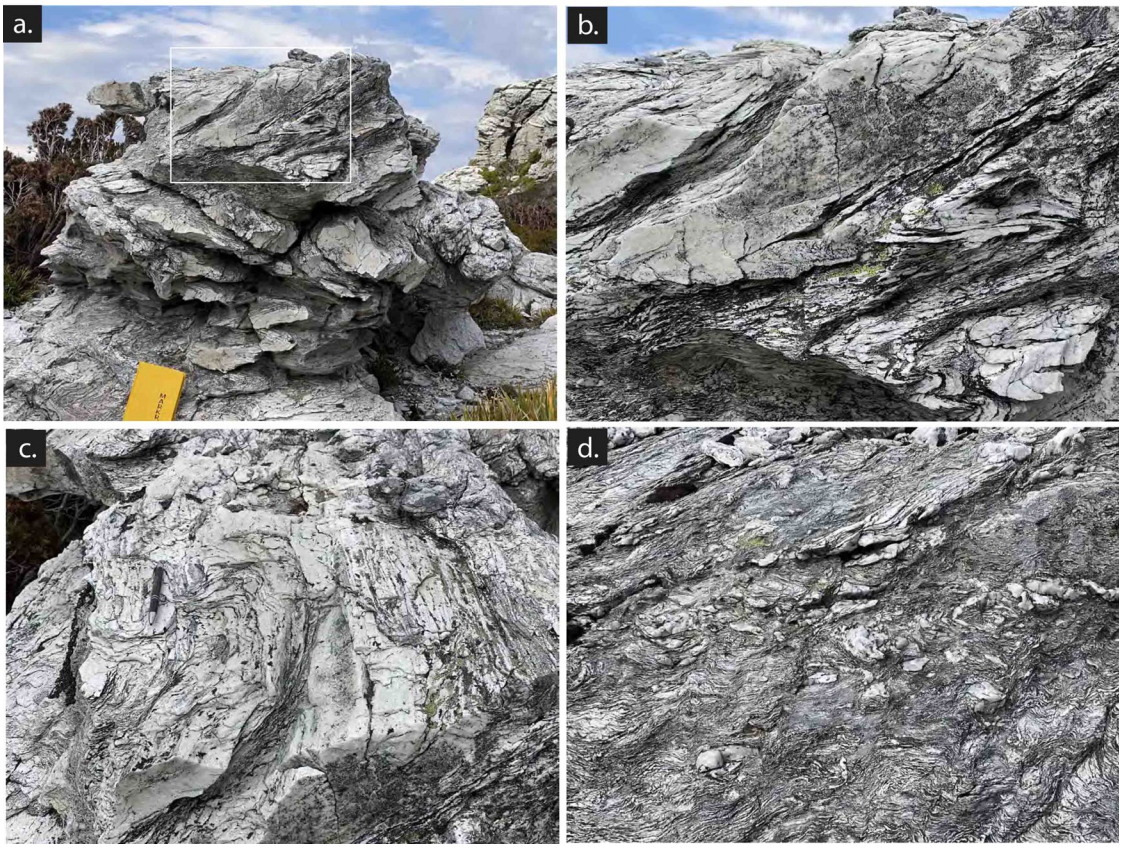

Figure 43. Clytemnestra fabrics and foliations. a) Fold hinges forming "pod" or augen within intensely foliated quartzite. b) Enlarged part of a) showing axial surface fabric development. c) Rodding fabric with preserved fold hinges. d) Typical intense foliation (Sm) with relict isoclines in Sm, zones of sub-horizontal crenulations and an overprinting northeast-dipping crenulation cleavage.

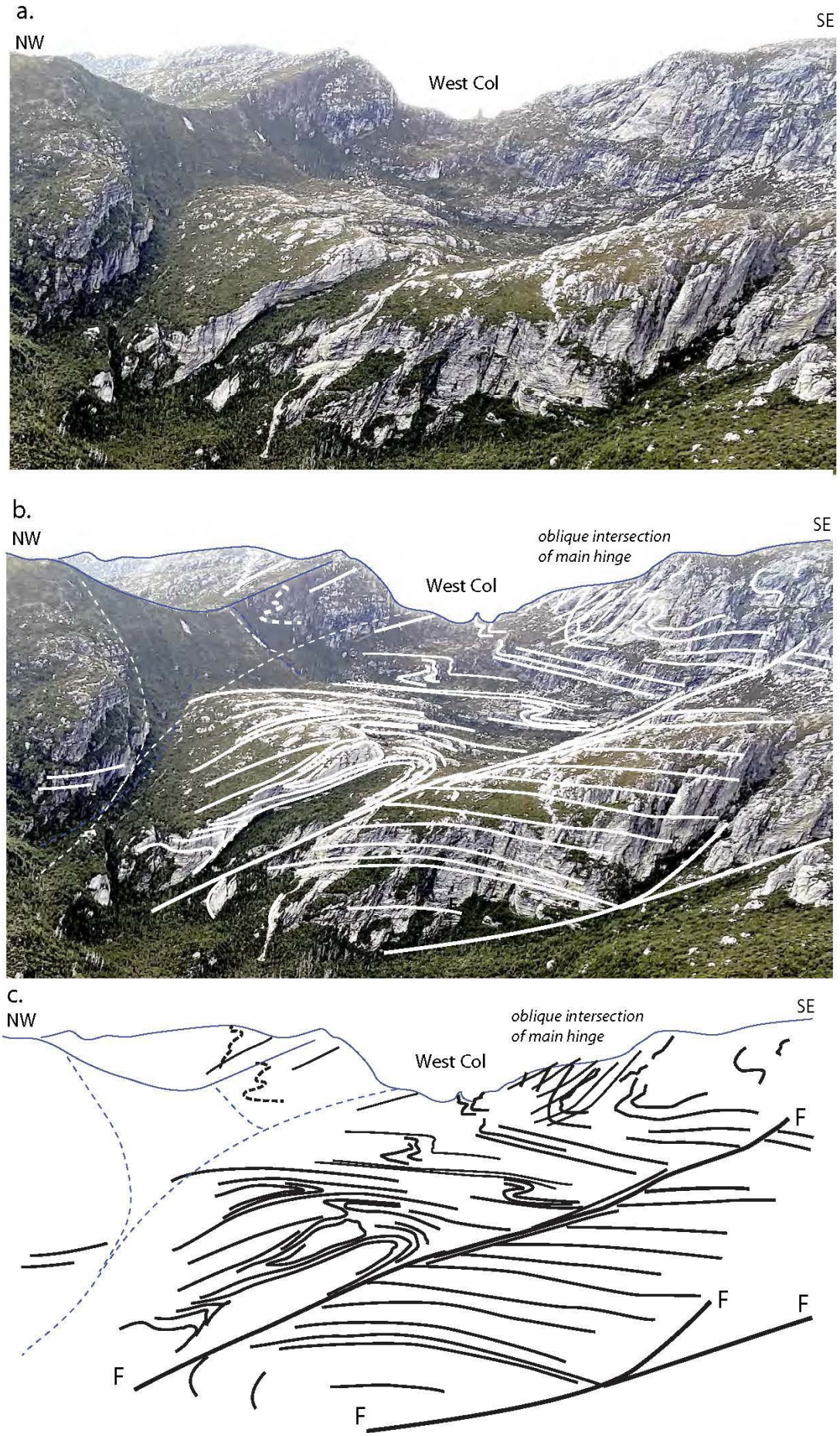

Figure 44. View of north wall of Sophie cirque and West Col (centre ridgeline) showing isoclinal folds below and south of the hinge of the major Frenchmans Cap recumbent fold. An oblique view of the synformal hinge can be seen at West Col. Close up views of the isoclines are shown in Figure 45. b) and c) are formline interpretations of the Sophie Cirque Fold Pod.

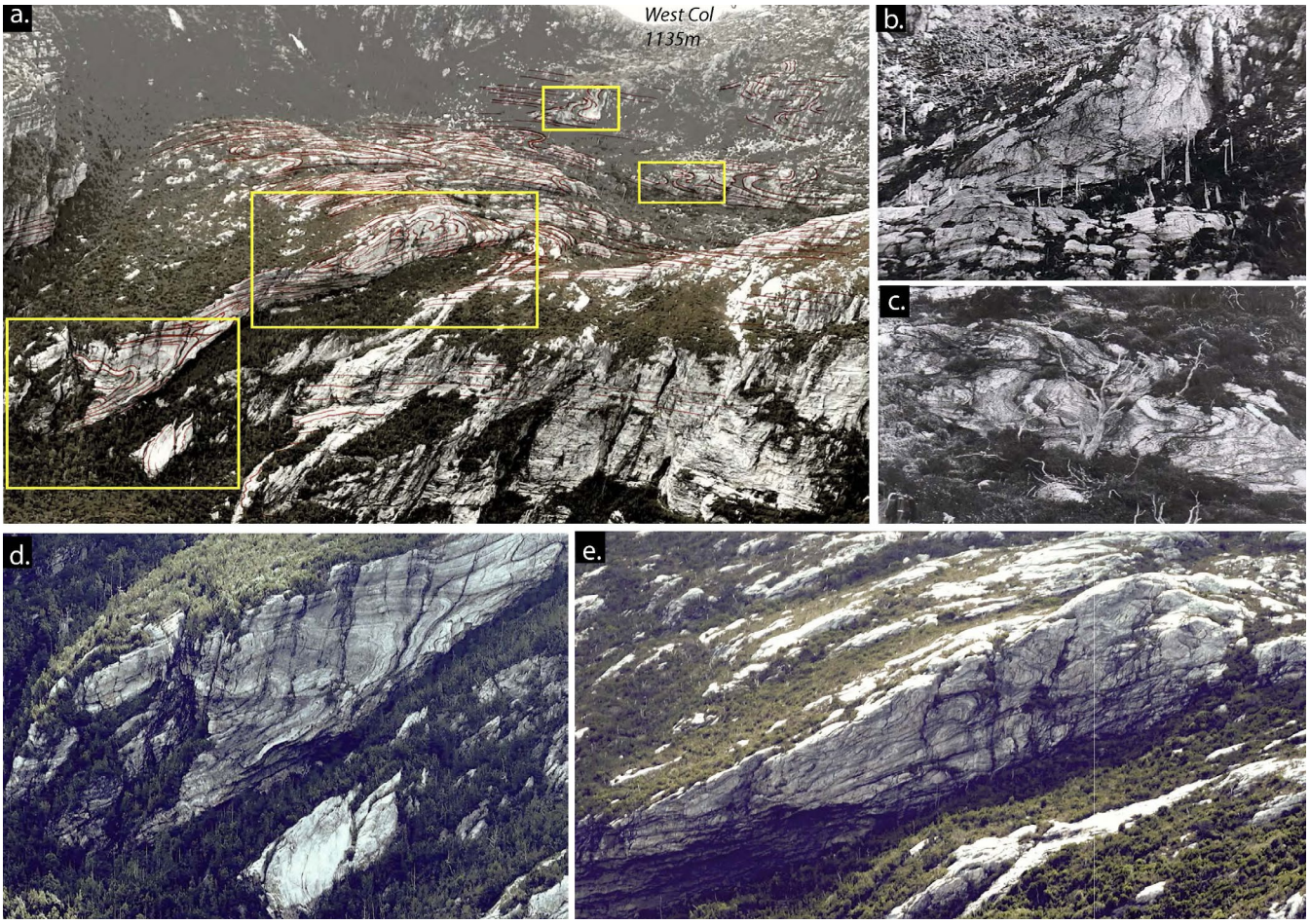

Figure 45. Sophie cirque north wall showing isoclinal fold pairs in the lower limb --strain transition zone beneath the Frenchmans Cap recumbent fold. a) Helicopter photo towards West Col. b) and c) are enlarged views of asymmetric fold pairs (upper yellow boxes in a.) along the recumbent fold lower limb (photos from Duncan, 2021). d) and e) are enlarged parts of the antiformal closure within the intensely foliated zone of the Sophie Cirque Fold Pod. Note the change in geometry along the fold length.

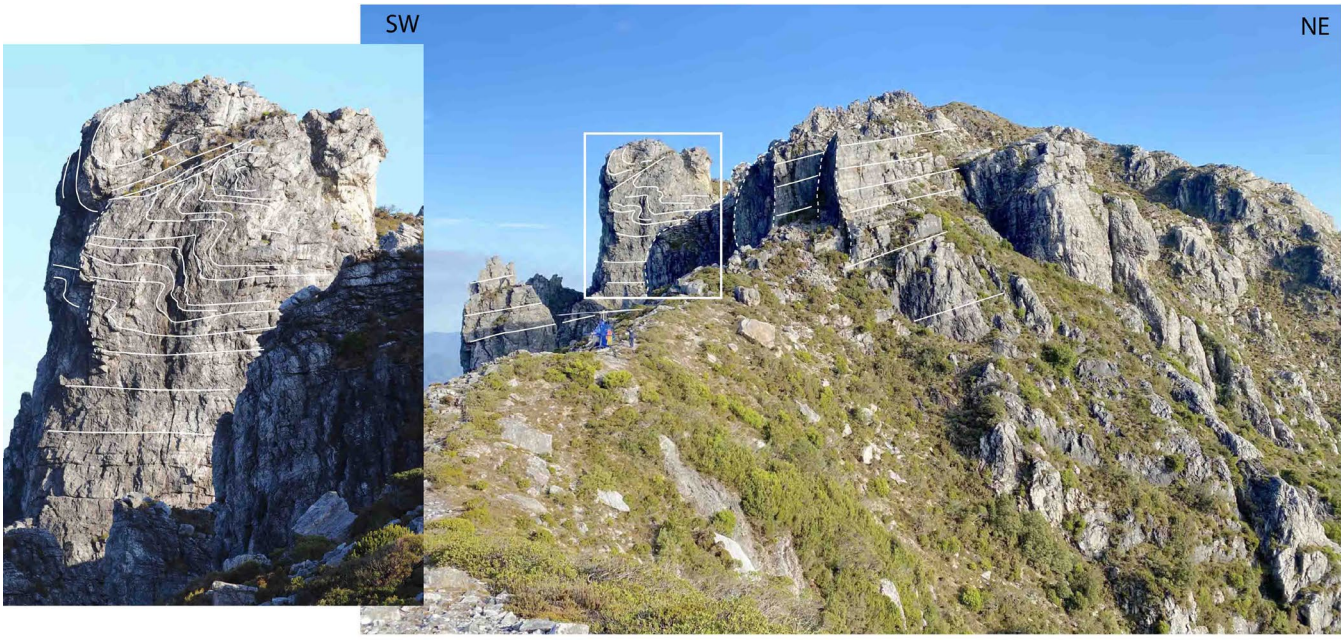

Figure 46. Southwest-closing recumbent fold hinge along the northwest continuation of Lions Head ridge above Lake Nancy. Helicopter for scale. The photo on the left shows an enlargement of the fold hinge.

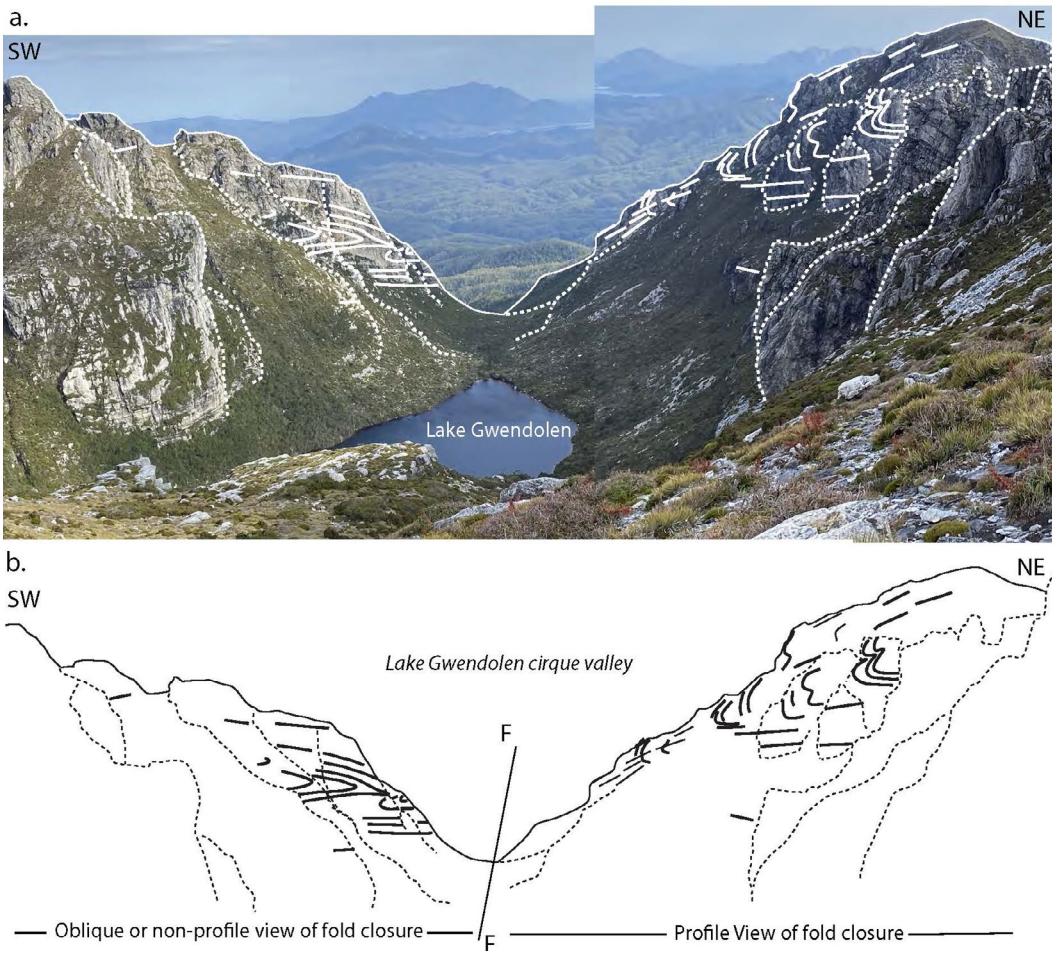

Figure 47. View to the northwest from North Col towards Lake Gwendolen (a) with structural interpretation in (b). F: North Col Fault trace. Note the So/Sm traces in the cirque west wall give an apparent closure to the east as the fold axis lies in or sub-parallel to the wall. The fold (Frenchmans Cap recumbent fold) actually closes to the southwest (see profile views in Figures 37 and 39). The traces in the east wall of the cirque show a profile view of the Lions Head Ridge recumbent fold. Note this is a probable continuation of the Frenchmans Cap recumbent fold across the Gwendolen cirque valley.

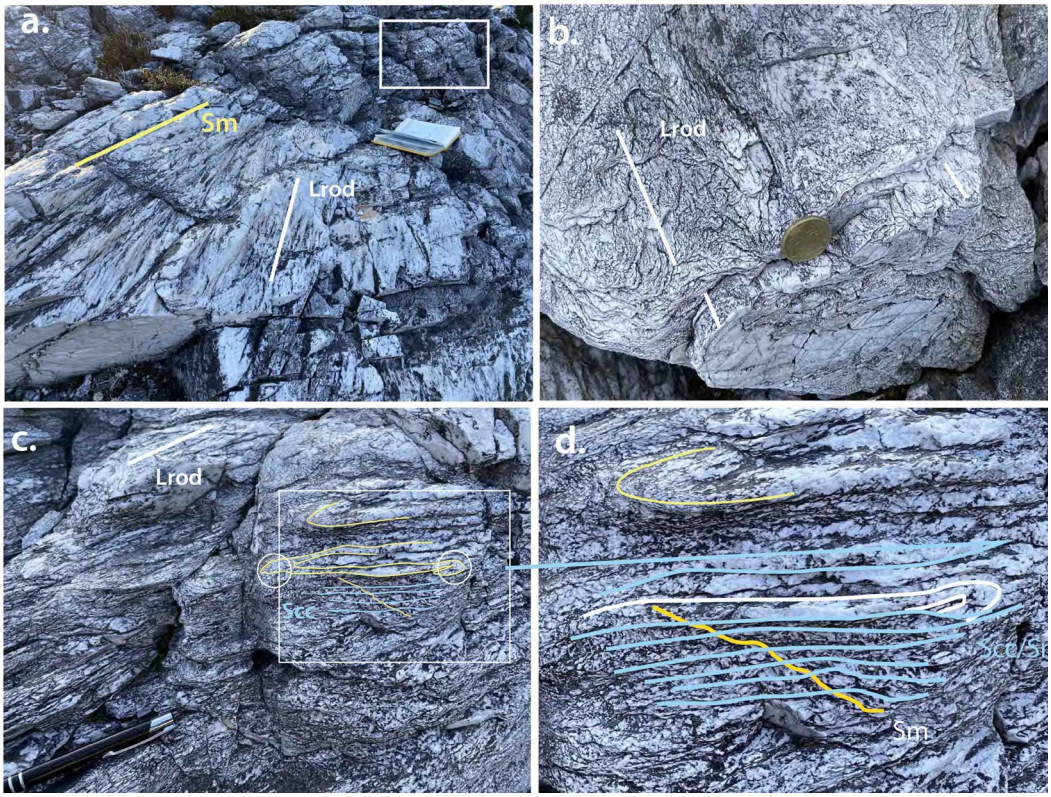

Figure 48. Photos of the complex and composite nature of the dominant foliation Sm in the col-ridge outcrop above Lake Nancy.
a). Gently northeast-dipping Sm with intense rodding fabric.
b) Isoclinal fold hinge folding an early variant of Sm with a boudinaged quartzite layer. Note the fold hinge is sub-parallel to the rodding fabric in the folded Sm.
c) and d) Photos showing the composite nature of the dominant fabric made up of compositional banding/transposition layering (yellow), a very early foliation (orange), and a crenulation foliation Scc (light blue) folding both the Sm (yellow) and early foliation (orange). Hinges of the crenulation folds and isoclines in Sm are sub-parallel and define Lrod. d) Enlargement view of part of c).

5.3 Agamemnon Recumbent Fold

The Agamemnon ridge crest is occupied by a major east-closing recumbent synform (Figure 49) with the flat-topped Agamemnon Plateau providing outcrop of the hinge and transition to the lower limb (Figures 50, 51 and 52). The recumbent fold lower-limb consists of intensely foliated and transposed quartzite with multiple fabrics. This quartzite varies between extremely rodded, platy quartzite and schistose quartzite in character (Figures 53, 54 and 55).

The structural interpretation is based on the apparent alignment of the macro-fold hinges on the Agamemnon plateau ridgeline (Figure 50). The lithology distribution (Figure 51a) is based on aerial photograph interpretation and examination of the photographs taken from the helicopter visit. The re-entrant valley between the main Agamemnon ridge and the ridge southeast of Lake Whitlam has been interpreted as being occupied by dolomitic phyllite (Ltpd) but could also be a phyllite unit within the Fincham-Mary metamorphic sheet. Clearly this will need field checking to resolve.

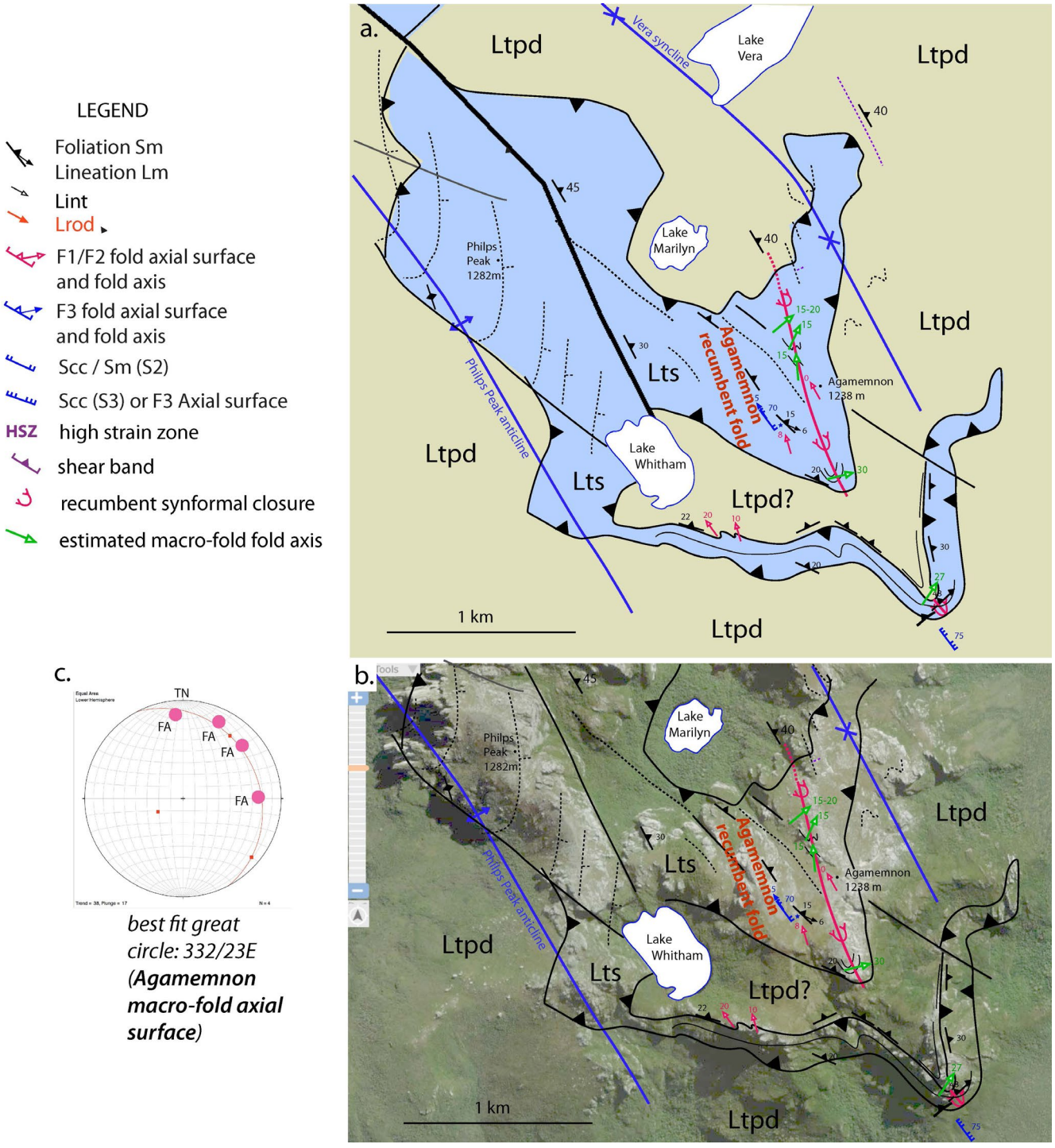

Figure 49. Structural summary map of the Philps Peak-Agamemnon region. a) Lithology map base showing the axial surface trace (red line) of the Agamemnon east-closing synform macro-fold. Macro-fold axes (green arrows) are estimates based on photograph interpretation. The inset stereonet shows macro-fold axis plot and best-fit great circle to give axial surface attitude (332/23E). Blue: quartzite (Lts); Khaki: dolomitic schist-phyllite (Ltpd). b) Google satellite Satellite image map-base showing the ridge forming quartzite outcrops with the recessive Scotchfire dolomitic phyllite occupying the valley areas.

The apparent curvature of the Agamemnon macro-fold axial surface trace (Figure 49) reflects 1) the outcrop intersection of the axial surface (332/23E) with the Agamemnon plateau, and 2) refolding by the younger Devonian northwest-trending fold sets (blue axial surface traces of the Philps Peak anticline and Lake Vera syncline).

Estimated fold axes of the main hinge reflect a change in geometry from reclined (south end) to inclined plunging (north end) (green arrows in Figures 49 and yellow arrows in Figure 50b). Meso-folds along the recumbent fold lower limb exposed in the plateau (Figures 52 and 53) show north-northwest plunges (red arrows in Figure 49).

Structures at the outcrop scale show:

1. High strain, intense transposition with transposition recycling of early fabric with Scc at low angles to dominant Sm (Figures 53, 54 and 55);
2. The L stretch trend is ~305°/125° (Figure 52d); and
3. Meso- to small-scale fold axes range from 290° to 025° (a range of 95°) (Figure 52d).

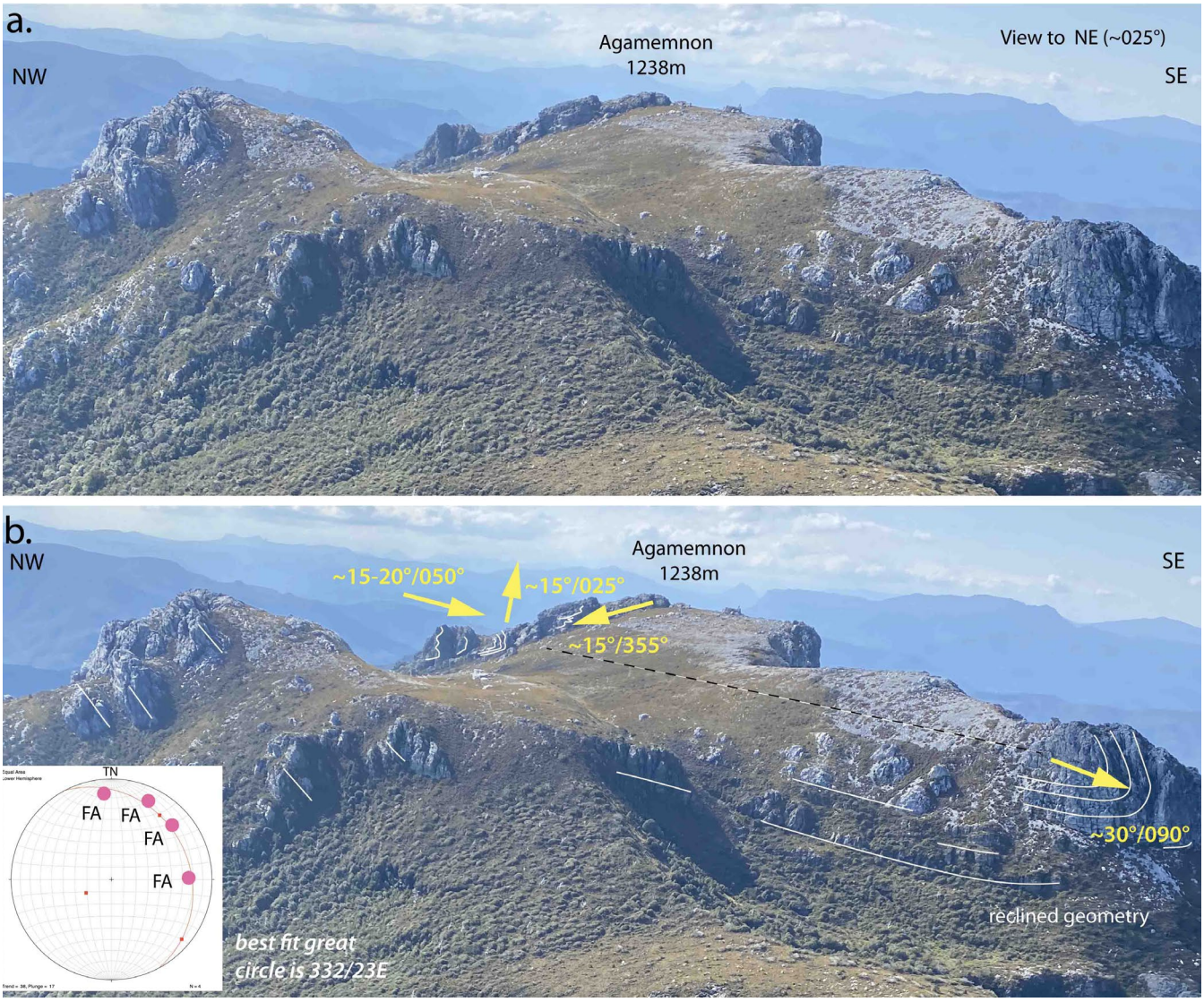

Figure 50. Aerial view of the Agamemnon Plateau showing position of the Agamemnon east-closing, isoclinal recumbent fold. Note macro-fold axis estimates (yellow arrows) are based on photograph interpretations. Fold geometry changes from reclined to inclined plunging with the lower limb preserved in the "plateau" and the upper limb removed by erosion. The stereonet inset shows a great circle best fit of 332/23E to the macro-fold axis determinations along the ridgeline. This equates to the Agamemnon recumbent fold axial surface. The fold closure is depicted by the white formline traces traces in So/Sm.

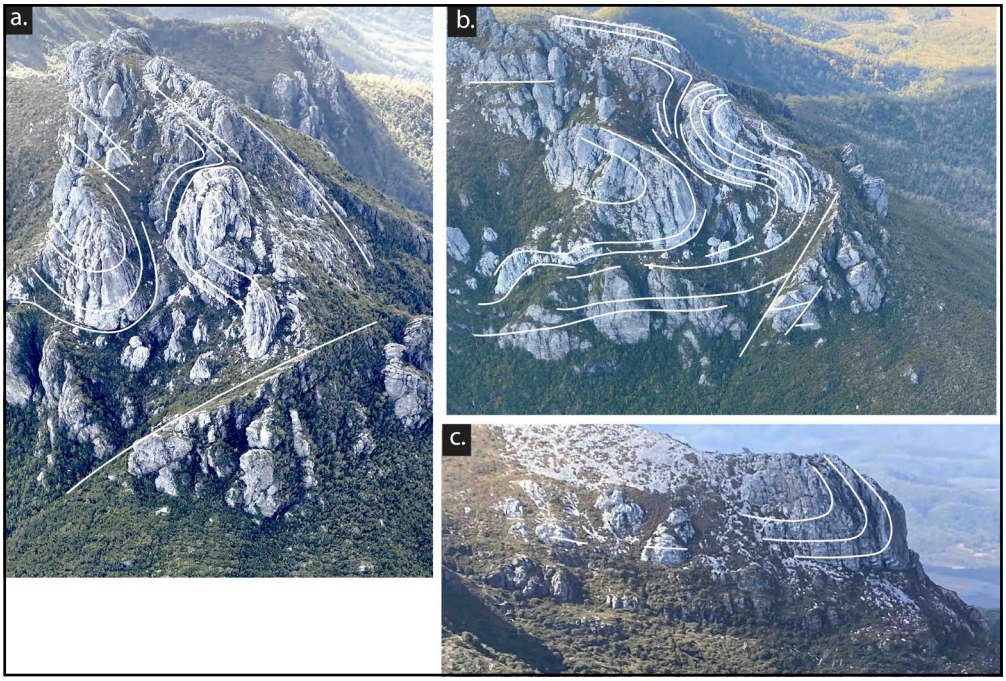

Figure 51. Hinge views of closures of the east-closing Agamemnon recumbent fold at the southern end of the ridgeline. Views are to the north or north-northeast. a) and b) are of the hinge in an isolated, erosional, klippe-like quartzite tongue where the closure sits directly on the contact with the underlying dolomitic phyllite (Scotchfire metamorphic sheet). The younger Devonian deformation distorts the fold closure with refolding of the upper limb and fault truncation of the hinge. Devonian cleavage also overprints the hinge. c) Reclined fold geometry of hinge between Agamemnon peak and the southern end of the plateau (see ridgeline right side of Figure 50).

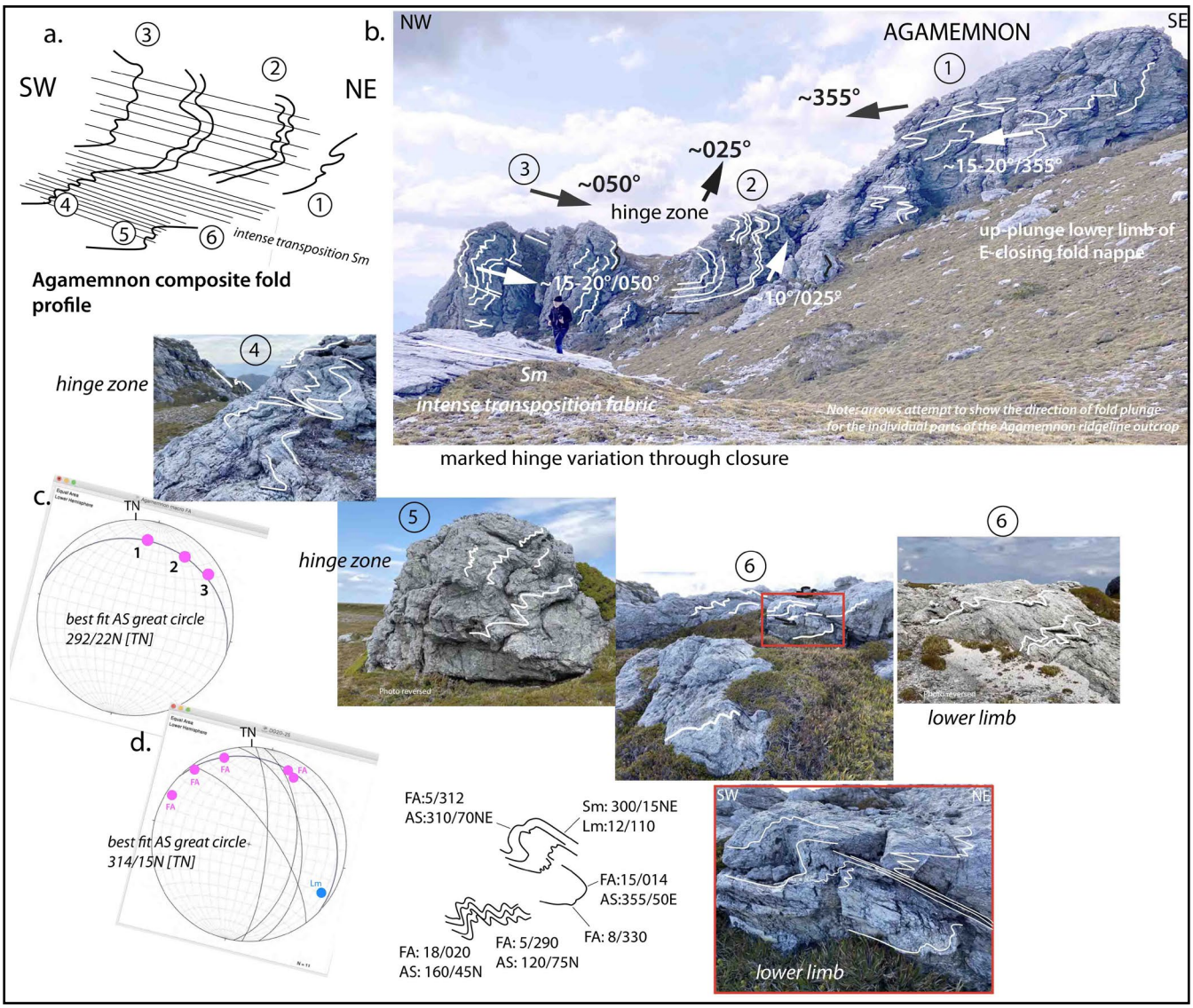

Figure 52. Agamemnon plateau outcrops with a) Composite profile construction of the east-closing Agamemnon recumbent fold. The circled numbers indicate positions of the observed outcrops in the reconstructed profile shown in a). b) Agamemnon summit with formline interpretation. Outcrop 1 closest is lower limb of the macro-fold with minor isoclinal folds plunging 15-20°/355°, whereas 2 and 3 are sections through the closure but showing changing fold axis plunge directions with hinge in outcrop 2 towards 025° and outcrop 3 more to the east at 040-050°. c) Stereonet showing fold axis plots for outcrops 1, 2 and 3 with a best fit axial surface of 292/22N. d) Stereonet with structural data plotted for Outcrop 6. Pink dots are fold-axis data. Blue dot is lineation Lm and great circles are axial surface (AS) plots. The best-fit axial surface is 314/15N. Enlarged part of outcrop 6 on bottom right with sketch and structural data listed as magnetic.

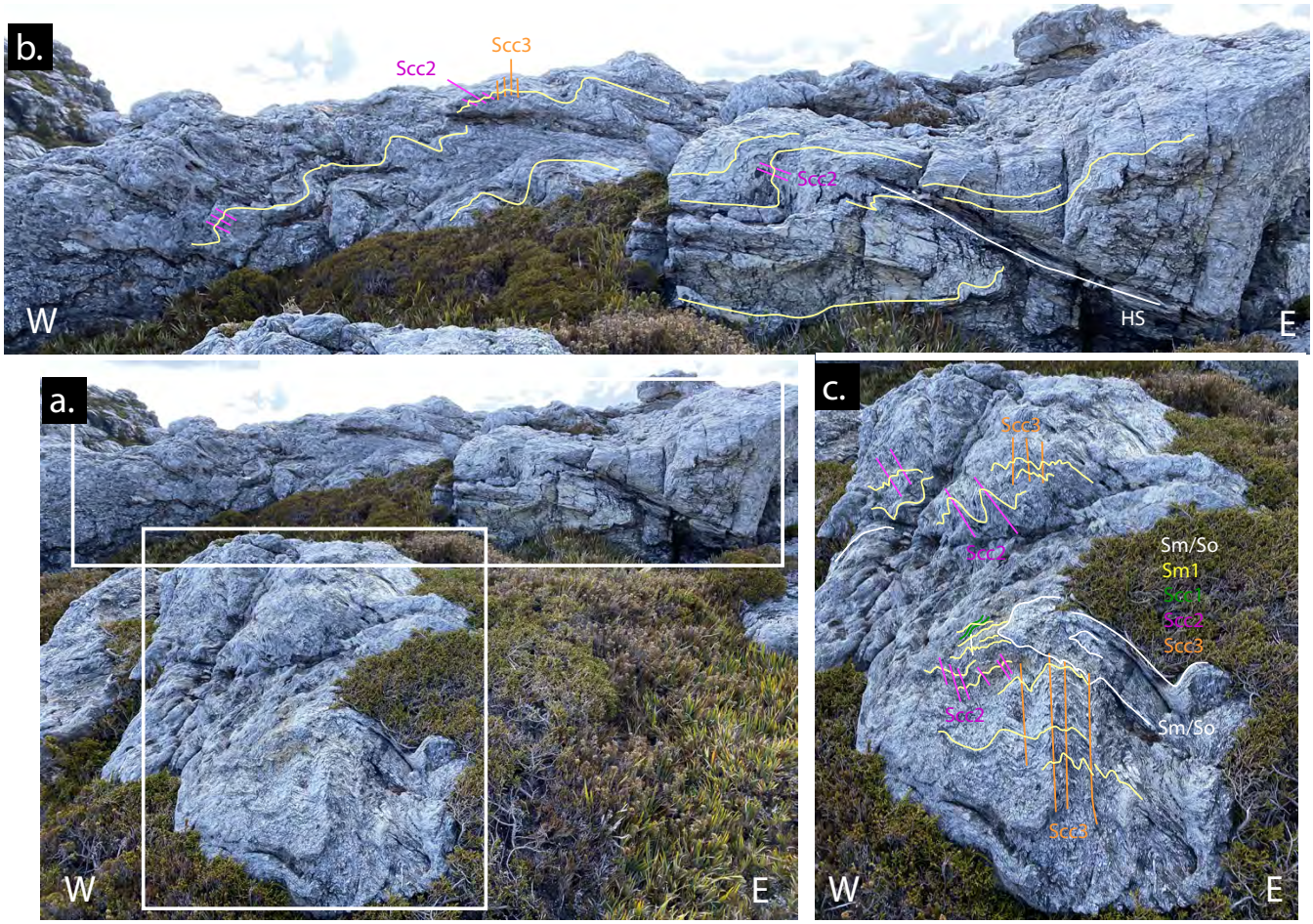

Figure 53. Agamemnon Plateau outcrop view to the north showing the complex structural character of the dominant foliation Sm (compare with Figures 54 and 55) and the overprinting fold phases of the lower limb of the Agamemnon recumbent fold. All views are towards north.

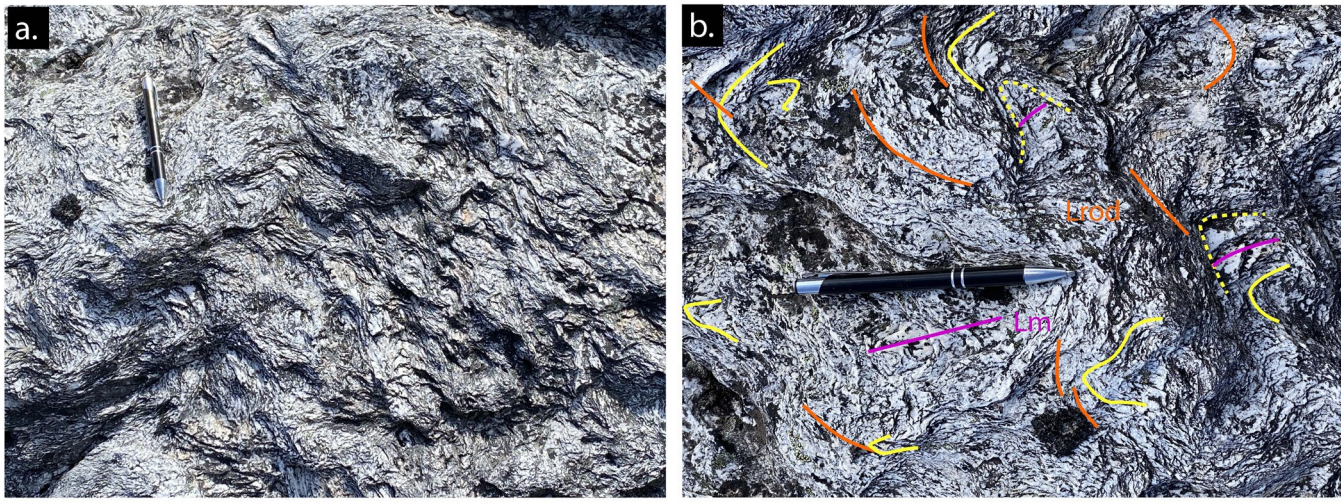

Figure 54. Transposition foliation Sm that dominates the lower limb of the Agamemnon east-closing recumbent fold. a) Typical "swirly" character of intense transposition fabric Sm. b) View onto transposition foliation showing isocline fold closures (yellow), isocline hinge-line traces (orange) and the quartz mineral elongation lineation (Lm) in purple. Most hinges are at high angles to the stretching direction indicated by Lm.

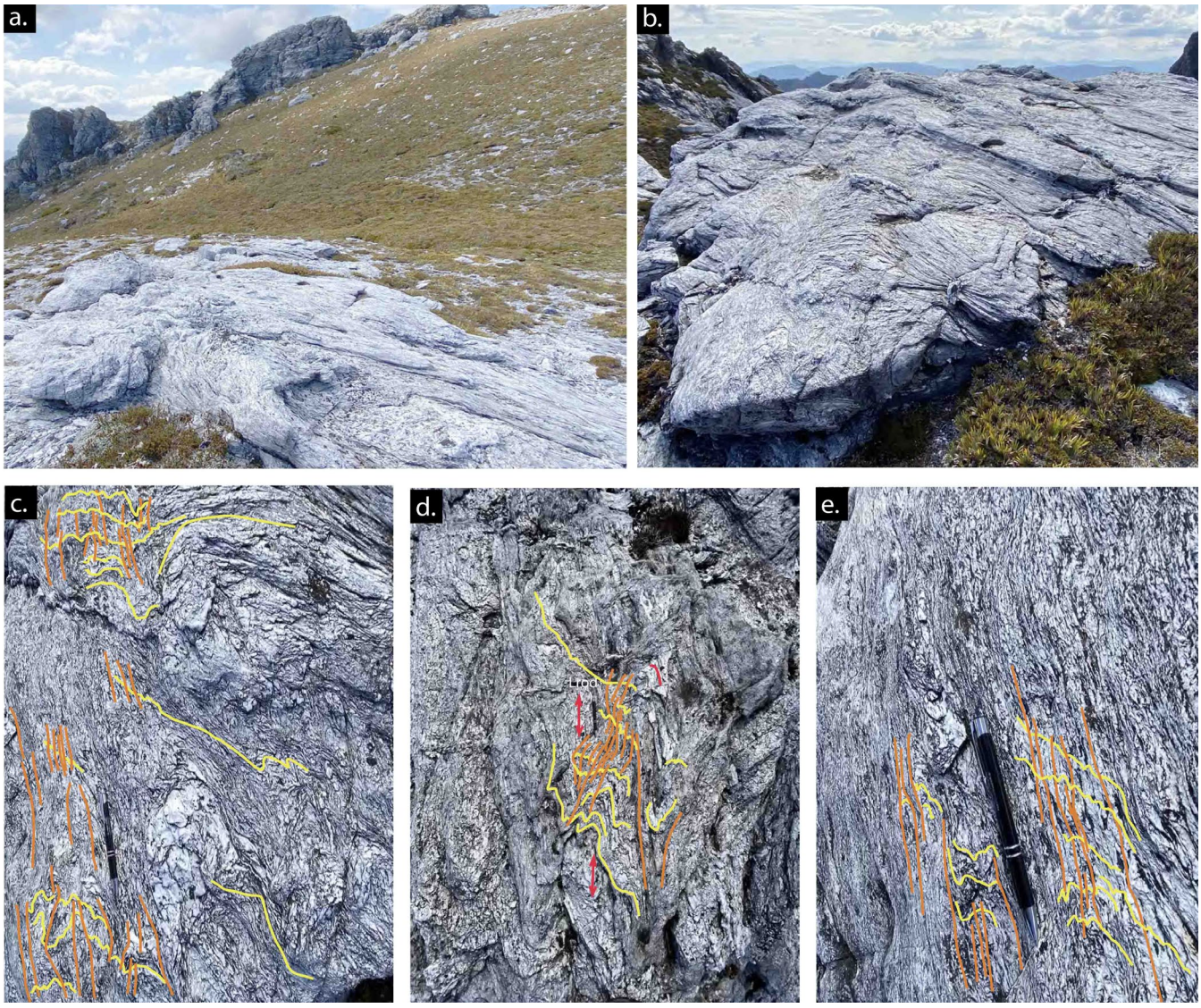

Figure 55. Agamemnon foliation photographs from Outcrop 4 in Figure 52. View is to the north. a) Core of mesoscopic isoclinal fold in "swirly" quartzite with the ridgeline outcrops containing the macroscopic Agamemnon fold hinge. b) Pod-like domains of relict crenulation cleavages and hinges of small-scale folds alternating with intensely foliated domains defining limbs of the "hinge pods". The dominant foliation displays internal-boudinage and quartz tension gash veins at high angle to the outcrop stretching direction (L stretch). c), d) and e) outcrop photographs showing intense transposition of quartzite early layering, multiple overprinting crenulation cleavage fabrics accompanied by marked rodding of small scale folds (see also Figure 54 above). They illustrate the composite nature of the dominant foliation. Early formed Sm (yellow traces) refolded and crenulated by a crenulation cleavage (orange traces) that intensifies and becomes another dominant sub-parallel foliation. Compare with fabrics in (e). Red arrows in d) indicate the lineation Lm traces on Sm surfaces that are oblique to the plane of the photo.

6. Geometry of the recumbent Folds - A Summary

Macro-recumbent folds overlie a zone of high-strain fabrics that reflect an increase in strain towards the basal part of the low-grade Fincham-Mary metamorphic sheet. The high-strain transposition fabrics are transitional into, or are part of, the recumbent fold lower limbs (Figures 56 and 57).

Given 1) the oppositely closing nature of the Frenchmans Cap and Agamemnon recumbent folds at the same structural level, and 2) the convergence of the quartzite outcrop belts containing the hingelines to the north, a possible geometry is a macro-sheath pod where both individual recumbent folds converge northwestwards (Figure 58). The implied geometry and 3D form of a northwest tapering wedge in quartzite matches the mapped outcrop pattern (Figures 4 and 5), although faulting along the Fincham-Mary sheet contact with the Scotchfire sheet and a younger Devonian folding overprint complicate the relationships (see discussion in Duncan, 1974, p. 193-194).

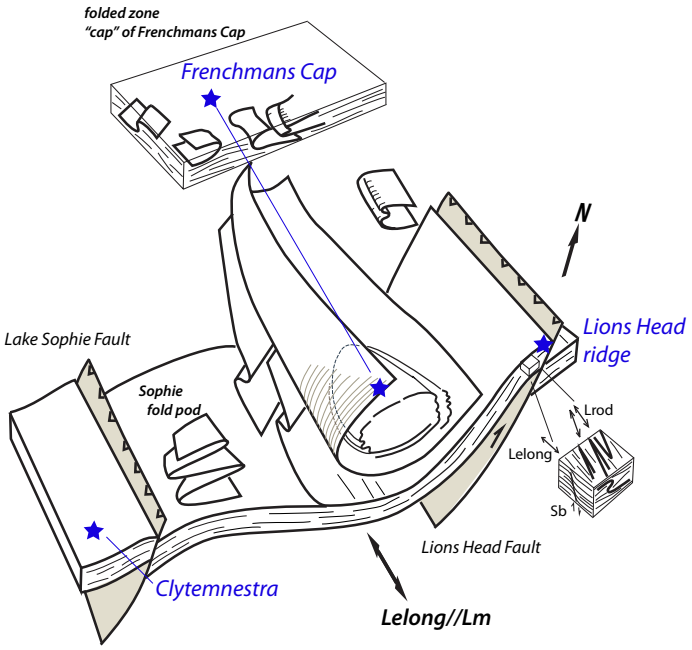

Figure 56 (Left). Schematic summary diagram of the Frenchmans Cap recumbent fold geometry with schematics of meso-fold attitudes and fabric relationships also shown. Distance from Clytemnestra (left side) to Lions Head ridge (right side) is ~3 km. The blue stars show geographic positions. Note the folded zone "cap" to Frenchmans Cap is offset from the actual position to enable the geometry below the cap zone to be shown. The blue location-stars for Frenchmans Cap are linked by the thin blue line to the actual position. The macro-fold hingelne is approximately sub-parallel to the stretching lineation Lelong/ Lm. The position of the Sophie Cirque Fold Pod above the basal lower limb high-strain zone is also shown. Late brittle faults with reverse west-over-east movement are included as the Lake Sophie and Lions Head Faults. Sb: shear band.

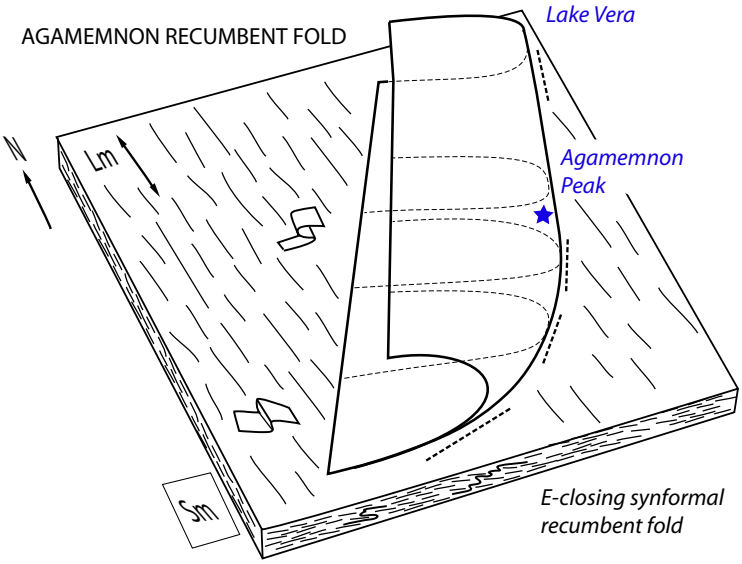

Figure 57 (Right). Schematic summary diagram of the east-closing Agamemnon recumbent fold showing the curvilinear hingeline of the fold relative to the lineation Lm (equivalent to the regional stretching direction) and the attitudes of meso-folds on the lower limb transition. These are transitional into the basal high-strain zone. The basal high-strain layer (dashed) has ~2 km width.

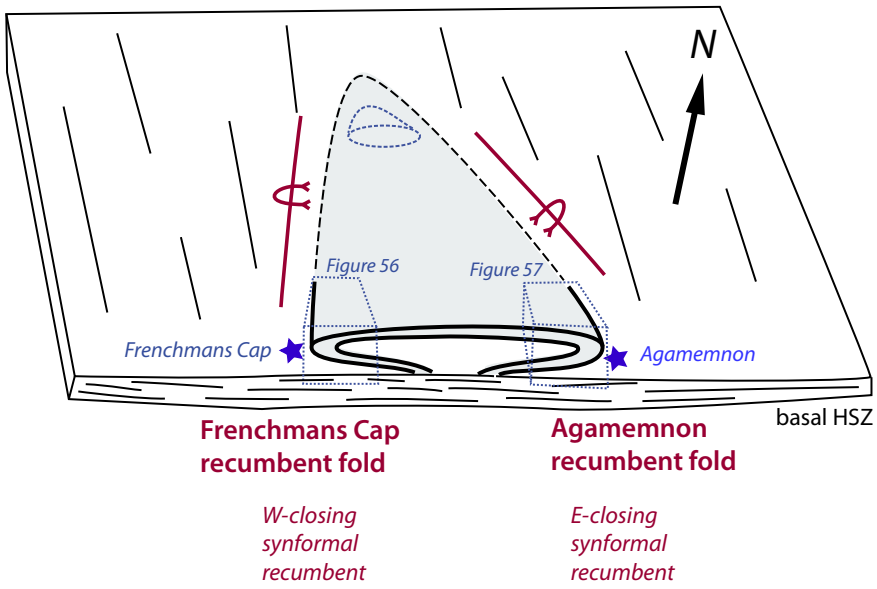

Figure 58 (Left). Possible geometrical relationships between the west-closing Frenchmans Cap and east-closing Agamemnon recumbent folds as a linked macro-regional sheath fold tapering to the northwest (see Frenchmans Cap map: Figure 4). Approximate scale of the macro-sheath pod is ~6 km width and ~10 km map length extent with sheath closure at or near the Franklin River to the north.

7. Conclusions

The Frenchmans Cap region shows the structure within the lower part of the low-grade Fincham-Mary metamorphic sheet, into and across the contact with the underlying dolomitic phyllite of the low-grade Scotchfire metamorphic sheet.

Two, kilometre-scale, recumbent isoclinal folds dominate the structure and occupy the quartzite ridges of Frenchmans Cap and Agamemnon. Their attenuated lower limbs are transitional into a basal high-strain zone towards the contact with the structurally lower Scotchfire sheet. This high-strain zone is defined by intensely foliated transposition layering within platy quartzite containing rare, isolated mesocopic isoclines as small pods or augens at metre scales, a strong rodding fabric, and relict sub-horizontal crenulation cleavage(s) at low angles to the dominant foliation Sm.

The two regional-scale recumbent folds formed during a west-over-east emplacement of the low-grade Fincham-Mary sheet quartzites over the low-grade Scotchfire dolomitic phyllites. The shear sense towards ~110° is recorded by shear bands (S-C' structures) and macro shear-band boudins.

Younger, open north-northwest-trending folds broadly warp the recumbent folds and associated fabrics, coupled with brittle west-over-east reverse faulting along the Fincham-Mary metamorphic sheet contact with the Scotchfire metamorphic sheet.

8. References

Alsop, G. I., Holdsworth, R. E. 1999. Vergence and facing patterns in large scale sheath fold. J. Struct. Geol., 21, 1335-1349.

Berry, R. F. AND Crawford, A. J. 1988. The tectonic significance of Cambrian allochthonous mafic-ultramafic complexes in Tasmania. *Australian Journal of Earth Sciences* 35, 523-533.

Berry, R. F. 2014. Chapter 4.2 Cambrian Tectonics – The Tyennan Orogeny. In Corbett, K.D., Quilty, P.G & Calver, C.R. editors, *Geological Evolution of Tasmania* pp 95-110. *Geological Society of Australia Special Publication 24*, Geological Society of Australia (Tasmania Division).

Brown, D. A., Hand, M. and Morrissey, L. J. 2021. Zircon petrochronology and mineral equilibria of the eclogites from western Tasmania: Interrogating the early Proterozoic East Gondwana subduction record. *Gondwana Research*, 93, 252-274.

Carey, S. W. 1953. Geological structure of Tasmania in Relation to Mineralisation. *5th Emp. Min. and Metall. Congr., 1*, 1108-1128.

Chmielowski, R. M. 2009. *The Cambrian metamorphic history of Tasmania*. PhD thesis, University of Tasmania.

Chmielowski, R. M. and Berry, R. F. 2012. The Cambrian Metamorphic History of Tasmania: The Metapelites. *Australian Journal of Earth Sciences* 59(7), 1007-1019.

Collins, K. 1990. *South-West Tasmania: A Natural; History and Visitors Guide*. Heritage Books. 368p.

Dietrich, D. and Casey, M. 1989. A new tectonic model for the Helvetic nappes, in Alpine Tectonics, (eds Coward, M.P., Dietrich, D. and Park, R.G.) *Geological Society of London Special Publication 45*, 47–63.

Duncan, D. McP. 1974. Reconnaissance geology of the Frenchmans Cap National Park. *Papers and Proceedings of the Royal Society of Tasmania*. vol 107, 191-195.

Duncan, D. McP. 2021. History of Structural Studies at Frenchmans Cap and Wards Bluff 1964/1965. Unpubl. Report Mineral Resources Tasmania. 4p.

Goscombe, B.D. 1990. Equilibrium thermodynamics of the Lyell Highway eclogites. Unpublished Report 1990_19. Tasmania Department of Energy and Minerals.

Kamperman, M. 1984. *The Precambrian metamorphic geology of the Lyell Highway-Collingwood River area*. B.Sc (Hons) Thesis, University of Tasmania: Hobart.

Kleinig, S. 2012. *Frenchmans Cap: Story of a Mountain*. Glass House Books. 271p.

Meffre, S., Berry, R. F. and Hall, M. 2000. Cambrian metamorphic complexes in Tasmania: tectonic implications. *Australian Journal of Earth Sciences 47,* 971-985.

Palmeri, R., Chmielowski, R., Sandroni, S., Talarico, F. and Ricci, C.A. 2009. Petrology of the eclogites from western Tasmania: Insights into the Cambro-Ordovician evolution of the paleo-Pacific margin of Gondwana. *Lithos 109*, 223-239.

Peterson, J.A. 1966, Glaciation of Frenchmans Cap-National Park. *Papers and Proceedings of the Royal Society of Tasmania*, vol. 100, 117-134.

Raheim, A. 1976. Petrology of Eclogites and Surrounding Schists from the Lyell Highway - Collingwood River Area. *J. Geol. Soc. Aust.*, 23, 313-328.

Ramsay, J. G., Casey, M., and Kligfield, R. 1983. Role of shear in development of Helvetic fold thrust belt of Switzerland. *Geology 11*, 439-442.

Spry, A.H. 1963. The occurrence of eclogite on the Lyell Highway, Tasmania. *Mineralogical Magazine 33,* 589-593.

Turner, N.J. 1989. Precambrian. In: BURRETT, C.F. and MARTIN, E.L. eds, *Geology and Mineral Resources of Tasmania. Geological Society of Tasmania Special Publication 15*, 5-46.

Wilkinson, B. edit. 2011. The Abels: A Comprehensive Guide to Tasmania's Mountains over 1100m High. Volume 2. *Tasmanian Outdoors Collection Publishers,* 204p.

9. Acknowledgements

- Andrew McNeill for providing support through the 2016-2020 Geoscience Initiative, reviewing the document and providing comments.
- Ron Berry for insightful comments and careful review of the document.
- Nic Turner and David Duncan for discussions and comments on the draft manuscript.
- Chris Large for editing and formatting of the final publication.
- David Duncan for providing access to his Frenchmans Cap and Wards Bluff B/W photographs and negatives.
- Parks and Wildlife Service (PWS) for access into the World Heritage area for data and sample collection.
- Jason Bradbury DPIPWE for assistance with WHA and PWS permits for scientific research.
- Nic Deka PWS for assistance with access into Mt McCall and Frenchmans Cap.
- Rodney Smith from Rotorlift for helicopter transport into Frenchmans Cap and skilled landings in difficult topography.
- Rick Allmendinger and Nestor Cardozzo for use of OSX Stereonet.

APPENDIX 1

TABULATED STRUCTURAL MEASUREMENTS

File Download

Tyennan Structural Measurements

Datum: GDA94 - MGA Zone 55

Project	Structure	Structure Type	Dip	D/Direct	Reliability	Secondary Dip	Secondary D/Direct	Comments	Originator	Chronostra-tigraphy	Collection Date	Field #	East	North	Accu-racy	Location Method
Tyennan	Fold axis	Haa + Pac	10	318	1 - Most reliable	15	254	FA/As	David Gray	Proterozoic	28/03/2020	DG20-17.1	403135	5320668	10m	GPS
Tyennan	Fold axis	Haa + Pac	20	144	1 - Most reliable	25	134	FA/AS	David Gray	Proterozoic	28/03/2020	DG.20.24.3	402773	5318138	10m	GPS
Tyennan	Fold axis	Haa + Pac	5	304	1 - Most reliable	75	34	FA/As	David Gray	Proterozoic	28/03/2020	DG.20.25.5	407514	5317016	10m	GPS
Tyennan	Lineation	Lao	4	314	1 - Most reliable			Lgrain	David Gray	Proterozoic	28/03/2020	DG20-17.2	403133	5320680	10m	GPS
Tyennan	Lineation	Lag	5	314	1 - Most reliable			Lrod	David Gray	Proterozoic	28/03/2020	DG20-17.2	403133	5320680	10m	GPS
Tyennan	Metamorphic Foliation	Sag	14	236	1 - Most reliable			Sm	David Gray	Proterozoic	28/03/2020	DG20-17.2	403133	5320680	10m	GPS
Tyennan	Fold axis	Haa + Pac	4	319	1 - Most reliable	62	39	A	David Gray	Proterozoic	28/03/2020	DG20.18.1	403550	5320381	10m	GPS
Tyennan	Bedding	Baf	75	89	1 - Most reliable			S0	David Gray	Proterozoic	28/03/2020	DG20.18.2	403550	5320381	10m	GPS
Tyennan	Cleavage	Cae	40	194	1 - Most reliable			S1	David Gray	Proterozoic	28/03/2020	DG20.18.2	403550	5320381	10m	GPS
Tyennan	Lineation	Laj	6	324	1 - Most reliable			Lcren	David Gray	Proterozoic	28/03/2020	DG20.18.3	403550	5320381	10m	GPS
Tyennan	Crenulation Cleav-age	Cai	53	54	1 - Most reliable			Scc	David Gray	Proterozoic	28/03/2020	DG20.18.3	403550	5320381	10m	GPS
Tyennan	Metamorphic Foliation	Sag	72	240	1 - Most reliable			Sm	David Gray	Proterozoic	28/03/2020	DG20.19.1	403484	5320339	10m	GPS
Tyennan	Metamorphic Foliation	Sah	90	149	1 - Most reliable			Sm	David Gray	Proterozoic	28/03/2020	DG20.19.1	403484	5320339	10m	GPS
Tyennan	Lineation	Lae	20	304	1 - Most reliable			Lm/Lrod	David Gray	Proterozoic	28/03/2020	DG20.19.2	403484	5320339	10m	GPS
Tyennan	Metamorphic Foliation	Sag	30	254	1 - Most reliable			Sm	David Gray	Proterozoic	28/03/2020	DG20.19.2	403484	5320339	10m	GPS
Tyennan	Lineation	Lao	15	310	1 - Most reliable			Lelong	David Gray	Proterozoic	28/03/2020	DG20.19.3	403484	5320339	10m	GPS
Tyennan	Lineation	Lag	14	319	1 - Most reliable			Lrod	David Gray	Proterozoic	28/03/2020	DG20.19.3	403484	5320339	10m	GPS
Tyennan	Metamorphic Foliation	Sag	20	294	1 - Most reliable			Sm	David Gray	Proterozoic	28/03/2020	DG20.19.4	403484	5320339	10m	GPS
Tyennan	Fold axis	Haa	5	319	1 - Most reliable			FA	David Gray	Proterozoic	28/03/2020	DG20.19.5	403484	5320339	10m	GPS
Tyennan	Lineation	Lao	18	294	1 - Most reliable			Lelong	David Gray	Proterozoic	28/03/2020	DG20.20.1	403615	5320007	10m	GPS
Tyennan	Fold axis	Haa + Pac	15	314	1 - Most reliable	45	14	FA/As	David Gray	Proterozoic	28/03/2020	DG20.20.2	403615	5320007	10m	GPS
Tyennan	Metamorphic Foliation	Sag	25	34	1 - Most reliable			Sm	David Gray	Proterozoic	28/03/2020	DG20.20.3	403615	5320007	10m	GPS
Tyennan	Metamorphic Foliation	Sag	85	54	1 - Most reliable			Sm	David Gray	Proterozoic	28/03/2020	DG20.20.4	403615	5320007	10m	GPS
Tyennan	Lineation	Lao	15	284	1 - Most reliable			Lelong	David Gray	Proterozoic	28/03/2020	DG20.20.5	403615	5320007	10m	GPS
Tyennan	Metamorphic Foliation	Sag	15	294	1 - Most reliable			Sm	David Gray	Proterozoic	28/03/2020	DG20.20.5	403615	5320007	10m	GPS

Project	Structure	Structure Type	Dip	D/Direct	Reliability	Secondary Dip	Secondary D/Direct	Comments	Originator	Chronostra-tigraphy	Collection Date	Field #	East	North	Accu-racy	Location Method
Tyennan	Lineation	Lao	4	290	1 - Most reliable			Lelong	David Gray	Proterozoic	28/03/2020	DG20.21.1	403716	5319950	10m	GPS
Tyennan	Shear Band	Sau	26	154	1 - Most reliable			Sb	David Gray	Proterozoic	28/03/2020	DG20.21.1	403716	5319950	10m	GPS
Tyennan	Metamorphic Foliation	Sag	15	54	1 - Most reliable			Sm	David Gray	Proterozoic	28/03/2020	DG20.21.1	403716	5319950	10m	GPS
Tyennan	Lineation	Lae	8	144	1 - Most reliable			Lm	David Gray	Proterozoic	28/03/2020	DG20.22.1	403718	5319934	10m	GPS
Tyennan	Metamorphic Foliation	Sag	40	64	1 - Most reliable			Sm	David Gray	Proterozoic	28/03/2020	DG20.22.1	403718	5319934	10m	GPS
Tyennan	Fold axis	Haa + Pac	8	194	1 - Most reliable	23	280	FA/As	David Gray	Proterozoic	28/03/2020	DG20.22.2	403718	5319934	10m	GPS
Tyennan	Fault	Fac	70	114	1 - Most reliable			Fault	David Gray	Proterozoic	28/03/2020	DG20.22.3	403718	5319934	10m	GPS
Tyennan	Fold axis	Haa	10	304	1 - Most reliable			FA	David Gray	Proterozoic	28/03/2020	DG.20.22b.1	403713	5319934	10m	GPS
Tyennan	Lineation	Lae	8	309	1 - Most reliable			Lm/ Lelong	David Gray	Proterozoic	28/03/2020	DG.20.22b.1	403713	5319934	10m	GPS
Tyennan	Fault	Fac	45	264	1 - Most reliable			Fault	David Gray	Proterozoic	28/03/2020	DG.20.22b.2	403713	5319934	10m	GPS
Tyennan	Fold axis	Haa	10	139	1 - Most reliable			FA	David Gray	Proterozoic	28/03/2020	DG.20.23	403762	5319866	10m	GPS
Tyennan	Fold axis	Haa	13	319	1 - Most reliable			FA	David Gray	Proterozoic	28/03/2020	DG.20.24.1	402773	5318138	10m	GPS
Tyennan	Lineation	Lao	22	294	1 - Most reliable			Lelong	David Gray	Proterozoic	28/03/2020	DG.20.24.1	402773	5318138	10m	GPS
Tyennan	Metamorphic Foliation	Sag	25	290	1 - Most reliable			Sm	David Gray	Proterozoic	28/03/2020	DG.20.24.1	402773	5318138	10m	GPS
Tyennan	Crenulation Cleav-age	Cai	80	224	1 - Most reliable			Scc	David Gray	Proterozoic	28/03/2020	DG.20.24.4	402773	5318138	10m	GPS
Tyennan	Fold axis	Haa + Pac	5	326	1 - Most reliable	70	54	FA/As	David Gray	Proterozoic	28/03/2020	DG.20.25.1	407514	5317016	10m	GPS
Tyennan	Lineation	Lae	12	124	1 - Most reliable			Lm	David Gray	Proterozoic	28/03/2020	DG.20.25.2	407514	5317016	10m	GPS
Tyennan	Metamorphic Foliation	Sag	15	44	1 - Most reliable			Sm	David Gray	Proterozoic	28/03/2020	DG.20.25.2	407514	5317016	10m	GPS
Tyennan	Fold axis	Haa + Pac	25	28	1 - Most reliable	50	99	FA/As	David Gray	Proterozoic	28/03/2020	DG.20.25.3	407514	5317016	10m	GPS
Tyennan	Fold axis	Haa	8	344	1 - Most reliable			FA	David Gray	Proterozoic	28/03/2020	DG.20.25.4	407514	5317016	10m	GPS
Tyennan	Fold axis	Haa + Pac	18	34	1 - Most reliable	45	84	FA/As	David Gray	Proterozoic	28/03/2020	DG.20.25.6	407514	5317016	10m	GPS
Tyennan	Fold axis	Haa	7	335	3			A	Duncan, D.McP.	Proterozoic	1/05/1964		401900	5317810	100m	Estimate
Tyennan	Metamorphic Foliation	Sag	22	255	3			Sm	Duncan, D.McP.	Proterozoic	1/05/1964		401900	5317810	100m	Estimate
Tyennan	Lineation	Lae	8	345	3			Lm	Duncan, D.McP.	Proterozoic	1/05/1964		402138	5318039	100m	Estimate
Tyennan	Metamorphic Foliation	Sag	30	52	3			Sm	Duncan, D.McP.	Proterozoic	1/05/1964		402138	5318039	100m	Estimate
Tyennan	Lineation	Lae	23	144	3			Lm	Duncan, D.McP.	Proterozoic	1/05/1964		402661	5318050	100m	Estimate
Tyennan	Metamorphic Foliation	Sag	40	210	3			Sm	Duncan, D.McP.	Proterozoic	1/05/1964		405211	5318434	100m	Estimate

Project	Structure	Structure Type	Dip	D/Direct	Reliability	Secondary Dip	Secondary D/Direct	Comments	Originator	Chronostra-tigraphy	Collection Date	Field #	East	North	Accu-racy	Location Method
Tyennan	Lineation	Lae	6	310	3			Lm	Duncan, D.McP.	Proterozoic	1/05/1964		403127	5318638	100m	Estimate
Tyennan	Metamorphic Foliation	Sag	27	25	3			Sm	Duncan, D.McP.	Proterozoic	1/05/1964		403127	5318638	100m	Estimate
Tyennan	Metamorphic Foliation	Sag	53	275	3			Sm	Duncan, D.McP.	Proterozoic	1/05/1964		405282	5318657	100m	Estimate
Tyennan	Fold axis	Haa	12	130	3			A	Duncan, D.McP.	Proterozoic	1/05/1964		403283	5318756	100m	Estimate
Tyennan	Metamorphic Foliation	Sag	15	268	3			Sm	Duncan, D.McP.	Proterozoic	1/05/1964		403283	5318756	100m	Estimate
Tyennan	Fold axis	Haa	19	330	3			A	Duncan, D.McP.	Proterozoic	1/05/1964		402524	5319286	100m	Estimate
Tyennan	Metamorphic Foliation	Sag	29	45	3			Sm	Duncan, D.McP.	Proterozoic	1/05/1964		402524	5319286	100m	Estimate
Tyennan	Fold axis	Haa	18	145	3			A	Duncan, D.McP.	Proterozoic	1/05/1964		405157	5319297	100m	Estimate
Tyennan	Metamorphic Foliation	Sag	24	270	3			Sm	Duncan, D.McP.	Proterozoic	1/05/1964		405157	5319297	100m	Estimate
Tyennan	Metamorphic Foliation	Sag	40	228	3			Sm	Duncan, D.McP.	Proterozoic	1/05/1964		404892	5319508	100m	Estimate
Tyennan	Metamorphic Foliation	Sag	20	90	3			Sm	Duncan, D.McP.	Proterozoic	1/05/1964		404771	5319538	100m	Estimate
Tyennan	Fold axis	Haa	10	330	3			A	Duncan, D.McP.	Proterozoic	1/05/1964		403094	5319586	100m	Estimate
Tyennan	Metamorphic Foliation	Sag	30	25	3			Sm	Duncan, D.McP.	Proterozoic	1/05/1964		403094	5319586	100m	Estimate
Tyennan	Metamorphic Foliation	Sah	90	38	3			Sm	Duncan, D.McP.	Proterozoic	1/05/1964		405199	5319601	100m	Estimate
Tyennan	Lineation	Lae	5	310	3			Lm	Duncan, D.McP.	Proterozoic	1/05/1964		403545	5319733	100m	Estimate
Tyennan	Metamorphic Foliation	Sag	14	15	3			Sm	Duncan, D.McP.	Proterozoic	1/05/1964		403545	5319733	100m	Estimate
Tyennan	Fold axis	Haa	11	142	3			A	Duncan, D.McP.	Proterozoic	1/05/1964		403771	5319934	100m	Estimate
Tyennan	Metamorphic Foliation	Sag	35	290	3			Sm	Duncan, D.McP.	Proterozoic	1/05/1964		403771	5319934	100m	Estimate
Tyennan	Metamorphic Foliation	Sag	17	270	3			Sm	Duncan, D.McP.	Proterozoic	1/05/1964		403830	5320069	100m	Estimate
Tyennan	Metamorphic Foliation	Sag	7	90	3			Sm	Duncan, D.McP.	Proterozoic	1/05/1964		404003	5320089	100m	Estimate
Tyennan	Metamorphic Foliation	Sag	15	102	3			Sm	Duncan, D.McP.	Proterozoic	1/05/1964		403532	5320128	100m	Estimate

Project	Structure	Structure Type	Dip	D/Direct	Reliability	Secondary Dip	Secondary D/Direct	Comments	Originator	Chronostra-tigraphy	Collection Date	Field #	East	North	Accu-racy	Location Method
Tyennan	Metamorphic Foliation	Sah	90	38	3			Sm	Duncan, D.McP.	Proterozoic	1/05/1964		403479	5320367	100m	Estimate
Tyennan	Lineation	Lae	44	279	3			Lm	Duncan, D.McP.	Proterozoic	1/05/1964		399792	5320419	100m	Estimate
Tyennan	Lineation	Lae	4	314	3			Lm	Duncan, D.McP.	Proterozoic	1/05/1964		403435	5320487	100m	Estimate
Tyennan	Fold axis	Haa	44	311	3			A	Duncan, D.McP.	Proterozoic	1/05/1964		399874	5320589	100m	Estimate
Tyennan	Metamorphic Foliation	Sag	63	275	3			Sm	Duncan, D.McP.	Proterozoic	1/05/1964		399874	5320589	100m	Estimate
Tyennan	Fold axis	Haa	12	355	3			A	Duncan, D.McP.	Proterozoic	1/05/1964		402117	5320713	100m	Estimate
Tyennan	Metamorphic Foliation	Sag	48	280	3			Sm	Duncan, D.McP.	Proterozoic	1/05/1964		402117	5320713	100m	Estimate
Tyennan	Metamorphic Foliation	Sag	33	285	3			Sm	Duncan, D.McP.	Proterozoic	1/05/1964		399829	5320786	100m	Estimate
Tyennan	Fold axis	Haa	24	330	3			A	Duncan, D.McP.	Proterozoic	1/05/1964		401478	5320838	100m	Estimate
Tyennan	Metamorphic Foliation	Sag	40	250	3			Sm	Duncan, D.McP.	Proterozoic	1/05/1964		401478	5320838	100m	Estimate
Tyennan	Metamorphic Foliation	Sag	40	241	3			Sm	Duncan, D.McP.	Proterozoic	1/05/1964		401138	5320840	100m	Estimate
Tyennan	Metamorphic Foliation	Sag	23	270	3			Sm	Duncan, D.McP.	Proterozoic	1/05/1964		399764	5320870	100m	Estimate
Tyennan	Metamorphic Foliation	Sag	30	290	3			Sm	Duncan, D.McP.	Proterozoic	1/05/1964		399630	5320875	100m	Estimate
Tyennan	Fold axis	Haa	23	330	3			A	Duncan, D.McP.	Proterozoic	1/05/1964		401824	5320899	100m	Estimate
Tyennan	Metamorphic Foliation	Sag	41	250	3			Sm	Duncan, D.McP.	Proterozoic	1/05/1964		401824	5320899	100m	Estimate
Tyennan	Fold axis	Had	0	120	3			A	Duncan, D.McP.	Proterozoic	1/05/1964		400953	5320957	100m	Estimate
Tyennan	Metamorphic Foliation	Sag	33	250	3			Sm	Duncan, D.McP.	Proterozoic	1/05/1964		400675	5321024	100m	Estimate
Tyennan	Metamorphic Foliation	Sag	34	305	3			Sm	Duncan, D.McP.	Proterozoic	1/05/1964		399415	5321055	100m	Estimate
Tyennan	Metamorphic Foliation	Sag	56	260	3			Sm	Duncan, D.McP.	Proterozoic	1/05/1964		400463	5321056	100m	Estimate
Tyennan	Fold axis	Haa	15	320	3			A	Duncan, D.McP.	Proterozoic	1/05/1964		402254	5321081	100m	Estimate

Project	Structure	Structure Type	Dip	D/Direct	Reliability	Secondary Dip	Secondary D/Direct	Comments	Originator	Chronostra-tigraphy	Collection Date	Field #	East	North	Accu-racy	Location Method
Tyennan	Fold axis	Haa	10	180	3			A	Duncan, D.McP.	Proterozoic	1/05/1964		402254	5321081	100m	Estimate
Tyennan	Metamorphic Foliation	Sag	12	302	3			Sm	Duncan, D.McP.	Proterozoic	1/05/1964		402254	5321081	100m	Estimate
Tyennan	Metamorphic Foliation	Sag	42	305	3			Sm	Duncan, D.McP.	Proterozoic	1/05/1964		399661	5321129	100m	Estimate
Tyennan	Fold axis	Haa	40	270	3			A	Duncan, D.McP.	Proterozoic	1/05/1964		399257	5321159	100m	Estimate
Tyennan	Metamorphic Foliation	Sag	47	280	3			Sm	Duncan, D.McP.	Proterozoic	1/05/1964		399257	5321159	100m	Estimate

Tasmanian
Government

Mineral Resources Tasmania
PO Box 56 Rosny Park
Tasmania Australia 7018
Ph: +61 3 6165 4800

info@mrt.tas.gov.au www.mrt.tas.gov.au